NASA Technical Paper 1918

Parametric Study of Microwave-Powered High-Altitude Airplane Platforms Designed for Linear Flight

Charles E. K. Morris, Jr.

NOVEMBER 1981

NASA

NASA Technical Paper 1918

Parametric Study of Microwave-Powered High-Altitude Airplane Platforms Designed for Linear Flight

Charles E. K. Morris, Jr.
Langley Research Center
Hampton, Virginia

National Aeronautics
and Space Administration

**Scientific and Technical
Information Branch**

1981

SUMMARY

The performance of a class of remotely piloted, microwave-powered, high-altitude airplane platforms was studied. The first part of each cycle of the flight profile consists of climb while the vehicle is tracked and powered by a microwave beam; this is followed by gliding flight back to a minimum altitude above a microwave station and initiation of another cycle. Parametric variations were used to define the effects of changes in the characteristics of the airplane aerodynamics, the energy-transmission systems, the propulsion system, and winds.

Results show that wind effects limit the reduction of wing loading and the increase of lift coefficient, two effective ways to obtain longer range and endurance for each flight cycle. Calculated climb performance showed strong sensitivity to some power and propulsion parameters. A simplified method of computing gliding endurance was developed.

INTRODUCTION

Remotely piloted vehicles operating at high altitude have been proposed to perform communication or observation tasks for various regions of the Earth's surface (refs. 1 and 2). A remote power supply, such as solar radiation or a microwave beam from a ground station, could give endurance limited only by systems reliability. Applications for such high-altitude aircraft platforms include mapping, resource monitoring, relaying communications, and conducting other tasks currently performed by satellites or manned aircraft.

Long-endurance aerial platforms offer advantages over alternate systems. Endurance of a manned aircraft is limited by fuel storage and human fatigue. Furthermore, the payload and equipment must include provisions for the pilot and his environmental control system. These factors adversely affect cost and complexity. A geosynchronous satellite has long endurance; however, it also has high cost, less resolution than airborne systems, and constraints for communications tasks because of the extreme range. A satellite operating in a low orbit passes only infrequently and briefly over a given region. Compared with a platform in the upper atmosphere, a low-orbit satellite requires observation systems to have resolutions at least six times as great for equivalent quality of results based on the ratio of operating altitudes.

Several types of high-altitude aircraft platforms have been proposed. Lighter-than-air concepts have been considered (ref. 3). Some of the difficulties of operating these vehicles at altitudes of 18 km (59 000 ft) and above relate to the atmospheric environment. The airships would have to generate lift at air densities less than one-tenth that of sea level (ref. 4), and, according to reference 5, have the capability to fly against winds of up to approximately 50 m/s (100 knots). Airplane configurations using solar power have been discussed in references 6 to 8. The study of reference 8 concludes that improved energy-storage technology and extremely low wing loadings would be required. (For a cruise altitude of 20 km (66 000 ft) and 12 hours of daylight, that study indicated that a specific energy-storage capability of 15 kJ/N (19 W-hr/lbf) required a wing loading of less than 5 Pa (0.1 lbf/ft^2) and 100 kJ/N (124 W-hr/lbf) required 55 Pa (1.1 lbf/ft^2).) In addition, a solar-powered

configuration would be constrained to operate with combinations of latitude and season that ensure an adequate daily supply of solar energy for a given configuration.

Studies of the design and operation of microwave-powered high-altitude airplane platforms (HAAP) have been reported in references 3 and 9 to 11. The HAAP configurations of all these reports were propeller-powered airplanes operating in the low-wind region near 20 km (66 000 ft) altitude. The lower surface of the wing contained a rectenna. (See ref. 12.) The rectenna received radio-frequency radiation at about 2.45 GHz and converted the impinging energy into direct electrical current for storage in batteries or use in electric motors driving the propellers. These studies indicated that the designs were feasible based on the assumption of some extrapolation of existing microwave technology (such as that described in ref. 12).

This study provides predictions of cruise performance for the class of HAAP configurations that use a "linear" mode of flight. In that mode, the flight profile consists of powered climb near a microwave ground station, followed by gliding flight that either returns the vehicle to the same microwave ground station or carries it to another station. (This mode is described further in the feasibility study of ref. 9 and the design sensitivity study of ref. 10.) Launch and recovery are not addressed in this study. Emphasis is placed on vehicle design and not energy transmission.

Analyses of the results of this parametric study define trends that apply to HAAP vehicles over a wide range of sizes and weights. Performance is characterized as a set of parameters: altitude at the end of climb, excess energy retained in storage, horizontal range between stations, and endurance for each cycle of the flight profile. Parametric studies are conducted for variations in the aerodynamic characteristics, energy-transmission system, propulsion system, flight profile, and winds. A minimum altitude of 18 km (59 000 ft) was selected for all cases as a probable constraint due to wind.

Operating characteristics of a microwave-powered airplane are sufficiently unconventional to require the development of a new computer program for performance prediction. The program used in this study is documented in appendix A.

SYMBOLS

Measurements and calculations were made in the International System of Units (SI). Except in the computer printouts and in some figures, dimensional quantities are presented in both SI and U.S. Customary Units to aid the reader.

A	wing aspect ratio
A_p	propeller-disk area, m^2 (ft^2)
a	constant defined in equation (11)
b	wing span, m; also, constant defined in equation (11)
C_D	drag coefficient, D/qS
$C_{D,o}$	profile-drag coefficient
C_L	lift coefficient, L/qS

C_p propeller-power coefficient, $P_p/\rho n^3 D_p^5$

D drag, N (lbf)

D_p propeller diameter, m (ft)

E_s stored energy, J (ft-lbf)

E_t total energy received, J (ft-lbf)

e Oswald efficiency factor; also, base of natural logarithms

g acceleration of gravity, 9.80 m/s^2 (32.2 ft/s^2) at sea level

h altitude above sea level, km (ft)

h_s altitude at beam intercept point, km (ft)

J propeller advance ratio, V/nD_p

k_a acceleration correction factor (see eq. (4))

k_r microwave-beam intensity factor (see eq. (12))

k_w wind-profile scale factor

L lift, N (lbf)

n propeller rotational speed, revolutions/second

P maximum power available in beam, W (hp)

P_p power absorbed by propellers, W (hp)

P_r power available at rectenna, W (hp)

q dynamic pressure, $1/2\ \rho V^2$, Pa (lbf/ft^2)

R reference value of radial distance from microwave ground station, km (n.mi.)

r actual radial distance from microwave ground station, km (n.mi.)

S wing area, m^2 (ft^2)

T propeller thrust, N (lbf)

T_d degraded propeller thrust, N (lbf)

t elapsed time, s

V true airspeed, m/s (knots, abbreviated kt on figures)

V_e equivalent airspeed, $V\sqrt{\rho/\rho_o}$, m/s (knots)

V_g ground speed, m/s (knots)

V_{tip} propeller tip speed, m/s (ft/s)

V_w local horizontal wind speed, m/s (knots)

W vehicle gross weight, N (lbf)

x horizontal range, km (n.mi.)

x_s horizontal distance between ground station and beam intercept point, km (n.mi.)

z dummy variable of integration (see eq. (B3)), km (ft)

γ flight-path angle, deg

Δ increment of parameter

η propeller efficiency factor

θ microwave-beam elevation angle, deg

μ angle between wind vector and required ground-track vector

ρ air density, kg/m^3

ρ_o sea-level air density, 1.255 kg/m^3 (0.08 lbm/ft^3)

ρ_R ratio of approximate density (appendix B) to density from reference 4

ϕ angle between airplane heading and required ground-track vector

Subscripts:

c end of climb or beginning of glide

g end of glide

max maximum

min minimum

t total for one climb and glide cycle

A dot over a symbol denotes differentiation with respect to time. A bar over a symbol denotes an average value.

CONCEPT DESCRIPTION

The remotely piloted, microwave-powered HAAP of this study is based on the concept described in reference 9. Drawings of representative vehicles are shown in figure 1. The description of the baseline vehicle and microwave system in table I is sufficiently generalized to apply to a wide variety of configurations and systems.

The linear mode of flight used in this study has the same two-part cycle as those of references 9 to 11. The climb segment begins when a microwave beam starts to track the vehicle and transmit energy to it. That energy is used for climbing or accumulating stored energy (for use by the payload, guidance, and control systems). Stored energy is not used for propulsion. Thus, after energy transmission terminates, the vehicle begins a long glide that either carries it to another ground station or back to the same station.

The transmission of microwave energy is modeled largely with the assumptions of reference 9. The multielement retrodirective array or equivalent antenna (ref. 11) transmits a linearly polarized beam that is focused on the rectenna built into the HAAP. (Linear polarization is preferred because most elements of the system are simpler than for circular polarization.) The two-dimensional tracking capability of the transmitter constrains the vehicle to fly in a vertical plane over the ground station. The cumulative effect of all range-related phenomena is assumed to be attenuation of the beam intensity as an inverse function of range.

The conceptual design of the vehicle for this study is similar to a powered version of a high-performance sailplane. The useful-load fraction of 0.3 contains allocations for the payload, energy-storage devices, and the guidance and control systems. The baseline configuration calls for high aerodynamic efficiency to be achieved with high-aspect-ratio wings and extensive amounts of natural laminar flow. The wing-mounted rectenna uses linear polarization unless otherwise noted. The power received by the rectenna is stored if it is below a minimum level for motor starting or above the power capacity of the motor. Power in the range required for propulsion is used by high-efficiency electric motors to drive variable-pitch, constant-speed propellers. When not in use, the propellers stop and fold streamwise to reduce drag. Since the propeller contributes drag rather than thrust during glide, the vehicle lift-drag ratio is decremented from that for climb. During both flight segments, the vehicle remains trimmed at one lift coefficient.

A more detailed study of HAAP should consider criteria for stability, control, aeroelasticity, reliability, and other factors. The design illustrated in figure 1(b) reflects some concern for reliability by minimizing the number of essential systems in comparison with the configuration of reference 9. The second configuration uses one rather than two propellers. Aerodynamic control is achieved through a total of two control surfaces at the end of the tail booms; differential inputs of the horizontal surfaces produce wing twist. This design was examined briefly in an unpublished study which indicated that the two vehicles of figure 1 can have the same performance, control power, and weight. Although these two configurations are significantly different, the approach of this study is sufficiently generalized to describe both of them with the same set of parameters. (See table I.)

ANALYSIS

The evaluation of vehicle performance for a microwave-powered airplane requires mathematical modeling of vehicle motion, wind effects, power transmission, and propulsion-system characteristics. The development of the equations used in the microwave-powered HAAP performance program of appendix A is given in the following sections.

Flight Mechanics

Equations for force balance along the body axes can be developed with the conventions shown in figure 2(a). The associated assumptions are that thrust and drag act along the same axis, the vehicle climbs or descends to maintain airspeed, vehicle lift coefficient remains constant, and excess thrust is used to climb. The resulting equations are as follows:

$$L - W \cos \gamma = 0 \tag{1}$$

$$T - D - W \sin \gamma - \frac{W}{g} \dot{V} = 0 \tag{2}$$

These equations can be modified to obtain the forms used in the performance program of appendix A. First, thrust can be described in terms of propeller efficiency as

$$T = \eta P_p / V \tag{3}$$

The term for the inertial acceleration force can be written as follows:

$$\frac{W}{g} \dot{V} = \frac{W}{g} \frac{dV}{dh} \frac{dh}{dt} = \frac{W}{g} \frac{dV}{dh} V \sin \gamma$$

For sufficiently small increments of altitude, an acceleration correction factor k_a can be defined as

$$k_a = \frac{V}{g} \frac{dV}{dh} \approx \frac{V}{g} \frac{\Delta V}{\Delta h} \tag{4}$$

Thus, equation (2) can be rewritten as

$$\eta P_p / V - D - (1 + k_a) W \sin \gamma = 0 \tag{5}$$

An expression for true airspeed, obtained from equation (1), may be written as

$$V = \sqrt{\frac{W}{S} \frac{2 \cos \gamma}{C_L}} \tag{6}$$

Except for the term $\cos \gamma$, equivalent airspeed is simply the equilibrium airspeed for a given configuration at sea level:

$$V_e = \sqrt{\frac{W}{S}\frac{2}{\rho_o C_L}} = \sqrt{\frac{\rho}{\rho_o}}\, V \tag{7}$$

The equations for the vehicle trajectory above a flat Earth are based on the conventions shown in figures 2(b) and 2(c):

$$V \cos \gamma \sin \phi - V_w \sin \mu = 0 \tag{8}$$

$$\dot{x} - V \cos \gamma \cos \phi + V_w \cos \mu = 0 \tag{9}$$

$$\dot{h} - V \sin \gamma = 0 \tag{10}$$

The use of these equations assumes that the airplane heading is automatically adjusted to compensate for the effects of wind. During climb, the resulting flight path must lie in the unique vertical plane swept out by the path of the microwave beam.

Several parameters are functions of altitude. Air density is modeled on the geometric standard atmosphere of reference 4. The ratio of local to sea-level values of air density is calculated as

$$\rho/\rho_o = e^{(-ah)-bh^2} \tag{11}$$

where the exponential coefficients (a and b) hold constant over a typical altitude increment of 2 km (6500 ft). At altitudes less than 30 km (98 000 ft), this method gives density data that differ from that of reference 4 by less than 0.4 percent. As in reference 10, it is assumed that L/D increases with altitude for the operating range of cruise altitudes because of the greater extent of laminar flow. The value of L/D is decremented (as a function of propeller size) for glide because of the drag of the folded propeller.

Energy Transmission

The available power (i.e., rate of energy reception) at the vehicle rectenna is assumed to be a function of both range and the angular orientation of the rectenna surface with respect to the beam. This analysis accounts for four factors that attenuate the power level between the ground-station antenna and its utilization for propulsion or storage.

Although the beam is considered to be focused, the effects of focusing precision and other factors are represented by a reciprocal relationship with range:

$$P_1 = (R/r)^{k_r} P \tag{12}$$

where R is a reference radial range from the ground station, r is the true radial range, and k_r has a nominal value of 1.0. The resulting level of available power P_1 is assumed to be further attenuated because of angular orientation that reduced the projected area of the rectenna that can be observed from the microwave ground station (p. 44 in vol. 2 of ref. 13). This effect can be approximated as

$$P_2 = P_1 \sin (\theta + \gamma) \tag{13}$$

If both transmitter and rectenna use linear polarization, the effect on the energy transfer can be conservatively approximated as a function of the phase angle between the two units (ref. 14 and p. 275 in vol. 1 of ref. 13):

$$P_r = P_2 \cos^2 \phi \tag{14}$$

If the antenna transmits with circular polarization, the linear polarization of the rectenna produces a sinusoidal variation in apparent amplitude of each wave form at the rectenna. As a result, the average energy level is only half that for polarization alignment. However, the system of mixed polarizations is insensitive to the relative alignment of antenna and rectenna in the horizontal plane.

All these power-transmission relationships (eqs. (12) to (14)) can be combined into one equation. It is convenient to describe power available at the rectenna for storage or propulsion in terms of power per unit weight:

$$\frac{P_r}{W} = \frac{P}{S}\left(\frac{S}{W}\right)\left(\frac{R}{r}\right)^{k_r} \sin (\theta + \gamma) \cos^2 \phi \tag{15}$$

where P/S is the maximum transmitted power per unit wing area available at the reference range R, W/S is wing loading, and both antenna and rectenna have linear polarization. The equation, as used in appendix A, also reduces the level of available energy by an efficiency factor of 74 percent. This reflects losses between the power reaching the rectenna surface and the power delivered to either the propeller shaft or the energy-storage system.

Propulsion

Representative values of propeller efficiency for equation (3) were developed from reference 15 and are given as functions of advance ratio J and propeller-power coefficient C_p. These latter quantities can be determined as functions of both calculated and input parameters of the program of appendix A:

$$J = \frac{\pi V}{V_{tip}} \tag{16}$$

$$C_p = \frac{\pi}{8}\left(\frac{P_p}{A_p}\right)\left(\frac{1}{V_{tip}}\right)^3 \tag{17}$$

$$\frac{P_p}{A_p} = \frac{P_p}{W}\left(\frac{W}{S}\right)\frac{S}{A_p} \tag{18}$$

where P_p/W is the power available at the propeller shaft. Net thrust for any number of propellers can be determined with this method if A_p is total propeller-disk area, P_p is total power absorbed by the propellers, and all propellers have the same value of both tip speed and power loading (P_p/A_p).

The program of appendix A imposes both an upper and a lower limit on the power-to-weight ratio of equation (18). As shown in sketch A, all energy not used for propulsion is stored. A limiting case may occur in which the minimum power level is never exceeded. (This could occur if the motor were large relative to the available power and the "projected area" of the rectenna were reduced by the combination of a negative γ and low θ (fig. 2(a)).)

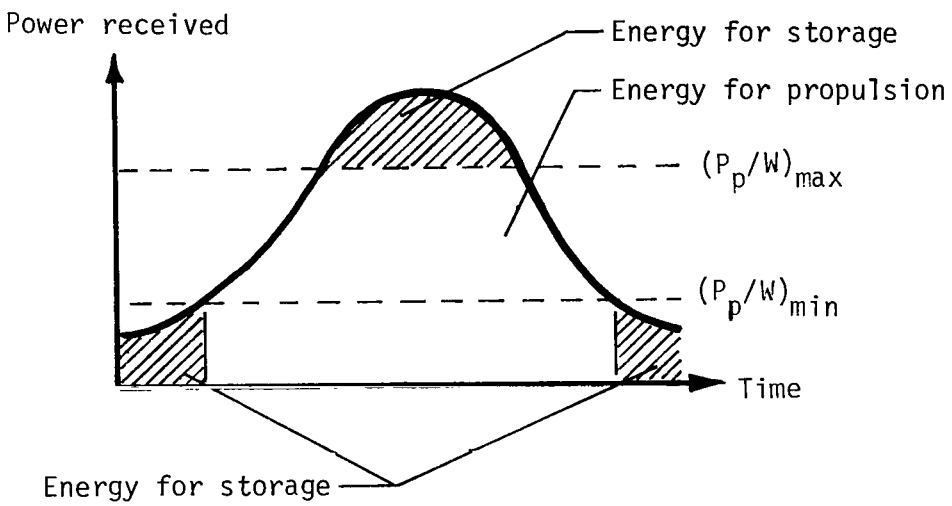

Sketch A.

Winds

The model of the wind aloft is based on one set of wind data. This standard set is the 99-percent profile (ref. 5 in fig. 3), which describes a wind profile that is exceeded only one percent of the time at five sites in the United States. Figure 3 also presents a 95-percent profile (one not exceeded 5 percent of the time) from reference 5. The second 99-percent profile of figure 3 is based on data from a worldwide set of sites (ref. 16) and indicates that the standard wind profile is generally conservative. In the computer program of appendix A, the magnitude of the wind at a given altitude is the product of the associated value from the reference profile and a scale factor k_w. In the program, the direction of the horizontal wind vector is assumed to remain constant.

DISCUSSION OF RESULTS

The results of calculations of HAAP system performance are presented to show the effect of variations in aerodynamic, power-system, and other parameters. Although not all the combinations of values represent reasonable systems, the more extreme sets help to define trends. In most cases, the results are compared with the performance of the baseline HAAP system described in table I. (This baseline system is similar to that of ref. 9. The primary differences are in specifications for h_s, x_s, and (P/W) limits.)

The variety of potential uses for a HAAP system has led to the use of several measures of performance to define results for most sections of this study. Requirements for following a specified ground track and the limited availability of sites for ground stations could produce emphasis on long endurance (total time per flight cycle) and zero-wind range. The need for high resolution in observation tasks and wide-area coverage in communications tasks may produce some differences in the specifications for attaining a maximum altitude. Wide variations may also occur in the level of stored energy required to operate each payload as well as guidance and control systems. Therefore, the results presented for each parametric variation usually include range, endurance, final climb altitude, and stored energy.

Typical Flights

One cycle of climb and glide is presented in figures 4 and 5 for each of three HAAP configurations with differing wing loadings. The essentially linear flight profile for gliding flight in figure 4 is a direct function of L/D. As shown in figure 5, the climb segment is affected by numerous parameters. The low wing-loading case (W/S = 50 Pa (1.0 lbf/ft^2)) has a fairly simple calculated history. During climb, the flight path is fairly linear, the rate of climb is nearly constant, and the propeller provides thrust all the time. The highest wing-loading case (W/S = 250 Pa (5.2 lbf/ft^2)) has an s-shaped climb profile (fig. 4) and climb history (fig. 5). Initially, the relatively smaller wing for W/S = 250 Pa does not receive enough power to start the motors. The airplane continues to store the received energy and to lose altitude as it glides nearer to the ground station (fig. 5(b)). When it is close enough to receive adequate power, the airplane uses all available power to climb. Near the end of the nominal climb period, the power received again drops below the minimum level. The airplane then glides and stores the received energy again. This latter glide segment illustrates the reasons that h_c can be less than the maximum altitude achieved in climb.

Figure 5 indicates that there are strong relationships between performance, power available, and the flight path (defined with respect to the ground station). Consequently, the flight profile could be changed to maximize stored energy or some other parameter. However, the results of this study are all obtained for the simple case of flight at constant lift coefficient.

Equivalent Airspeed

The design value of V_e is important for a HAAP vehicle. As shown in equation (7) and figure 6, V_e is a function of both C_L and W/S. Maximizing L/D to improve range leads to the selection of the highest value of C_L that allows some

margin of safety against stall. Requirements for adequate rectenna area and for long endurance (i.e., slow descent rate) can produce design emphasis on low values of W/S. Figure 6 shows that these design trends lead to low values of V_e.

The effect of winds produces constraints on the minimum acceptable level of V_e. Figure 7 presents a wind profile that is exceeded only 1 percent of the time at five sites (ref. 5). As shown subsequently in this report, this profile can provide a reasonable design criterion for HAAP vehicles that must avoid being blown away from a given site. The data suggest that V_e above 16.6 m/s (32.3 knots) is required if flight profiles extend to as low as 18 km (59 000 ft) in altitude. Application of this criterion to the data of figure 6 limits C_L as a function of W/S.

Airplane Aerodynamic Characteristics

The effects of W/S and L/D on HAAP performance are evaluated in figure 8. The parameter W/S also affects the power and propulsion system, since the rectenna is assumed to cover all the wing area S. Thus, decreasing W/S increases available power per unit weight. Large propulsion systems can then operate the propeller continuously at full power during climb. As shown in figure 5, this effect can result in a sustained high rate of climb. Figure 8 also shows that reductions in W/S produce substantial improvements in attainable altitude and, below about W/S = 100 Pa (2.1 lbf/ft^2), large increases in stored energy. Variations in L/D have relatively less effect on altitude and energy performance than variations in W/S. Range and endurance are both increased by reduced W/S or by increased L/D. In the case of the baseline HAAP, Reynolds number effects are estimated to change L/D for the baseline vehicle from 44.1 at 8.1 km (27 000 ft) altitude to 46.6 at 24 km (79 000 ft). However, analyses show that an average L/D yields results in good agreement with those for the variable L/D. (For example, performance results for the baseline vehicle, with the variable L/D and W/S = 100 Pa, were within 1 percent for the case with L/D = 45, an average value.)

The effect of L/D can also be considered in light of the independent effects of C_L and $C_{D,o}$ (fig. 9). The value of C_D is calculated as

$$C_D = C_{D,o} + C_L^2/\pi Ae$$

The set of $C_{D,o}$ values used provides reasonable agreement between the maximum values of calculated L/D and those obtained from references 17 and 18. Both C_L and $C_{D,o}$ appear to have significant effects on range and endurance. All the trends for aerodynamic changes are in agreement with those determined in reference 10.

Gliding Flight

A simplified analysis of gliding-flight endurance can be accomplished with an approximate solution to equation (29) of reference 8, an expression for glide time between specified altitudes. Appendix B presents the development of an expression for a glide-time parameter $t_g V_e(D/L)$ which is independent of configuration.

An approximation for air density as a function of altitude allows the glide-endurance equation to assume integrable form. Figures 10 and 11 provide a means of comparing results from the approximate function with the values given in refer-

ence 4. Figure 11 shows that the two density models are in good agreement between 18 and 23 km (59 000 and 75 000 ft), which is the altitude range of interest.

The glide-time parameter can be used to determine the relative endurance achieved by gliding between different sets of initial and final altitudes. Figure 12 presents the glide-time parameter as a function of initial altitude and altitude decrements. The computed results show that for a given altitude decrement, glide time is longer at lower altitudes. This occurs because the vehicle travels more slowly through the denser atmosphere at lower altitudes.

Results of glide-endurance calculations are compared in figures 13 and 14 for the computer program of appendix A and the closed-form solution of appendix B. The computer program has the advantage of accounting for acceleration effects and using a more detailed model of density variation with altitude. The figures show that agreement between the methods is best at low values of W/S, L/D, and h_c. If the acceleration correction factor is removed from the computer program, the computer yields glide times which are virtually identical to those given by the closed-form method of appendix B.

Energy-Transmission System

Climb performance is strongly affected by numerous interrelated parameters that characterize the energy-transmission system. As shown in equation (15), these include P/S, R, and k_r. Parametric variations are considered here even though further development of microwave technology may lead to revisions of equation (15). The review of the present results is simplified by presenting only climb performance since gliding flight has already been treated.

The character of beam-range effects is controlled by the exponent k_r in equation (15). (Even though k_r is considered separately here, the formulation of the governing equation is based on the interrelationships between P/S, R, and k_r.) As shown in figure 15, focused power is independent of range only for $k_r = 1$. For any value of $k_r > 0$, the equation requires that received power increases indefinitely as r/R approaches 0. In the present study, the values of r/R range from about 0.4 to 1.0, and the effect of k_r does not reach physically implausible proportions for $k_r = 1$. In a real system the transmitter would have a finite value of beam intensity at zero range; beyond a given range some value of k_r would model the beam attenuation. Thus, increases in only k_r imply a disproportionately large increase in actual transmitter power. Because of the large value of R, $r/R \leq 1$ during climb; since the effect of k_r is amplification at those regions, power intensity is always equal to or greater than the P/S reference value of 1.1 kW/m^2 at 50 km range (100 W/ft^2 at 27 n.mi. range).

Climb performance is presented as a function of k_r in figure 16 and several climb histories are presented in figure 17. Increasing k_r allows the value of final climb altitude to increase asymptotically to a maximum and stored energy to increase exponentially. Since $r/R \leq 1$, increasing k_r simply increases available power at the vehicle. The calculated results appear to be opposite of the effects that would be anticipated from an increasing decay of beam intensity with distance; however, the short ranges and the implied large increase in transmitted power overcome the effects of decay rate.

Climb performance is also sensitive to reference range R and the power density at that range P/S. Increasing P/S leads to large increases in stored energy (fig. 18) and allows the vehicle to climb higher. However, as in the case of $(P_p/W)_{max}$ = 4 W/N (0.002 hp/lbf) in figure 18, motor size can limit altitude, regardless of the power received. Similar trends are shown for increasing R in figure 19. Increases in R or P/S are also associated with large increases in transmitted power.

The initial range and altitude for beam intercept also affects climb performance. Figure 20 shows that beam interceptions at longer range permit higher altitudes to be attained. However, power received at the vehicle is attenuated as a function of range; thus, the higher flying vehicles can accumulate less stored energy per cycle of flight. This attenuation and the decrease of density with altitude combine to determine vehicle ceiling. As shown in figure 21, both the rate of climb and the energy storage for the baseline configuration are negligible at an altitude of about 29 km (95 000 ft).

Propulsion System

The effects of variations in propeller efficiency are shown in figure 22. The computer program of appendix A determines η as a function of J and C_p from a conventional propeller-performance table (ref. 15). These tabulated data do not reflect any effects of high-altitude, low Reynolds number phenomena on propeller aerodynamics. This omission, and other simplifications, may lead to optimistic predictions of propeller performance. The result of operating with degraded thrust T_d is a nearly linear decrease in attainable altitude (fig. 22). This indicates that even a small degradation in propeller efficiency translates into noticeable performance decreases.

The effect of relative motor size is shown in figure 23. The parameter $(P_p/W)_{max}$ reflects not only the maximum power that the propulsion system can absorb, but also the ratio of motor size to total vehicle weight. The largest value of $(P_p/W)_{max}$ considered here is twice that of the baseline configuration. The computed results show that increasing the relative size of the motor generally leads to decreases in stored energy and to increases in attainable altitude until a maximum performance level is achieved. Beyond that point, increasing $(P_p/W)_{max}$ is detrimental to performance. This variation indicates that the optimization of propulsion parameters is a function of wing loading (and rectenna size).

A review of the calculated flight histories leading to the results of figure 23 reveals that the variation in performance is related to both trajectory characteristics and limits on the minimum power required. The vehicle with the larger motor may have to glide closer to the ground station before receiving enough power to overcome starting loads and other constraints. The more powerful vehicle climbs faster and generally flys a higher trajectory as it passes over the ground station. The more powerful vehicle then reaches the minimum P_p/W condition and begins its glide phase sooner. Detailed design of a HAAP will apparently be sensitive to constraints on minimum and maximum motor power.

The effects of two propeller parameters on climb performance are shown in figures 24 and 25. The baseline value of tip speed 172 m/s (564 ft/s) appears to be a good selection (fig. 24), although performance appears to be fairly insensitive to small variations in that parameter until compressibility effects are encountered. The area ratio S/A_p is a somewhat artificial parameter that is a convenient element

in equation (18). As indicated in figure 25, that measure of relative propeller size is also set at a good value in the baseline configuration ($S/A_p = 2.65$).

Winds Aloft

Although winds aloft can greatly influence the results of any given mission, wind effects on HAAP design are difficult to quantify. The statistical nature of basic wind data (refs. 5, 16, and 19) must be properly evaluated to avoid developing excessively stringent design criteria. Wind profiles that are exceeded only 1 percent of the time probably provide adequate design guidelines. The winds that exceed those limits tend to be associated with large storms occurring at lower altitudes. These more detectable, lower-altitude phenomena may provide enough warning to make appropriate changes in the flight program, such as maintaining as much altitude as possible. In addition, the relationships of wind direction at different altitudes are not considered in most sources of data. Nonuniformity of wind direction at different altitudes may make HAAP operations easier than predicted for uniform wind direction.

Operational limits imposed by winds tend to affect HAAP operations at lower altitudes. Figure 7 shows that for $V_e \geq 10$ m/s (19 knots), the selection of a design value of V_e for lower altitudes ensures an adequate margin of true airspeed V at higher altitudes. Thus, operations need not be restricted to the nominal low-wind region of about 20 km (66 000 ft).

HAAP operations with actual wind effects will be more complex than for the simplified wind model of this study. Profiles for mean wind values from reference 19 show consistent trends with altitude for different seasons in figure 26(a); however, the associated data of figure 26(b) show that there is a considerable variation possible between the mean and instantaneous values. Below 18 km (59 000 ft) altitude, the mean winds blow predominately from west to east, although the instantaneous value appears to vary considerably (fig. 26(b)). Data from references 16 and 19 clearly indicate that winds at 18 km and above are typically much stronger in winter. Despite the evidence of complexity, this study models winds on the basis of the profile shown in figure 7 and on the assumption of uniform wind direction. The wind-profile scale factor k_w affects only the magnitude of the nominal profile (ref. 5); k_w does not directly reflect the probability level of encountering that profile.

Studies were conducted of the effect on performance of wind-profile magnitude and wind direction relative to required ground track. The first cases to be considered are those for the baseline HAAP configuration with a head wind or tail wind over the nominal ground track (fig. 27). Increases in wind-profile magnitude for a head wind of $\mu = 0°$ reduce ground speed and increase the amount of time spent in passing over the ground station. The additional energy available through the extended climb period produces substantial increases in attainable altitude; however, the head winds affect the glide for a longer period of time and can substantially reduce total range. The reverse relationships appear to be true for tail winds. The data for $\mu = 0°$ terminate at $k_w = 0.97$ because head winds at 18 km (59 000 ft), the initial altitude, can become no stronger without blowing the vehicles away from the ground station.

As shown in figure 2(c), adjustments to vehicle heading can cause the vector summation of wind and airspeed velocities to produce the desired ground track for the HAAP (for sufficiently low wind speeds). However, if the vehicle rectenna is not

exactly aligned with the transmitting antenna, the use of linear polarization results in a reduction in energy-transmission efficiency (eq. (14)). The effect of parametric variations in wind conditions is shown in figure 28. As shown in figure 27, the absence of calculated results for a given condition indicates that the baseline HAAP configuration could not fly in those winds. Typical performance near limiting conditions is shown in figure 28(a) for $\mu = 45°$ and $k_w = 0.74$. As winds approach limiting conditions, the vehicle spends a large part of its climb time in slowly making headway at the lowest altitudes (near 18 km (59 000 ft)); power storage increases significantly, but final altitude decreases. Figure 28 shows that as amplitude of the wind profile increases, only tail winds permit flight. In all cases, the unsuccessful attempts at flight were terminated by winds at 18 km blowing the vehicle away from the ground station.

Flight with more severe wind profiles would be possible for all wind directions if the baseline configuration or flight plan were modified. Previously discussed results show that increasing the design value of equivalent airspeed could allow the vehicle to operate in the presence of stronger winds. Another solution would be to increase the value of minimum altitude. As shown in figure 7, the nominal wind profile for this study is more severe at the lower altitudes. Figure 26 shows that such data are representative. An alternate solution would be to accept the cost and complexity of circular polarization, at least for the transmitter. The relative benefits of the last two methods are suggested in figure 29. If stored energy is not a limiting factor, the restriction of the flight profile to higher altitudes appears to offer a simple, viable solution.

Although turbulence and wind shear affect the development of HAAP design criteria, these effects are not considered herein. Some limited data on these phenomena at high altitude are available in references 20 and 21.

CONCLUDING REMARKS

A parametric study of performance has been conducted for remotely piloted, microwave-powered, high-altitude airplane platforms. The flight profile consists of climb and glide cycles: while receiving power, the vehicle climbs and stores excess energy; it then glides back down to some minimum altitude above a microwave ground station.

Calculated results identified several basic trends. Low values of wing loading and high values of lift coefficient were shown to result in long range, long endurance, and low equivalent airspeed. Wind effects constrain the lower limits of both equivalent airspeed and operating altitude. Calculations also showed that energy-transmission and propulsion-system characteristics could strongly affect climb performance. An approximate, closed-form solution was developed to predict gliding endurance.

Langley Research Center
National Aeronautics and Space Administration
Hampton, VA 23665
August 18, 1981

APPENDIX A

COMPUTER PROGRAM FOR HAAP PERFORMANCE

A computer program has been developed to calculate the performances of a microwave-powered high-altitude airplane platform (HAAP) vehicle. This appendix contains a listing of the program, a sample input file, and the corresponding sample set of output listing. The results presented in the output listing can be interpreted with the description of variable names given in tables AI and AII.

The program calculations and logic are based on the HAAP operating procedures as described in the main text. The program calculates the flight trajectory and system performance at specified intervals of time. These intervals are 10 seconds for climb and 20 seconds for glide unless the end of climb or glide is approached; at that point, the intervals are adjusted to be one-tenth their previous value. The only configuration change allowed during a given flight is the folding or unfolding of the propellers.

The program yields results for parametric studies. The first set of output information describes initial conditions in terms of the characteristics of the airplane aerodynamics, propeller and power system variables, and wind and trajectory parameters. The listings presented in columns provide histories of performance and flight mechanics. For each run, the input parameter being varied is listed in the first column on the left. Each set of parametric variations may be conducted for performance at a single point (with respect to the ground station), during climb or glide only, or throughout an entire climb and glide cycle.

The sample case included in this appendix illustrates the effect of wind magnitude. Performance is calculated for the baseline configuration HAAP with winds at right angles to the nominal ground track ($\mu = 90°$). The required inputs are: N1 = 3, N2 = 10, AMU = 90., SI = 0., SF = 1.0, and SS = 0.2. Results indicate that a full-strength wind profile does not allow the vehicle to initiate climb at 18 km (59 000 ft).

TABLE AI.- INPUT PARAMETERS FOR PERFORMANCE PROGRAM

Array element	Input name	Description
1	WOS	W/S
2	C_L	C_L
3	BLOD	L/D component independent of altitude
4	HLOD	Coefficient of altitude-dependent term in L/D equation, per km
5	TS	V_{tip}
6	SOAP	S/A_p
7	POS	P/S
8	RR	R
9	POWL	Maximum P/W used by propulsion system
10	WK	k_w
11	AMU	μ
12	XS	x_s
13	HS	h_s
14	POWR	Ratio of minimum P/W to maximum P/W for propulsion system
15	TDOT	T_d/T
16	HI	h_c
17	RKR	k_r
	N1	Code for flight mode calculation (1 - single point; 2 - climb; 3 - climb plus glide; 4 - glide only)
	N2	Element in input array to be varied
	N3	Number of calculation points per listed line
	N4	Tansmitter polarization code (1 - linear; 2 - circular)
	SF	Final value of variation set
	SI	Initial value of variation set
	SS	Step size of variation set

TABLE AII.- OUTPUT PARAMETERS FOR PERFORMANCE PROGRAM

Output name given in listing sequence	Parameter
X	x
H	h
R/C	$\dot{h}$
P/W-P	P/W available for propulsion
P/W-S	P/W available for storage
GAMMA	γ
THETA	θ
R	r
VG	V_g
VT	V
VEC	$V_e\sqrt{\cos \gamma}$
T	t
AK	k_a
ETA	η
CP	C_p
J	J
PSI	ϕ
XC	x_c
HC	h_c
TC	t_c
E/W-S	E_s/W
E/W-T	E_t/W
XT	x_t
TT	t_t

```
      PROGRAM HAAP (INPUT,OUTPUT,TAPE5=INPUT,TAPE6=OUTPUT)
C
      DIMENSION A(5), BDN(17), BD(17) ,Z(8,20)
C     A- ALPHANUMERIC LABEL, BDN- NAMES OF ELEMENTS OF BASELINE DATA ARRAY
C     BD- BASEINE DATA ARRAY, Z- FINAL OUTPUT ARRAY
C
      COMMON /PAAH/ WOS,CL, BLOD,HLOD, TS,SOAP, POS,RR, POWL,WK, AMU,
     1      XS,HS, POWR,TDOT,HI,RKR, AK,ETA, GAMMA,POW, POWP,POWS, PSID,
     2      R,RLOD, ROC,THETA, VE,VG, VT,PCP, PJ,N4,N5,X,H
      EQUIVALENCE (BD(1),WOS)
C
      NAMELIST/DD/ WOS,CL,BLOD,HLOD,TS,SOAP,POS,RR,POWL,WK,AMU,XS,HS,
     1             SI,SF,SS,N1,N2,N3,N4,TDOT,POWR,HI,RKR
C
      DATA         WOS,CL,BLOD,HLOD,TS,SOAP,POS,RR,POWL,WK,AMU,XS,HS,
     1             SI,SF,SS,N1,N2,N3,N4,TDOT,POWR,HI,RKR/
     2             144.,0.9,36.6,.418,172.,2.653,1.1,50.,8.62,0.0,0.0,
     3             40.,18.0,0.,0.,0.,2,2,50,1,1.0,0.25,25.,1./
C
      DATA BDN/7H    W/S, 6H    CL, 8H   L/D-B, 8H   L/D-H,6H    TS,
     1          8H   S/A-P, 7H    P/S, 6H    RR, 8H   P/W-L, 6H    WK,
     2          6H    MU, 5H   XS, 5H   HS, 9H  P/W M-M, 7H   TDOT,
     3          6H    HI, 6H   PKR/
C
C     BASELINE DATA ARRAY   1.W/S  2.CL  3.L/D-B  4.L/D-H 5.TS  6.S/A-P
C
C                           7.P/S  8.RR  9.P/W-L  10.WK  11.MU  12.XS
C
C                           13.HS   14.POWR   15.TDOT   16.HI   17.RKR
C
C     PARAMETER VARIATION CODE  SI- INITIAL VALUE
C                               SF- FINAL VALUE
C                               SS- STEP INCREMENT (POSITIVE OR NEGATIVE)
C
C     CONTROL CODE  N1-(SINGLE POINT, CLIMB, TOTAL FLIGHT, GLIDE ONLY)
C                   N2-(ELEMENT IN ARRAY BD TO BE VARIED)
C                   N3-(NUMBER OF CALCULATION POINTS PER LISTED LINE)
C                   N4-(RECTENNA POLARIZATION- LINEAR OR CIRCULAR)
C                   N5-(CODE=1 WHEN VG< 0)
C
  100 FORMAT (1H1,5X,5A10// 5X, 14HAIRCRAFT AERO., 7X,9HPROPELLER, 11X,
     1  5HPOWER, 14X,5HWINDS, 9X,11HSTART POINT, 4X,12HVARIABLE SET,
     2  9X,4HCODE// 5X,4HW/S=,F6.1, 5H N/M2, 6X, 3HTS=,F6.1, 4H M/S,7X,
     3 4HP/S=,F5.2, 6H KW/M2, 4X, 3HWK=,F5.2, 6X, 3HXS=,F6.2, 3H KM, 4X,
     4 6HFIRST=,F8.3, 5X, 3HN1=,I3/  114X,3HN2=,I3/  6X,3HCL=,F5.2, 9X,
     5 6HS/A-P=,F6.3, 12X,3HRR=,F5.1, 3H KM, 7X, 3HMU=,F5.1, 4H DEG, 2X,
     6 3HHS=,F6.2, 3H KM, 4X, 6HFINAL=,F8.3, 5X, 3HN3=,I3/ 114X, 3HN4=,
     7 I3/5X,4HL/D=,F5.1, 28X, 8HMAX P/W=,F5.2, 6H KW/KN, 18X, 3HHI=,
     8 F6.2, 3H KM, 4X, 5HSTEP=, F8.3, 6X, // 2X, 7HL/D(H)=,
     9 F6.3,27X,8HMIN P/W=, F4.2, 10H X MAX P/W ///)
  101 FORMAT (5A10)
  111 FORMAT (2X,A10,4X,1HX,5X,1HH,5X,3HR/C,3X,5HP/W-P,2X,5HP/W-S,2X,
     1         5HGAMMA,2X,5HTHETA,4X,1HR,6X,2HVG, 4X,2HVT,5X,3HVEC,5X,
     2         1HT,6X,2HAK,4X, 3HETA, 3X, 2HCP, 4X, 1HJ ,5X, 3HPSI//
     3         16X,2HKM, 5X,2HKM,4X,3HM/S, 4X,3HW/N,4X, 3HW/N,4X,
     4         3HDEG, 4X,3HDEG, 5X,2HKM,4X,3HM/S, 4X,3HM/S, 4X,3HM/S,
     5         4X,3HSEC,29X, 3HDEG //)
  113 FORMAT (2X,F9.5,1X,,6F7.2,F7.1,F7.2,3F7.1,F8.0,2F6.3,2F6.3,F6.1)
  114 FORMAT (5X/)
  115 FORMAT (2X,F9.5,1X, 3F7.2, F21.2, 14X, 3F7.1, F8.0, F8.4)
  200 FORMAT (//2X,A10, 4X,2HXC, 5X,2HHC, 4X,2HTC, 4X,5HE/W-S, 3X,
     1         5HE/W-T, 4X,2HXT, 7X,2HTT// 16X, 2HKM, 5X,2HKM, 4X,2HHR,
     2         4X,4HKJ/N, 4X,4HKJ/N, 5X,2HKM, 7X,2HHR/)
  201 FORMAT (110X,3HTG=, F6.3, 3H HR //)
  202 FORMAT (3X,F8.3,1X,2F7.2,F6.3,2F8.3,2F8.2)
C
C
      GO TO 3
    2 X= 0.0
```

```
      H= HS
      IF (N1.EQ.1.OR.N1.EQ.4) GO TO 3
      WRITE (6,200) BDN(N2)
      DO 300 I=1,N
      WRITE (6,202) Z(1,I),Z(2,I),Z(3,I),Z(4,I),Z(5,I),Z(6,I),Z(7,I),
     1              Z(8,I)
  300 CONTINUE
    3 READ (5,101) A
      IF (EOF(5)) 199,4
    4 READ (5,DD)
      WRITE (6,100) A,WOS,TS,POS,WK,XS,SI,N1, N2, CL,SOAP,RR,AMU,HS,SF,
     2              N3,N4, BLOD,POWL,HI,SS, HLOD,POWR
      N= 0
C
C     N2- PARAMETER FOR VARIATION, CHOSEN FROM ARRAY BD

    7 WRITE (6,111) BDN(N2)
C     INITIALIZE PARAMETER ---  NEW STARTING POINT IS NEW X OR Y
      N5= 0
      BD(N2)= SI
      GO TO 17
C
   13 Z (2,N)= X
      Z (3,N)= H
      Z (4,N)= TT
      Z (5,N)= EOWS
      Z (6,N)= EOWT
      IF (N1.EQ.3) GO TO 40
C
C     INCREMENT PARAMETER
   14 CONTINUE
      N5= 0
      IF (N1.EQ.3) Z(7,N)= X
      IF (N1.EQ.3) Z(8,N)= TG
      IF (N1.EQ.4) WRITE (6,201) TG
C
C
   16 BD(N2)= BD(N2) +SS
      DELTA= SF -BD(N2)
      IF (SS.GT.0..AND.DELTA.GE.0.) GO TO 17
      IF (SS.LT.0..AND.DELTA.LE.0.) GO TO 17
      GO TO 2
   17 N= N+1
      Z(1,N)= BD(N2)
      GO TO (20,30,30,39) ,N1
C
C     CALCULATE VALUES AT ONE POINT
   20 T= 0.
      X= 0.
      H= HS
      EOWS= 0.
      EOWT= 0.
      GAMMA= 0.
      CALL RCLIMB
      WRITE (6,113) BD(N2), X,H, ROC,POWP, POWS,GAMMA, THETA,R, VG,VT,
     1              VE,T, AK,ETA, PCP,PJ, PSID
      WRITE (6,114)
      GO TO 14

C
C     CALCULATE TOTAL CLIMB PHASE
   30 NK= 0
      POW1= 0.0
      POWS1= 0.
      GAMMA= 0.
      THETA= 0.0
      T= 0.
      EOWS= 0.
      EOWT= 0.
      RR95= RR* .95
      TT= 0.
      X= 0.0
```

```
140                H= HS
                   TDEL= 10.
                   WRITE (6,114)
             C
             C     N3 - PRINTOUT INCREMENT FOR COMPLETE CLIMB
145             31 IF (NK.EQ.N3) NK= 0
                   GAMMA= GAMMA/57.2957
                32 CALL RCLIMB
                   IF (N5.GE.1) GO TO 14
                   IF (R.GT.RR95.AND.THETA.LT.50.) TDEL= 1.
150                IF (T.EQ.0.) GO TO 35
                   NK= NK+1
             C
             C     X AND H GIVEN IN KM
                33 X= X +VG*TDEL/1000.
155                H= H +ROC*TDEL/1000.
             C
             C     SPECIFIC-ENERGY INCREMENTS FROM AVERAGED POWER FOR TIME INCREMENT
             C     STORED SPECIFIC ENERGY (E/W-S) AND TOTAL UTILIZED SPECIFIC
             C     ENERGY (E/W-T) ARE GIVEN IN KJ/N
160                EOWS= EOWS +(POWS+POWS1)*TDEL/2000.
                   POWS1= POWS
                   EOWT= EOWT +(POW +POW1)*TDEL/2000.
                   POW1= POW
                   IF (R.GT.RR.AND.THETA.LT.90) GO TO 35
165                IF (X.LT.0.) GO TO 35
                   IF (NK.EQ.N4) GO TO 35
                   T= T+TDEL
                   GO TO 31
             C     WRITE DATA FOR ONE INCREMENT OF CLIMB OR FINAL CLIMB POINT
170             35 CONTINUE
                   WRITE (6,113) BD(N2), X,H, ROC,POWP, POWS,GAMMA, THETA,R, VG,VT,
                  1              VE,T, AK,ETA, PCP,PJ, PSID
                   TT= T/3600.
                   T= T+TDEL
175                IF (X.LT.0.) GO TO 13
                   IF (R.GT.RR.AND.THETA.LT.90) GO TO 13
                   GO TO 31
             C
             C
180          C     CALCULATE GLIDE PHASE
             C
                39 T= 20.
                   TDEL= 20.
                   X= 0.
185                H= HI
                40 NG = 0
                   HS101= 1.01* HS
                   T= T -TDEL
                   PDF= 2.653/SOAP
190          C     PDF IS PROP DRAG FACTOR-PROPORTIONAL TO RATIO OF DISK AREA TO WING AREA
                   TDEL = 20.
                   GAMMA= 0.0
                41 GAMMA= GAMMA/57.2957
             C
195          C     BEGIN CALCULATION FOR NEW GAMMA AT NEW ALTITUDE
                42 RLOD= BLOD +HLOD*H
                   IF (NG.EQ.N3) NG= 0
             C     DECREMENT L/D DUE TO DRAG OF FOLDED PROPELLER
                   IF (N1.LT.4) RLOD= RLOD -1.5*PDF
200                KK= 0
             C
             C     ITERATE FOR GAMMA
                43 KK= KK +1
                   IF (KK.EQ. 10) GO TO 50
205                VE= 1.27775*SQRT (WOS*COS(GAMMA)/CL)
                   CALL ALTF (AMU, VE, WK, H, PSI, VT, VG, N5)
                   VY= -VT*COS(GAMMA) /RLOD
                   CALL ACCEL(VY,H,VG,AMU,VE,WK,GAMMA,AK)
                   ROC= VY/(1. +AK)
```

```
210         C     CALCULATE RESULTING CLIMB ANGLE
                  GAMMAC= ASIN(ROC/VT)
                  DELG= ABS(GAMMAC-GAMMA)
                  IF (DELG.LT..0002) GO TO 50
            C     AJUST CLIMB ANGLE AND REPEAT
215               GAMMA= GAMMAC
                  GO TO 43
               50 NG = NG + 1
            C
            C     X AND H GIVEN IN KM
220            54 X= X +VG*TDEL/1000.
                  H= H +ROC*TDEL/1000.
                  T= T + TDEL
                  IF (H.LT.HS101) TDEL= 2.
                  IF (NG.EQ.N3) GO TO 55
225               IF (H.GT.HS) GO TO 42
               55 GAMMA= GAMMA*57.2957
            C     WRITE DATA FOR ONE INCREMENT OF GLIDE OR FINAL POINT
                  WRITE (6,115) BD(N2),X,H, ROC, GAMMA, VG, VT, VE, T, AK
                  IF (H.GT.HS) GO TO 41
230               TG= T/3600.
                  Z(7,N)= X
                  Z(8,N)= TG
                  GO TO 14
            C
235            199 STOP
                  END
```

```
      C
      C
            SUBROUTINE DENSITY (CH, SIGMA)
      C
      C     CURVE FIT TO 62 ATMOS.†FOR CALCULATION OF DENSITY RATIO
      C
      C     INPUT: ALTITUDE IN KM; OUTPUT: DIMENSIONESS DENSITY RATIO (SIGMA)
            DIMENSION DC1(15),DC2(15)
      C
      C     SIGMA= E **(CC1*H +CC2*H**2) WHERE H IS IN KM
      C
            DATA (DC1(I),I=1,15)/.0958554,.0948554,.0955529,.0950089,.0942258,     DC1
           1                     .0942258,.0770834,.0879373,.0962238,.1027082,     DC1
           2                     .1045655,.1107329,.1160101,.1204581,.1243220/     DC1
            DATA (DC2(J),J=1,15)/.117337,.117337,.124898,.133965,.143754,          DC2
           1                     .143754,.307572,.230044,.178253,.142229,          DC2
           2                     .132942,.104908,.082920,.065812,.052013/          DC2
      C
            ICH= 1+ IFIX(CH/2.)
      C
            CC1= DC1(ICH)
            CC2= DC2(ICH)
      C
            IF (CH.LE.11..OR.CH.GE.12.) GO TO 20
            CC1= .0675418
            CC2= .387085
      C
         20 SIGMA= EXP(-CC1*CH -CC2*CH*CH/100.)
            RETURN
            END
```

†1962 U.S. Standard atmosphere, reference 4.

```
      C
      C
            SUBROUTINE ALTF(AMU,VE,WK,H,PSI,VT,VG,N5)
      C     CALCULATE TRUE AIRSPEED, WINDSPEED, AND GROUNDSPEED - SI UNITS
      C     INPUTS: WIND AZIMUTH, EQUIVALENT AIRSPEED, WIND SCALE FACTOR, AND
      C     ALTITUDE; OUTPUT: GROUND-TRACK OFFSET ANGLE, TRUE AIRSPEED, AND
      C     GROUND SPEED. (ALL SPEEDS IN M/S; ALL ANGLES IN DEGREES.)
      C         FOR WK= 1., RESULTING WIND PROFILE IS FOR 99% INCLUSIVE
      C         PROFILE FOR 5 LAUNCH SITES FROM NASA TM 78118.
      C
        300 FORMAT (4X, 24HWIND SPEED TOO LARGE AT ,F4.1, 4H KM.)
      C
            CALL DENSITY (H,SIGMA)
            VT= VE*(SIGMA)**(-.5)
            IF (H.GE.14.) GO TO 50
            VW= WK*88.
            GO TO 62
         50 IF (H.GE.15.) GO TO 51
            VW= WK* (88. -18.*(H -14.))
            GO TO 62
         51 IF (H.GE.20.) GO TO 52
            VW= WK* (70. -5.8*(H -15.))
            GO TO 62
         52 IF (H.GE.23.) GO TO 53
            VW= WK*41.
            GO TO 62
         53 VW= WK* (41. +4.7778*(H -23.))
         62 SPSI= VW*SIND(AMU)/VT
            IF (SPSI.GE.1.) GO TO 64
            PSI= ASIN(SPSI)
            VG= VT*COS(PSI) -VW*COSD(AMU)
            GO TO 65
         64 WRITE (6,300) H
            N5= 1
         65 CONTINUE
            RETURN
            END
```

```
      C
      C
            SUBROUTINE PROPCAL (PCP,PJ,ETA)
            DIMENSION PT(15,41)
      C     INPUT: PROPELLER POWER COEFFICIENT AND ADVANCE RATIO
      C     OUTPUT: PROPELLER EFFICIENCY FACTOR
      C
      C                                                                    J
      C     EACH DATA STATEMENT GIVES VALUES OF ETA AS CP, RANGES FROM .0 TO .35
      C
            DATA (PT(I, 1),I=1,15)/.0,.74,.66,.57,.48,.42,.37,.33,.28,.24,.22,     .40
           1.19,.17,.16,.14/                                                       .40
            DATA (PT(I, 2),I=1,15)/.0,.78,.71,.61,.54,.47,.41,.36,.32,.28,.24,     .45
           1.22,.19,.175,.16/                                                      .45
            DATA (PT(I, 3),I=1,15)/.0,.80,.76,.66,.58,.52,.45,.41,.35,.31,.27,     .50
           1.24,.22,.19,.18/                                                       .50
            DATA (PT(I, 4),I=1,15)/.0,.83,.80,.71,.62,.56,.49,.45,.39,.35,.30,     .55
           1.27,.24,.22,.19/                                                       .55
            DATA (PT(I, 5),I=1,15)/.0,.84,.82,.75,.67,.60,.54,.48,.43,.38,.33,     .60
           1.29,.26,.24,.22/                                                       .60
            DATA (PT(I, 6),I=1,15)/.0,.85,.84,.78,.70,.63,.57,.52,.46,.41,.37,     .65
           1.32,.28,.25,.24/                                                       .65
            DATA (PT(I, 7),I=1,15)/.0,.87,.86,.80,.73,.67,.61,.55,.50,.44,.40,     .70
           1.35,.31,.28,.25/                                                       .70
            DATA (PT(I, 8),I=1,15)/.0,.88,.87,.82,.76,.70,.64,.59,.53,.47,.43,     .75
           1.38,.34,.30,.28/                                                       .75
            DATA (PT(I, 9),I=1,15)/.0,.88,.88,.84,.78,.73,.67,.62,.57,.52,.46,     .80
           1.40,.37,.34,.29/                                                       .80
            DATA (PT(I,10),I=1,15)/.0,.88,.89,.86,.81,.75,.70,.65,.60,.55,.49,     .85
           1.44,.39,.36,.33/                                                       .85
            DATA (PT(I,11),I=1,15)/.0,.88,.90,.87,.82,.78,.72,.68,.63,.58,.52,     .90
           1.47,.42,.39,.34/                                                       .90
            DATA (PT(I,12),I=1,15)/.0,.87,.90,.88,.84,.80,.75,.70,.65,.61,.56,     .95
           1.5,.45,.41,.38/                                                        .95
            DATA (PT(I,13),I=1,15)/.0,.87,.914,.89,.85,.81,.77,.72,.68,.63,.6,    1.00
           1.54,.48,.45,.40/                                                      1.00
            DATA (PT(I,14),I=1,15)/.0,.86,.913,.9,.87,.83,.78,.74,.7,.66,.62 ,    1.05
           1.56,.51,.47,.44/                                                      1.05
            DATA (PT(I,15),I=1,15)/.0,.85,.915,.901,.88,.84,.8,.76,.72,.68,       1.10
           1 .64,.60,.55,.50,.475/                                                1.10
            DATA (PT(I,16),I=1,15)/.0,.84,.916,.91,.89,.85,.82,.78,.74,.7,.67,    1.15
           1.62,.575,.54,.49/                                                     1.15
            DATA (PT(I,17),I=1,15)/.0,.84,.917,.912,.895,.86,.83,.79,.75,.73,     1.20
           1 .69,.65,.60,.55,.53/                                                 1.20
            DATA (PT(I,18),I=1,15)/.0,.83,.918,.915,.9,.87,.84,.81,.77,.74,.7,    1.25
           1.67,.63,.58,.55/                                                      1.25
            DATA (PT(I,19),I=1,15)/.0,.82,.917,.916,.902,.88,.85,.82,.79,.75,     1.30
           1 .73,.69,.66,.61,.58/                                                 1.30
            DATA (PT(I,20),I=1,15)/.0,.8,.916,.92,.91,.89,.86,.83,.8,.77,.74 ,    1.35
           1.71,.675,.64,.60/                                                     1.35
            DATA (PT(I,21),I=1,15)/.0,.8,.915,.92,.912,.895,.87,.84,.81,.78,      1.40
           1 .75,.72,.70,.67,.63/                                                 1.40
            DATA (PT(I,22),I=1,15)/.0,.8,.915,.92,.914,.9,.88,.85,.82,.8,.77 ,    1.45
           1.74,.71,.68,.65/                                                      1.45
            DATA (PT(I,23),I=1,15)/.0,.8,.915,.92,.916,.905,.885,.86,.83,.81,     1.50
           1 .78,.75,.73,.70,.67/                                                 1.50
            DATA (PT(I,24),I=1,15)/.0,.8,.912,.92,.918,.91,.89,.87,.84,.82,.8,    1.55
           1.77,.74,.72,.69/                                                      1.55
            DATA (PT(I,25),I=1,15)/.0,.8,.91,.92,.92,.911,.90,.88,.85,.83,.8 ,    1.60
           1.78,.755,.73,.70/                                                     1.60
            DATA (PT(I,26),I=1,15)/.0,.8,.91,.92,.92,.914,.9,.885,.86,.84,.81,    1.65
           1.79,.77,.74,.72/                                                      1.65
            DATA (PT(I,27),I=1,15)/.0,.79,.905,.92,.92,.915,.905,.89,.87,.845,    1.70
           1 .82,.80,.78,.755,.735/                                               1.70
            DATA (PT(I,28),I=1,15)/.0,.78,.902,.92,.92,.917,.909,.895,.875,       1.75
           1 .85,.83,.81,.79,.77,.75/                                             1.75
            DATA (PT(I,29),I=1,15)/.0,.77,.9,.92,.92,.917,.91,.90,.88,.86,.84,    1.80
           1.82,.80,.78,.76/                                                      1.80
            DATA (PT(I,30),I=1,15)/.0,.77,.9,.917,.92,.92,.913,.903,.89,.87,      1.85
```

```
     1 .85,.83,.81,.79,.77/                                                    1.85
      DATA (PT(I,31),I=1,15)/.0,.76,.89,.915,.92,.92,.915,.907,.893,.88,       1.90
     1 .86,.84,.82,.80,.78/                                                    1.90
      DATA (PT(I,32),I=1,15)/.0,.75,.88,.914,.92,.92,.916,.909,.895,.88,       1.95
     1 .86,.85,.83,.81,.79/                                                    1.95
      DATA (PT(I,33),I=1,15)/.0,.74,.87,.911,.92,.92,.917,.912,.9,.89,         2.00
     1 .87,.855,.835,.82,.80/                                                  2.00
      DATA (PT(I,34),I=1,15)/.0,.72,.86,.91,.92,.92,.919,.914,.903,.89,        2.05
     1 .87,.86,.845,.825,.81/                                                  2.05
      DATA (PT(I,35),I=1,15)/.0,.7,.86,.905,.919,.92,.92,.915,.908,.9,         2.10
     1 .88,.865,.85,.83,.82/                                                   2.10
      DATA (PT(I,36),I=1,15)/.0,.7,.85,.9,.917,.92,.92,.917,.91,.9,.89 ,       2.15
     1.87,.86,.84,.825/                                                        2.15
      DATA (PT(I,37),I=1,15)/.0,.7,.85,.9,.915,.92,.92,.918,.912,.902,         2.20
     1 .89,.88,.865,.85,.83/                                                   2.20
      DATA (PT(I,38),I=1,15)/.0,.7,.85,.89,.913,.92,.92,.918,.913,.907,        2.25
     1 .895,.885,.87,.855,.84/                                                 2.25
      DATA (PT(I,39),I=1,15)/.0,.7,.84,.88,.911,.92,.92,.918,.915,.908,        2.30
     1 .9 ,.89,.875,.86,.845/                                                  2.30
      DATA (PT(I,40),I=1,15)/.0,.7,.83,.88,.91,.918,.92,.918,.915,.91,         2.35
     1 .902,.89,.88,.865,.85/                                                  2.35
      DATA (PT(I,41),I=1,15)/.0,.7,.82,.87,.907,.916,.918,.918,.916,           2.40
     1 .912,.905,.895,.885,.87,.86/                                            2.40
C
C
      RCP= 40.*PCP +1.
      ICP= IFIX(RCP)
      DCP= RCP -FLOAT(ICP)
      RJ= 20.*PJ -7.
      IJ= IFIX(RJ)
      DIJ= RJ -FLOAT(IJ)
C     POINTS A & B AT GIVEN CP VALUE; POINT A AT LOWER J VALUE THAN POINT B
      PTA= (1.-DCP)*PT(ICP,IJ) +PT(ICP+1,IJ)*DCP
      PTB= (1.-DCP)*PT(ICP,IJ+1) +PT(ICP+1,IJ+1)*DCP
      ETA= PTA +(PTB-PTA)*DIJ
      RETURN
      END
```

```
C
C
      SUBROUTINE ACCEL (VY,H,VG,AMU,VE,WK,GAMMA,AK,N5)
C     INPUT: VERTICAL VELOCITY IN M/S, ALTITUDE IN KM, GROUND SPEED
C     IN M/S, WIND AZIMUTH IN DEG, EQUIVALENT AIRSPEED IN M/S, WIND SCALE
C     FACTOR, AND FLIGHT PATH ANGLE IN DEG; OUTPUT: ACCELERATION CORRECTION
C     FACTOR
      IF (VY.LT.0) GO TO 84
      Y1= H+.1
      Y2= H-.1
      GO TO 85
   84 Y1= H-.1
      Y2= H+.1
   85 VAV= SQRT (VY*VY +VG*VG)
      CALL ALTF (AMU,VE,WK,Y1,PSI1,VT1,VG1,N5)
      IF (N5.EQ.1) GO TO 87
      CALL ALTF (AMU,VE,WK,Y2,PSI2,VT2,VG2,N5)
      IF (N5.EQ.1) GO TO 87
      V1= SQRT (VG1**2 +(VT1*SIN(GAMMA))**2)
      V2= SQRT (VG2**2 +(VT2*SIN(GAMMA))**2)
      DELV= V1-V2
      AK= DELV*VAV/1950.
   87 CONTINUE
      RETURN
      END
```

```
      C
      C
            SUBROUTINE RCLIMB
            COMMON /PAAH/ WOS,CL, BLOD,HLOD, TS,SOAP, POS,RR, POWL,WK, AMU,
           1     XS,HS, POWR,TDOT, H1,RKR, AK,ETA, GAMMA,POW, POWP,POWS, PSID,
           2     R,RLOD, ROC,THETA, VE,VG, VT,PCP, PJ,N4,N5,X,H
            DATA C1/ 9.9397/
      C     C1 EQUALS (PI**4 )/(8.(S.L. DENSITY))
      C
      C     BASIC PARAMETERS
            XR= X -XS
            R= SQRT (XR*XR +H*H)
            THETA= ATAN2(H,XR)
            RLOD= BLOD +HLOD*H
            KODE= 1
            KK= 0.0
         60 VE= 1.27775*SQRT(WOS*COS(GAMMA)/CL)
      C     NOTE: VE IS CORRECTED FOR FLIGHT PATH ANGLE, GAMMA
            CALL ALTF (AMU,VE,WK,H,PSI,VT,VG,N5)
            IF (N5.EQ.1) GO TO 90
            CALL DENSITY(H,SIGMA)
      C
      C     CALCULATION OF POWER - RECEIVED,AVAILABLE AND STORED
      C     740 FACTOR IS 1000 W/KW X .74 EFFICIENCY FACTOR
            ANGLE= 3.1415926 -THETA +GAMMA
         70 POW=((RR/R)**RKR)* 740.*(POS/WOS)*SIN(ANGLE)
            IF (N4.EQ.1) POW= POW* (COS(PSI))**2
            KK= KK+1
            IF (KK.GT.10) GO TO 90
            POWERL= POW/POWL
            IF (POWERL.GT.POWR) GO TO 75
      C     KEEP PROP FOLDED AND STORE ALL INCOMING ENERGY
            ETA= 0.0
            POWP= 0.0
            PJ= 0.0
            PCP= 0.0
      C     DECREMENT L/D TO ACCOUNT FOR DRAG OF FOLDED PROPELLERS
            RLOD= RLOD -1.5
            KODE= -1
            POWS= POW
            GO TO 83
         75 DPOW= POW -POWL
            IF (DPOW)  76,76,77
      C     ALL POWER TO PROP
         76 POWP= POW
            POWS= 0.0
            GO TO 78
      C     POWER TO PROP AND REMAINDER TO STORAGE
         77 POWP= POWL
            POWS= DPOW
         78 IF (KODE) 79,79,82
         79 RLOD= RLOD +1.5
      C
      C     CALCULATION OF NONDIMENSIONAL CHARACTERITICS OF PROPELLER
         82 PJ= 3.14159*VT/TS
            POAP=  POWP*WOS* SOAP
            PCP= C1*POAP/(SIGMA*TS**3)
            CALL PROPCAL (PCP,PJ,ETA)
      C
      C     CALCULATION OF RATE OF CLIMB - THRUST AND DRAG COMPONENTS
      C     TDOT IS RATIO OF ACTUAL, DEGRADED THRUST TO THRUST FROM TABLE LOOK-UP
            ETA= ETA*TDOT
         83 VYT= ETA*POWP
            VYD= VT*COS(GAMMA)/RLOD
            VY= VYT-VYD
            CALL ACCEL(VY,H,VG,AMU,VE,WK,GAMMA,AK)
            IF (N5.GE.5) GO TO 90
            ROC= VY/(1.+AK)
      C
```

```
      C     CALCULATE RESULTING CLIMB ANGLE
            GAMMAC= ASIN(ROC/VT)
            DELG= ABS(GAMMAC-GAMMA)
            IF (DELG.LT..001) GO TO 90
      C
      C     AJUST CLIMB ANGLE AND REPEAT
            GAMMA= GAMMAC
            GO TO 60
      C
      C     CALCULATION FOR GAMMA (FLIGHT PATH ANGLE) HAS CONVERGED
         90 THETA= THETA*57.2957
            GAMMA= GAMMA*57.2957
            PSID= PSI*57.2958
            RETURN
            END
```

SAMPLE CASE: VARIATION OF WIND-PROFILE MAGNITUDE

AIRCRAFT AERO.	PROPELLER	POWER	WINDS	START POINT	VARIABLE SET		CODE
W/S= 144.0 N/M2	TS= 172.0 M/S	P/S= 1.10 KW/M2	WK= 0.00	XS= 40.00 KM	FIRST=	0.000	N1= 3
CL= .90	S/A-P= 2.653	RR= 50.0 KM	MU= 90.0 DEG	HS= 18.00 KM	FINAL=	1.000	N2= 10
L/D= 36.6		MAX P/W= 8.62 KW/KN		HI= 25.00 KM	STEP=	.200	N3= 50
L/D(H)= .418		MIN P/W= .25 X MAX P/W					N4= 1

WK	X	H	R/C	P/W-P	P/W-S	GAMMA	THETA	R	VG	VT	VEC	T	AK	ETA	CP	J	PSI
	KM	KM	M/S	W/N	W/N	DEG	DEG	KM	M/S	M/S	M/S	SEC					DEG
0.00000	0.00	18.00	.78	2.73	0.00	.85	155.8	43.86	51.3	51.3	16.2	0.	.021	.716	.021	.937	0.0
0.00000	.51	18.01	.78	2.73	0.00	.85	155.8	43.86	51.3	51.3	16.2	10.	.021	.716	.021	.937	0.0
0.00000	27.52	19.89	6.18	8.62	1.95	6.01	123.4	23.75	59.0	59.0	16.1	510.	.029	.889	.086	1.078	0.0
0.00000	60.98	22.79	4.16	6.58	0.00	3.19	48.3	30.44	74.6	74.6	16.1	1010.	.045	.907	.105	1.363	0.0
0.00000	83.61	23.41	.67	2.66	0.00	.54	28.3	49.43	78.7	78.7	16.2	1312.	.051	.902	.047	1.438	0.0
0.00000	84.32	23.41	.60	2.60	0.00	.48	27.9	50.05	78.8	78.8	16.2	1321.	.051	.897	.046	1.439	0.0
0.00000	157.90	21.68	-1.62			-1.35			68.8	68.8	16.2	2321.	-.0394				
0.00000	222.49	20.16	-1.44			-1.36			60.9	60.9	16.2	3321.	-.0301				
0.00000	280.07	18.79	-1.30			-1.36			54.6	54.6	16.2	4321.	-.0239				
0.00000	309.28	18.09	-1.24			-1.37			51.7	51.7	16.2	4871.	-.0211				
0.00000	313.19	18.00	-1.23			-1.37			51.3	51.3	16.2	4947.	-.0212				
.20000	0.00	18.00	.59	2.60	0.00	.65	155.8	43.86	50.2	51.3	16.2	0.	.022	.681	.020	.937	11.8
.20000	.50	18.01	.59	2.60	0.00	.65	155.8	43.86	50.2	51.3	16.2	10.	.022	.681	.020	.937	11.8
.20000	26.93	19.78	6.19	8.62	1.51	6.08	124.7	23.98	57.9	58.5	16.1	510.	.029	.890	.085	1.068	8.4
.20000	59.85	22.70	4.37	6.83	0.00	3.37	49.8	29.64	73.6	74.1	16.1	1010.	.045	.904	.107	1.353	6.4
.20000	83.64	23.38	.63	2.63	0.00	.51	28.2	49.44	78.1	78.5	16.2	1330.	.050	.898	.046	1.435	6.3
.20000	84.34	23.38	.57	2.57	0.00	.45	27.8	50.06	78.1	78.6	16.2	1339.	.050	.893	.045	1.435	6.3
.20000	157.30	21.66	-1.62			-1.34			68.2	68.7	16.2	2339.	-.0393				
.20000	221.25	20.14	-1.44			-1.36			60.2	60.8	16.2	3339.	-.0300				
.20000	278.04	18.77	-1.30			-1.37			53.7	54.5	16.2	4339.	-.0250				
.20000	305.76	18.09	-1.24			-1.37			50.6	51.7	16.2	4871.	-.0224				
.20000	309.69	18.00	-1.23			-1.37			50.2	51.3	16.2	4949.	-.0225				

.40000	0.00	18.00	.11	2.21	0.00	.12	155.8	43.86	46.8	51.3	16.2	0.	.026	.579	.017	.937	24.2
.40000	.47	18.00	.11	2.21	0.00	.12	155.8	43.86	46.8	51.3	16.2	10.	.026	.579	.017	.937	24.2
.40000	24.96	19.37	6.23	8.62	.01	6.31	128.9	24.81	53.7	56.6	16.1	510.	.031	.891	.079	1.034	18.5
.40000	56.01	22.36	5.13	7.75	0.00	4.07	55.5	27.06	70.2	72.1	16.1	1010.	.042	.892	.115	1.317	13.1
.40000	83.02	23.26	.60	2.59	0.00	.45	28.4	48.84	76.0	77.8	16.2	1384.	.046	.891	.045	1.422	12.5
.40000	84.39	23.27	.47	2.47	0.00	.39	27.7	50.05	76.0	77.9	16.2	1402.	.046	.882	.043	1.423	12.5
.40000	155.32	21.56	-1.61			-1.34			66.1	68.1	16.2	2402.	-.0386				
.40000	217.19	20.05	-1.43			-1.35			58.1	60.4	16.2	3402.	-.0300				
.40000	271.40	18.69	-1.30			-1.36			50.6	54.2	16.2	4402.	-.0281				
.40000	293.92	18.10	-1.24			-1.38			47.3	51.7	16.2	4862.	-.0261				
.40000	297.87	18.00	-1.24			-1.38			46.8	51.3	16.2	4946.	-.0262				
.60000	0.00	18.00	-1.29	0.00	1.55	-1.39	155.8	43.86	40.4	51.3	16.2	0.	-.032	0.000	0.000	0.000	38.0
.60000	.40	17.99	-1.24	0.00	1.55	-1.39	155.8	43.86	40.4	51.3	16.2	10.	-.032	0.000	0.000	0.000	38.0
.60000	20.00	18.11	2.81	4.60	0.00	3.11	138.5	27.27	41.0	51.6	16.2	510.	.032	.883	.035	.942	37.4
.60000	44.80	20.84	6.08	8.62	2.23	5.52	78.5	21.20	58.7	63.7	16.1	1010.	.034	.891	.100	1.163	22.7
.60000	77.76	22.69	1.00	2.96	0.00	.77	31.5	43.45	70.1	74.3	16.2	1510.	.045	.900	.047	1.357	19.3
.60000	84.66	22.75	.30	2.27	0.00	.26	27.0	50.06	70.6	74.7	16.2	1617.	.045	.852	.036	1.365	19.2
.60000	150.21	21.10	-1.55			-1.35			60.9	65.7	16.2	2617.	-.0356				
.60000	206.85	19.64	-1.40			-1.37			52.4	58.4	16.2	3617.	-.0370				
.60000	254.42	18.31	-1.27			-1.38			42.9	52.6	16.2	4617.	-.0328				
.60000	262.37	18.07	-1.25			-1.38			40.9	51.6	16.2	4807.	-.0323				
.60000	264.57	18.00	-1.24			-1.38			40.4	51.3	16.2	4861.	-.0325				
.80000	0.00	18.00	-1.30	0.00	.82	-1.40	155.8	43.86	29.3	51.3	16.2	0.	-.041	0.000	0.000	0.000	55.1
.80000	.29	17.99	-1.25	0.00	.82	-1.40	155.8	43.86	29.3	51.3	16.2	10.	-.041	0.000	0.000	0.000	55.1
.80000	12.50	17.37	-1.20	0.00	.68	-1.40	147.9	32.69	19.1	48.8	16.2	510.	-.041	0.000	0.000	0.000	66.9

WIND SPEED TOO LARGE AT 16.9 KM.
WIND SPEED TOO LARGE AT 16.9 KM.
WIND SPEED TOO LARGE AT 16.9 KM.
WIND SPEED TOO LARGE AT 16.9 KM.
WIND SPEED TOO LARGE AT 16.9 KM.
WIND SPEED TOO LARGE AT 16.9 KM.
WIND SPEED TOO LARGE AT 16.8 KM.
WIND SPEED TOO LARGE AT 16.8 KM.
WIND SPEED TOO LARGE AT 16.8 KM.
WIND SPEED TOO LARGE AT 16.9 KM.

WIND SPEED TOO LARGE AT 18.0 KM.

WK	XC	HC	TC	E/W-S	E/W-T	XT	TT
	KM	KM	HR	KJ/N	KJ/N	KM	HR
0.000	84.32	23.41	.367	1.452	9.803	313.19	1.37
.200	84.34	23.38	.372	1.377	9.730	309.69	1.37
.400	84.39	23.27	.389	1.154	9.508	297.87	1.37
.600	84.66	22.75	.449	1.187	9.203	264.57	1.35
.800	-I	-I	-I	-I	-I	17.38	1.35
1.000	-I	-I	-I	-I	-I	0.00	1.35

APPENDIX B

GLIDE-TIME PARAMETER

An expression for the time required to glide between two altitudes is given as equation (29) of reference 8. The development of that equation assumes that the aerodynamic characteristics (C_L and C_D) remain constant and that acceleration effects (eq. (4)) are negligible. That endurance equation for gliding flight is written as

$$t_g = \frac{L}{D}\sqrt{\frac{C_L}{W/S(\cos\gamma)^{-3/2}}}\int_{h_1}^{h_2}\sqrt{\frac{\rho}{2}}\,dh \tag{B1}$$

where h_1 and h_2 are the final and initial altitudes, respectively. Equation (B1) can be simplified in two ways. First, since γ is a small angle, the cosine term can be approximated as 1.0. Second, if the range of altitudes lies between about 16 and 26 km (52 000 and 85 000 ft) equation (11) can be used to approximate density variation by choosing $a = 0.105$ and $b = 0.0013$ throughout that altitude range.

Substituting equation (11) into equation (B1) yields the integrable expression

$$t_g = \frac{L}{D}\sqrt{\frac{C_L\rho_o}{2W/S}}\,e^{(a^2/8b)}\int_{h_1}^{h_2} e^{-(b/2)[h+(a/2b)]^2}\,dh$$

$$= \frac{L}{D}\frac{1}{V_e}\,e^{(a^2/8b)}\sqrt{\frac{2}{b}}\int_{z_1}^{z_2} e^{-z^2}\,dz \tag{B2}$$

$$t_g = \frac{L}{D}\frac{1}{V_e}\,e^{(a^2/8b)}\sqrt{\frac{\pi}{2b}}\,[\mathrm{erf}(z_2) - \mathrm{erf}(z_1)] \tag{B3}$$

where

$$z = \sqrt{b/2}\,[h + (a/2b)]$$

and erf is the error function, as described in reference 22. Equation (B3) may be rearranged to produce an expression independent of vehicle aerodynamic characteristics. After substituting the values of a and b, the equation becomes

$$t_g V_e \frac{D}{L} = 27.873[\mathrm{erf}(z_2) - \mathrm{erf}(z_1)] \tag{B4}$$

where

$$z = 1.0296 + 0.025495h$$

Here h is expressed in km, V_e in m/s, and t_g in hours. As in equation (B1), h_1 is the final altitude because of the negative rate of climb.

Glide time can be determined for a specific vehicle where L/D and V_e are given. For the class of vehicles considered in this study, the values of $L/(DV_e)$ lie approximately between 10 and 0.1. The largest value yields the longest glide time and is produced by low W/S and high L/D.

REFERENCES

1. Kuhner, M. B.; and McDowell, J. R.: User Definition and Mission Requirements for Unmanned Airborne Platforms (Revised). NASA CR-156861, 1979.

2. Youngblood, James W.; Darnell, Wayne L.; Johnson, Robert W.; and Harriss, Robert C.: Airborne Spacecraft - A Remotely Powered, High-Altitude RPV for Environmental Applications. NASA paper presented at Electronics and Aerospace Systems Conference (Arlington, Virginia), Oct. 9-11, 1979.

3. Sinko, James W.: High Altitude Powered Platform: A Microwave Powered Airship. A Collection of Technical Papers - AIAA Lighter-Than-Air Systems Technology Conference, July 1979, pp. 212-218. (Available as AIAA Paper 79-1606.)

4. U.S. Standard Atmosphere, 1962. NASA, U.S. Air Force, and U.S. Weather Bur., Dec. 1962.

5. Kaufman, John W., ed.: Terrestrial Environment (Climatic) Criteria Guidelines for Use in Aerospace Vehicle Development, 1977 Revision. NASA TM-78118, 1977.

6. Irving, F. G.; and Morgan, D.: The Feasibility of an Aircraft Propelled by Solar Energy. AIAA Paper No. 74-1042, Sept. 1974.

7. Boucher, R. J.: Project Sunrise. AIAA Paper 79-1264, June 1979.

8. Phillips, William H.: Some Design Considerations for Solar-Powered Aircraft. NASA TP-1675, 1980.

9. Heyson, Harry H.: Initial Feasibility Study of a Microwave-Powered Sailplane as a High-Altitude Observation Platform. NASA TM-78809, 1978.

10. Turriziani, R. Victor: Sensitivity Study for a Remotely Piloted Microwave-Powered Sailplane Used as a High-Altitude Observation Platform. NASA CR-159089, 1979.

11. Fordyce, Samuel W.; and Brown, William C.: Applications of Free-Space Microwave Power Transmission. Astronaut. & Aeronaut., vol. 17, no. 9, Sept. 1979, pp. 54-59, 61.

12. Brown, William C.: A Profile of Power Transmission by Microwaves. Astronaut. & Aeronaut., vol. 17, no. 5, May 1979, pp. 50-55.

13. Hansen, R. C., ed.: Microwave Scanning Antennas. Academic Press.
    Volume I - Apertures, 1964.
    Volume II - Array Theory and Practice, 1966.

14. Dickinson, Richard M.: Beamed Microwave Power Transmitting and Receiving Subsystems Radiation Characteristics. Publ. 80-11, Jet Propul. Lab., California Inst. Technol., 1980. (Available as NASA CR-163362.)

15. Generalized Method of Propeller Performance Estimation. PDB 6101A, Hamilton Standard, United Aircraft Corp., June 1963.

16. Strganac, Thomas W.: Wind Study for High Altitude Platform Design. NASA RP-1044, 1979.

17. Hoerner, Sighard F.: Fluid-Dynamic Drag. Hoerner Fluid Dynamics (Brick Town, N. J.), c.1965.

18. Taylor, John W. R., ed.: Jane's All the World's Aircraft, 1980-1981, Jane's Pub., Inc., c.1980.

19. Cochrane, James A.; Henry, Robert M.; and Weaver, William L.: Revised Upper-Air Wind Data for Wallops Island Based on Serially Completed Data for the Years 1956 to 1964. NASA TN D-4570, 1968.

20. Tolefson, H. B.: An Investigation of Vertical-Wing-Shear Intensities From Balloon Soundings for Application to Airplane- and Missile-Response Problems. NASA TN 3732, 1956.

21. Coleman, Thomas L.; and Steiner, Roy: Atmospheric Turbulence Measurements Obtained From Airplane Operations at Altitudes Between 20,000 and 75,000 Feet for Several Areas in the Northern Hemisphere. NASA TN D-548, 1960.

22. Kreyszig, Erwin: Advanced Engineering Mathematics, Second Ed. John Wiley & Sons, Inc., c.1967.

TABLE I.- DESCRIPTION OF BASELINE CONFIGURATION OF

HIGH-ALTITUDE AIRPLANE PLATFORM

Airplane aerodynamics:	
Aspect ratio, A	30
Lift coefficient, C_L	0.9
Lift-drag ratio	
Altitude function, L/D	36.6 + 0.418h
Folded propeller decrement, L/D	1.5
Oswald efficiency factor, e	0.96
Wing loading, W/S, Pa (lbf/ft^2)	144 (2.92)
Propeller(s):	
Activity factor	80
Design lift coefficient	0.3
Ratio of wing area to propeller-disk area, S/A_p	2.653
Tip speed, V_{tip}, m/s (knots)	172 (334)
Motor(s):	
Maximum specific power (available), $(P/W)_{max}$, W/N (hp/lbf)	8.62 (0.0514)
Minimum specific power (required), $(P/W)_{min}$, W/N (hp/lbf)	2.16 (0.0129)
Power transmission:	
Power intensity at reference range, P/S, kW/m^2 (W/ft^2)	1.10 (100)
Reference range, R, km (n.mi.)	50 (27)
Range-power attenuation factor	R/r
Transmission-initiation point	
Altitude, h_s, km (ft)	18 (59 000)
Horizontal range, x_s, km (n.mi.)	40 (22)
Transmission-termination slant range, km (n.mi.)	50 (27)

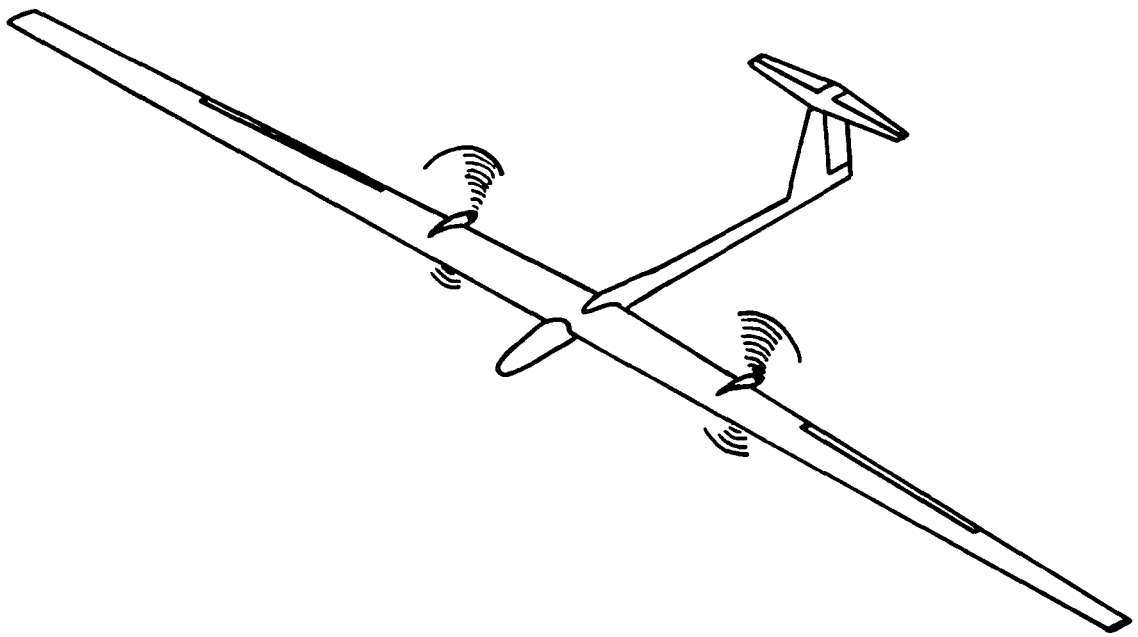

(a) Configuration of reference 9.

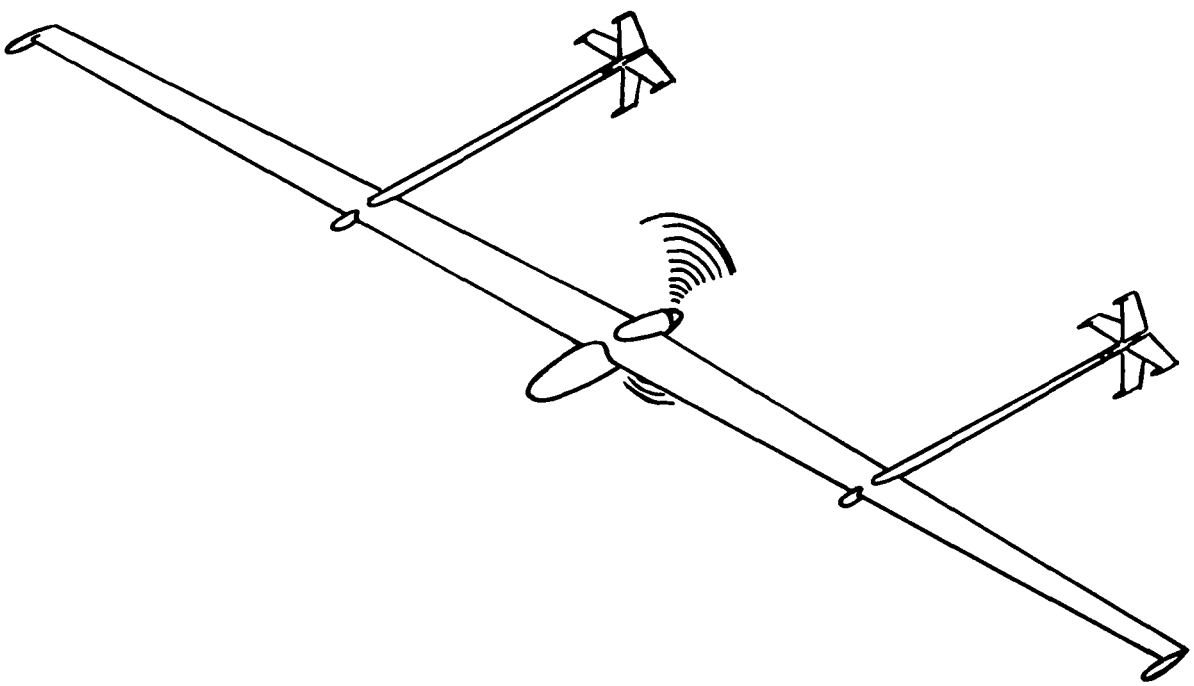

(b) Alternate configuration.

Figure 1.- Representative HAAP designs.

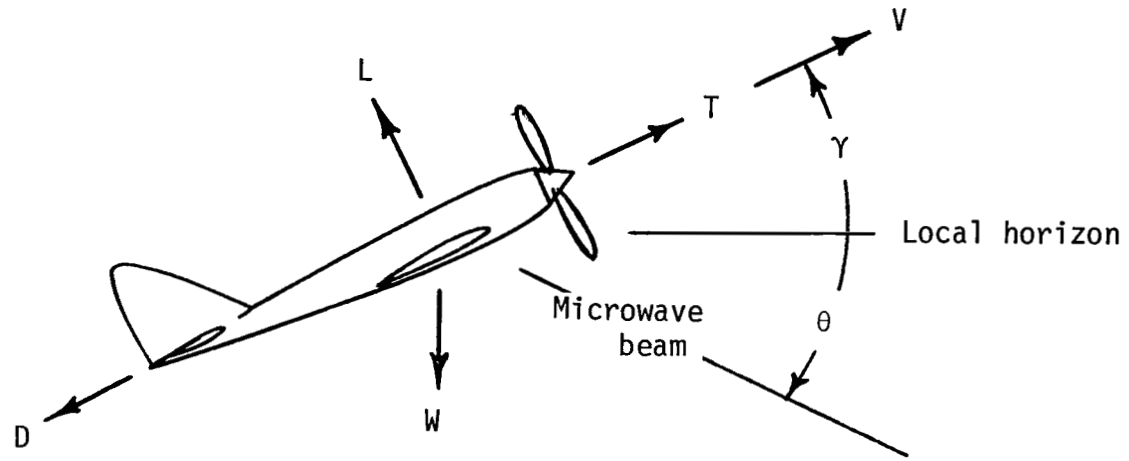

(a) Forces and angles in vertical plane.

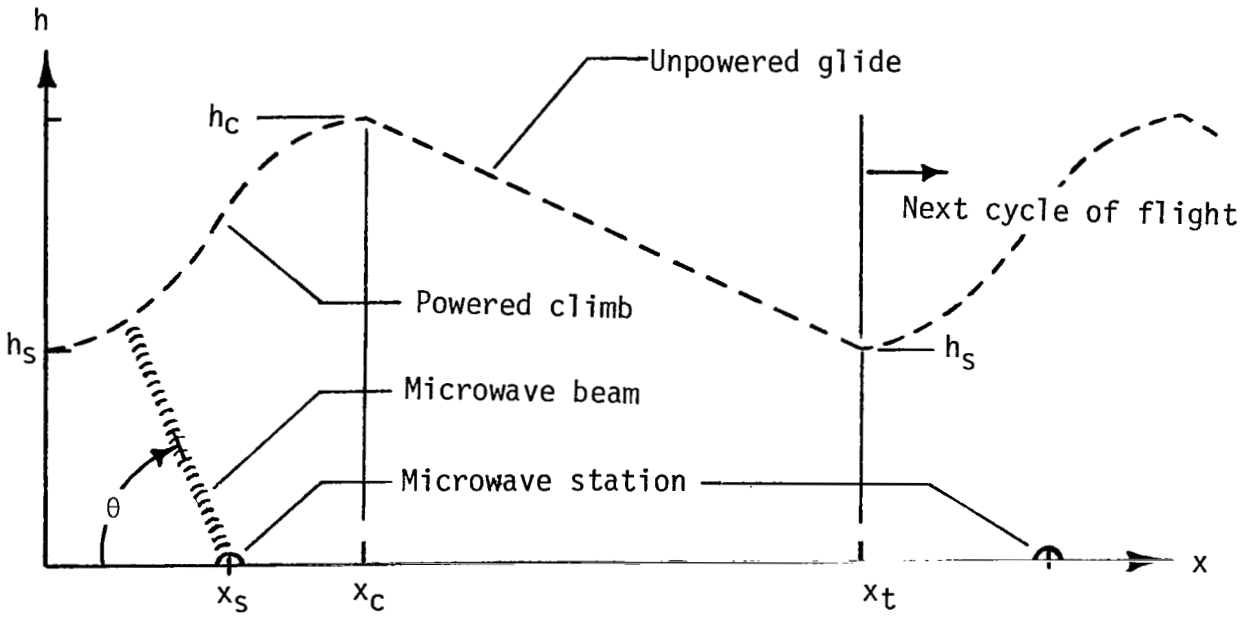

(b) Flight-path profile.

Figure 2.- Conventions used to define senses of displacements, forces, angles, and velocities.

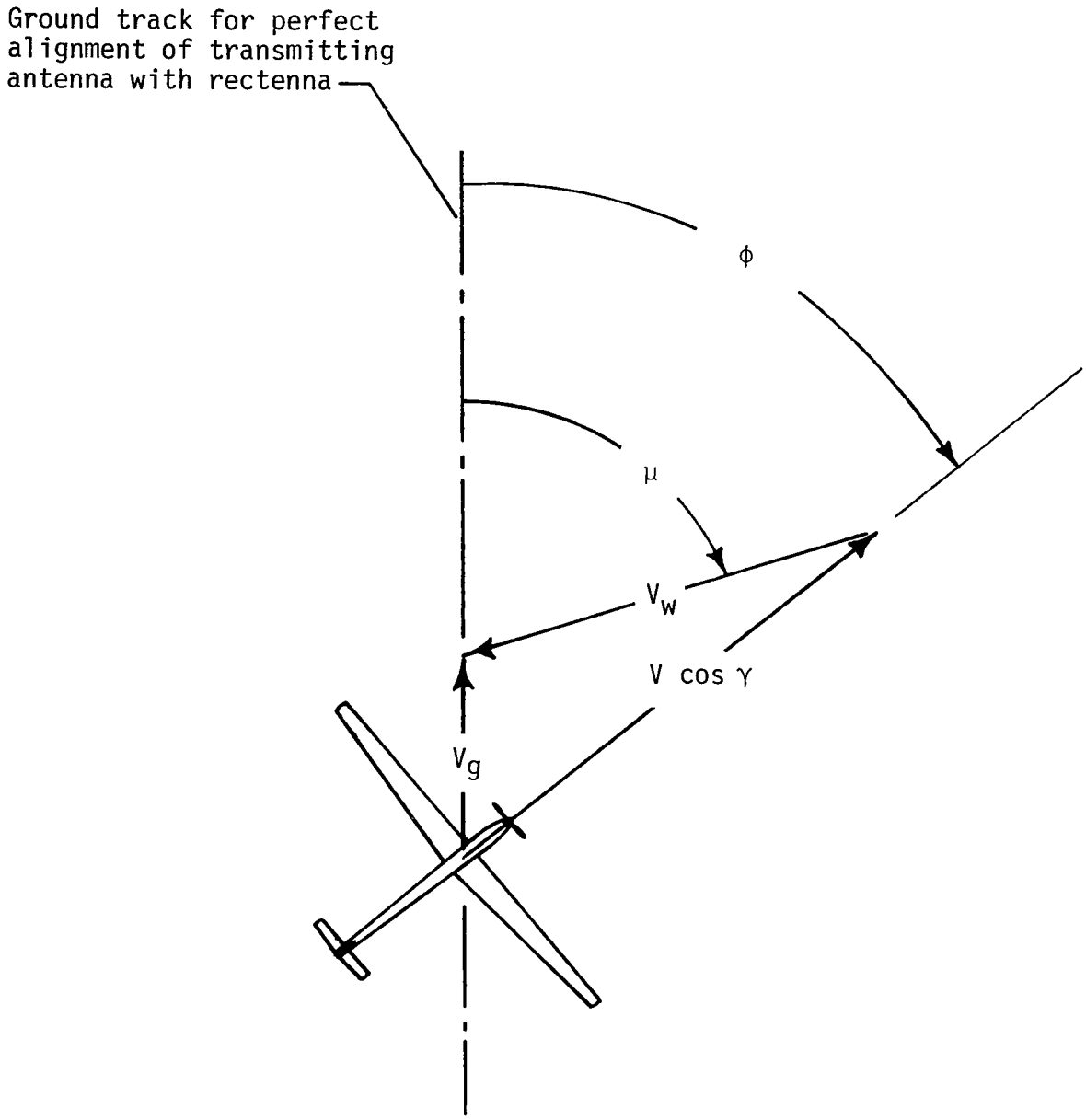

(c) Velocities and angles in horizontal plane.

Figure 2.- Concluded.

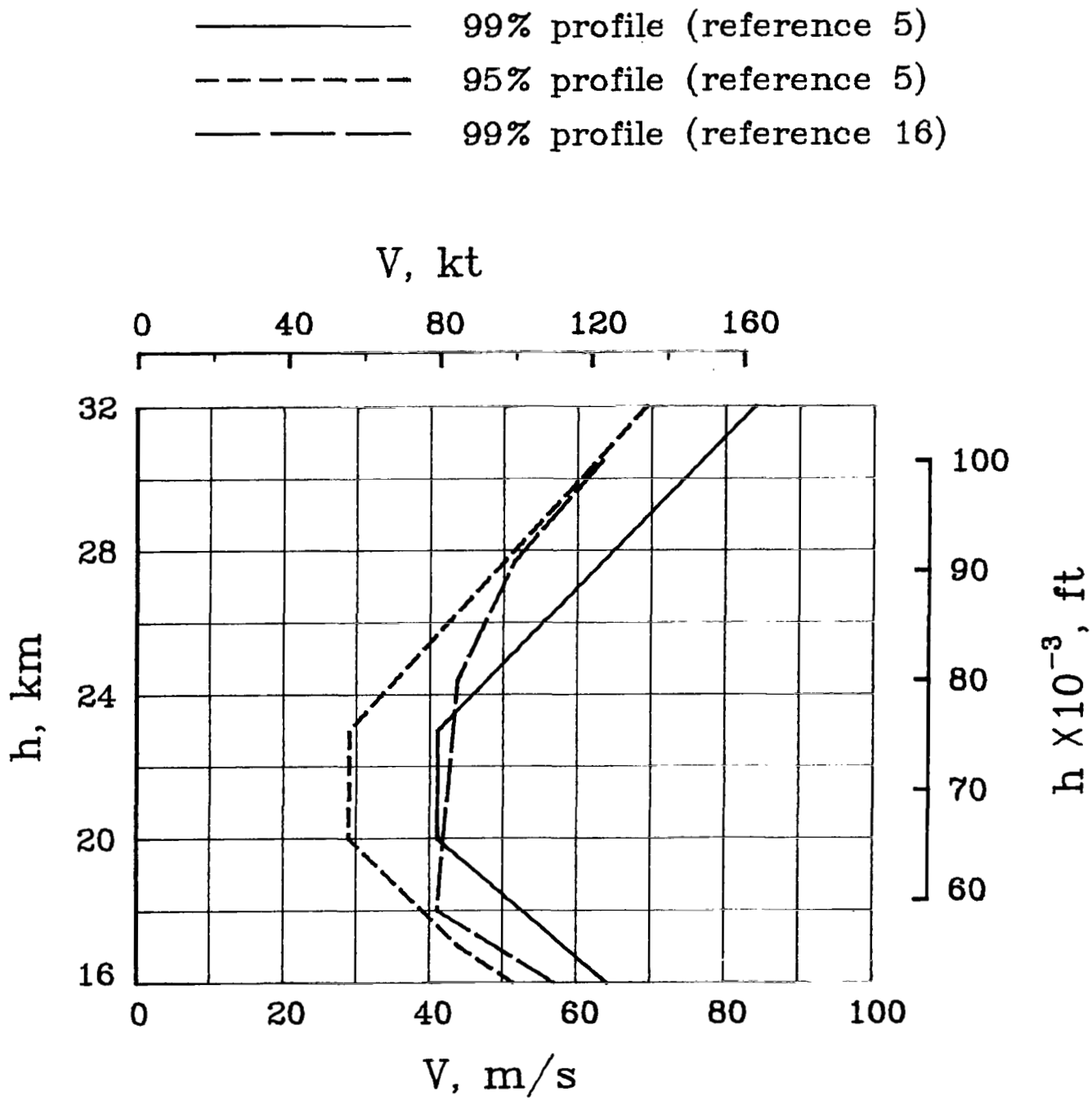

Figure 3.- Statistical wind-profile data.

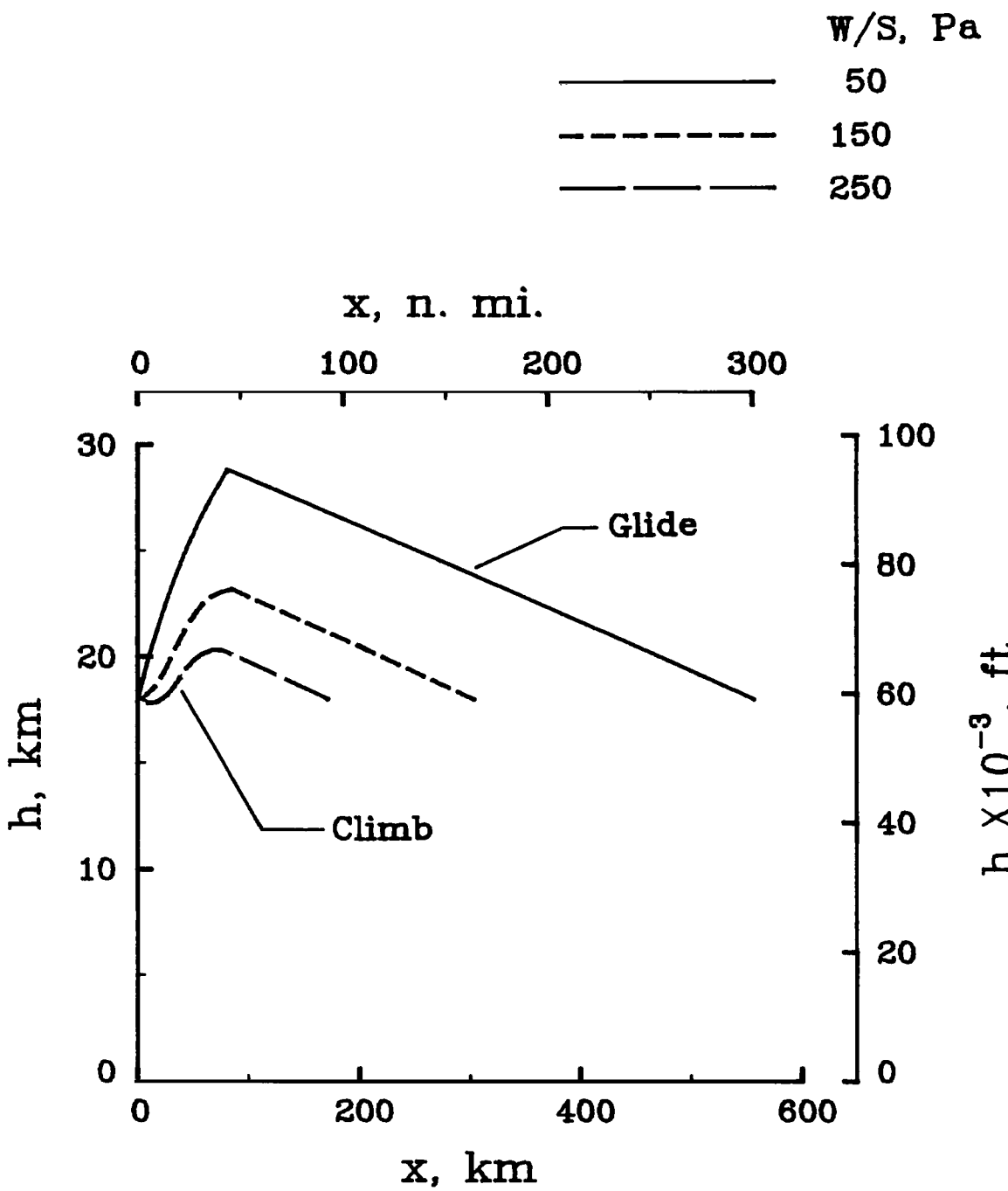

Figure 4.- Flight profiles for baseline configuration with three values of wing loading.

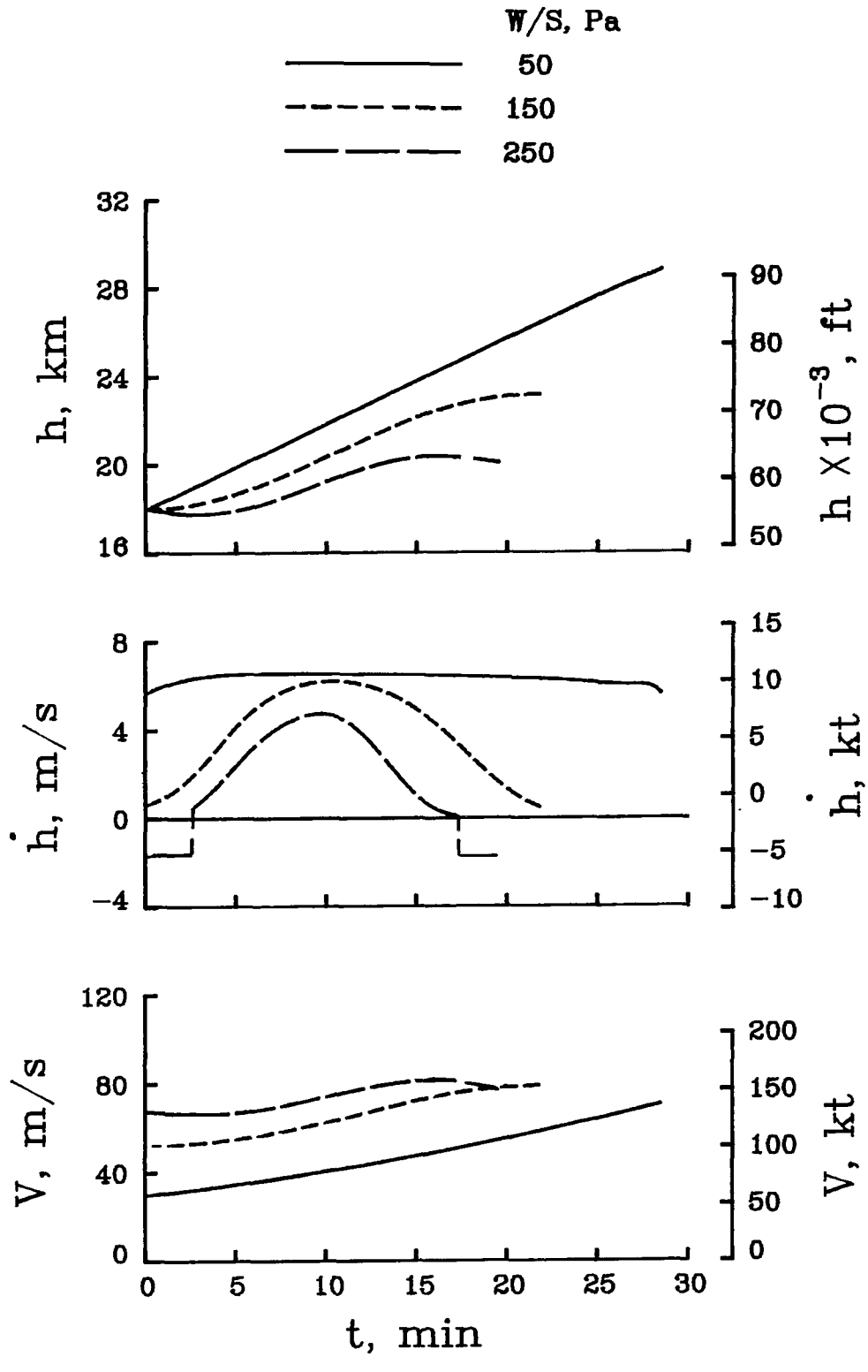

(a) Trajectory.

Figure 5.- History of flight parameters for baseline configuration with three values of wing loading.

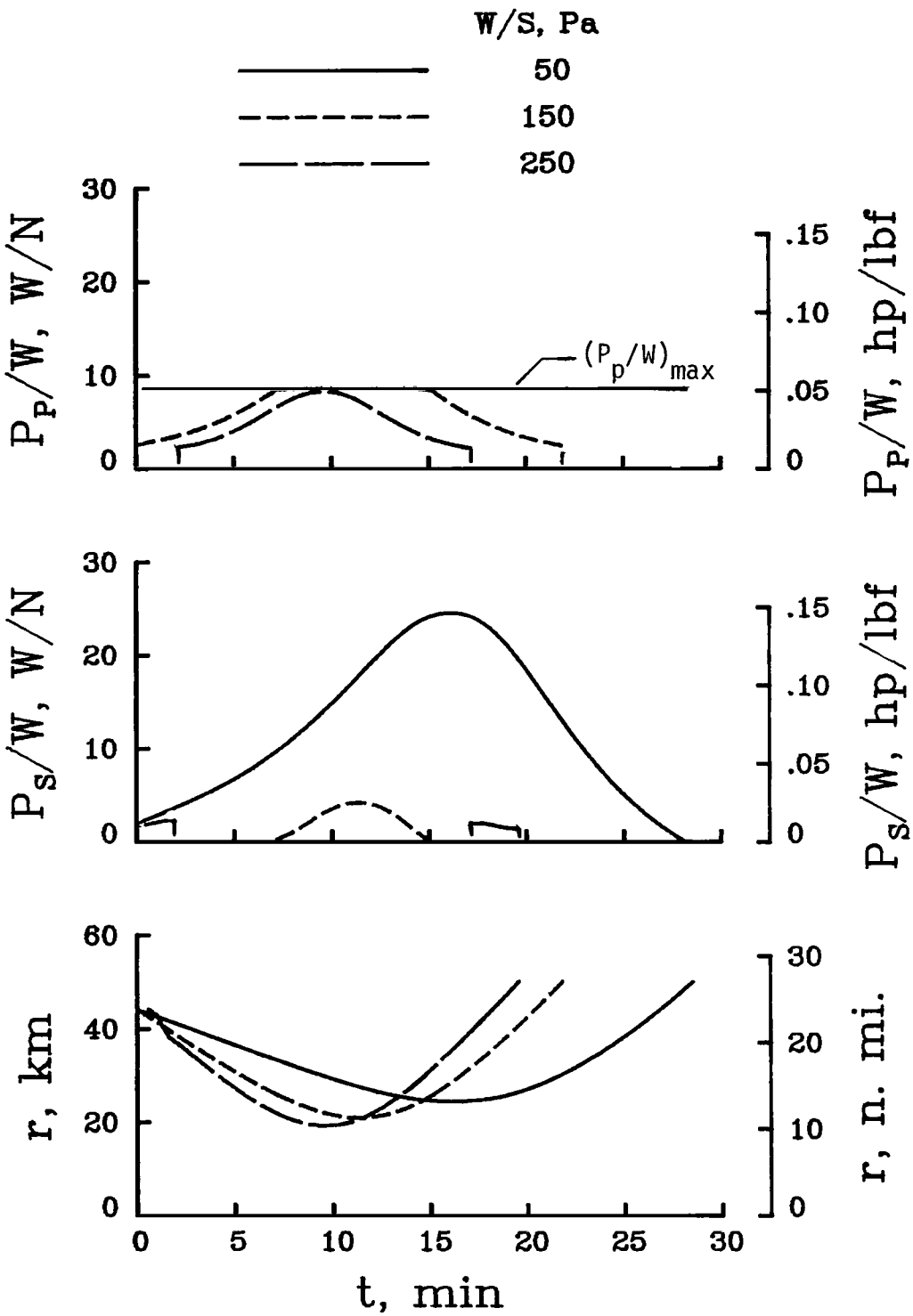

(b) Power and range parameters.

Figure 5.- Continued.

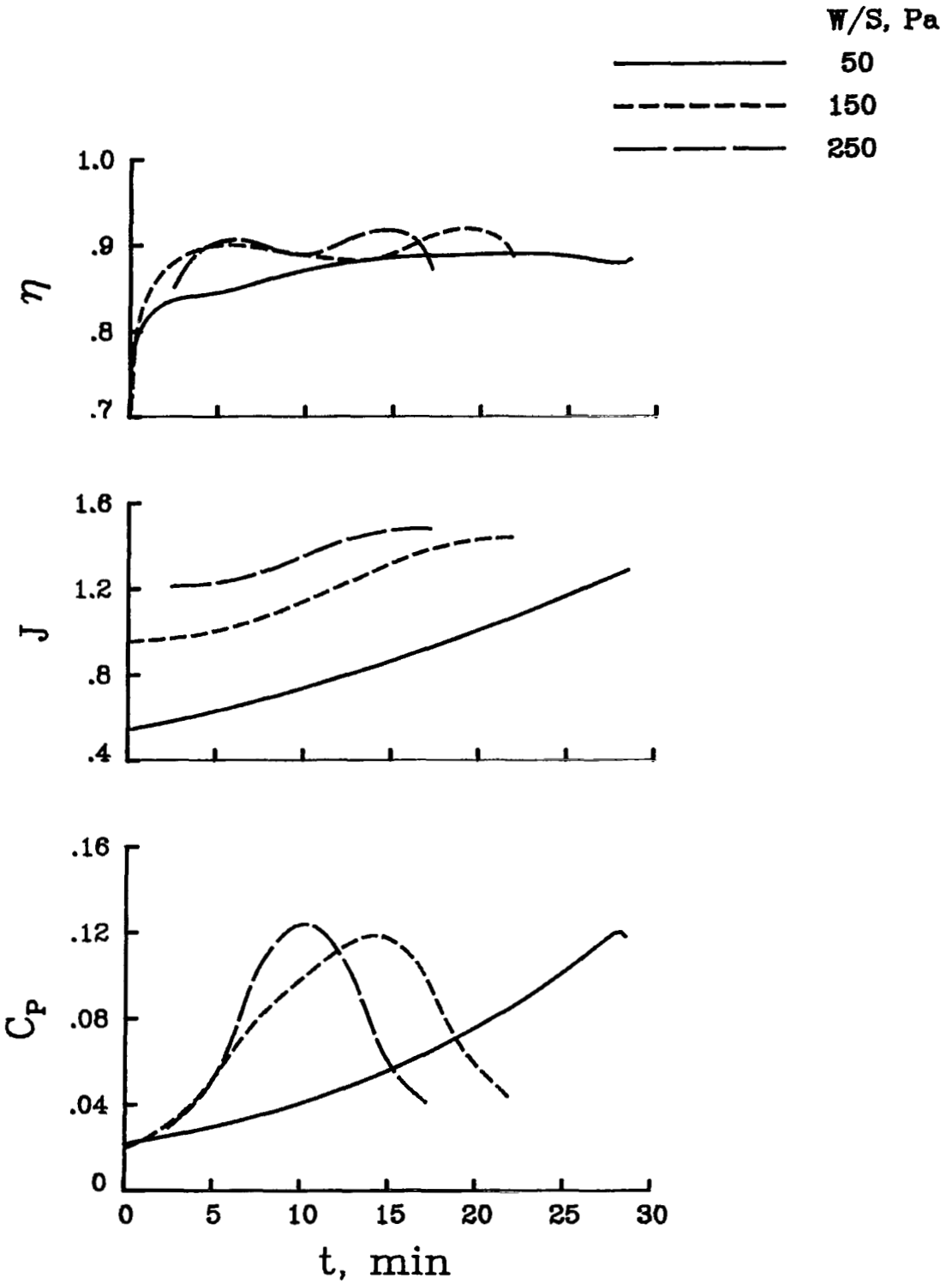

(c) Propeller parameters.

Figure 5.- Concluded.

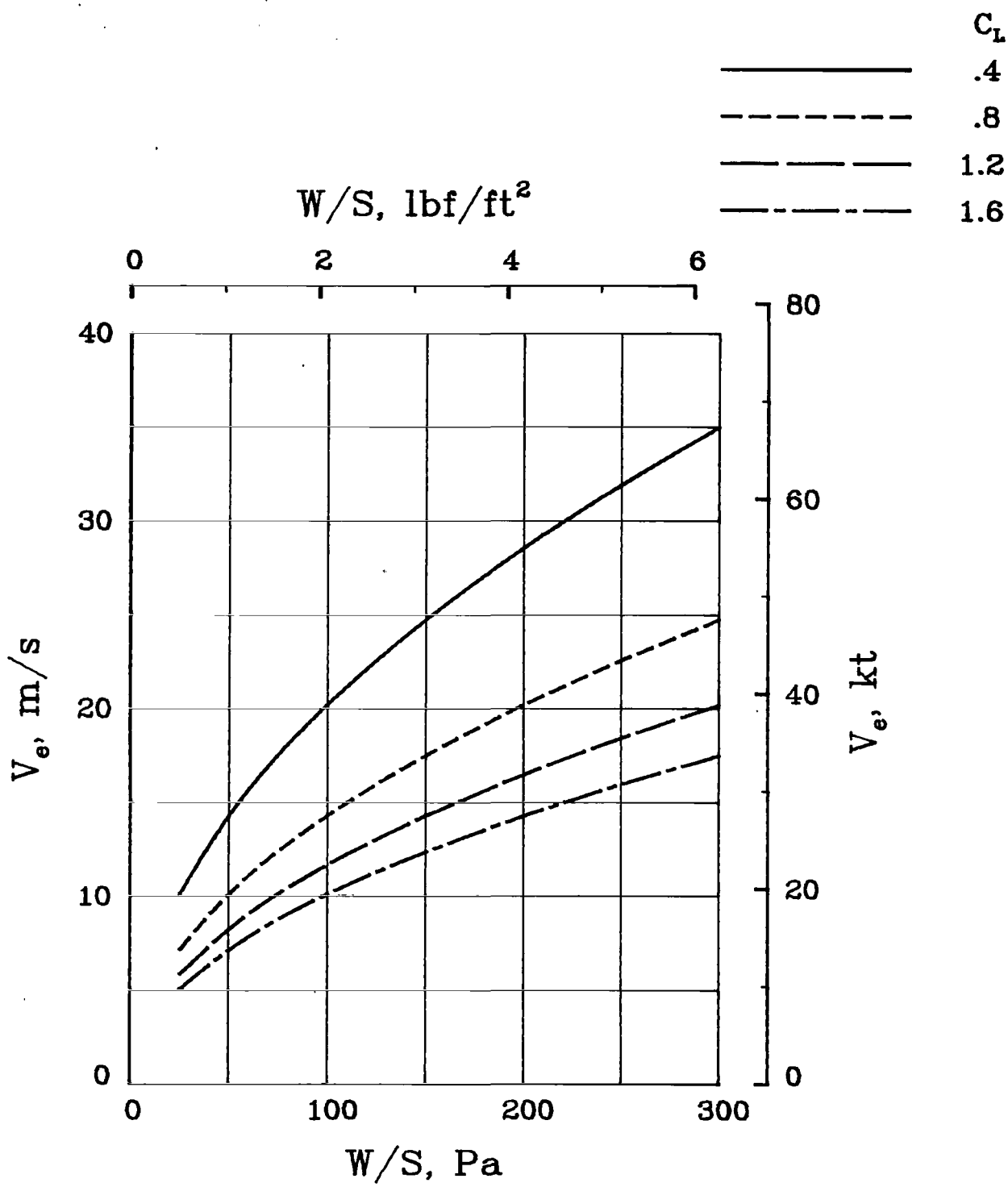

Figure 6.- Variation of equivalent airspeed with wing loading and lift coefficient.

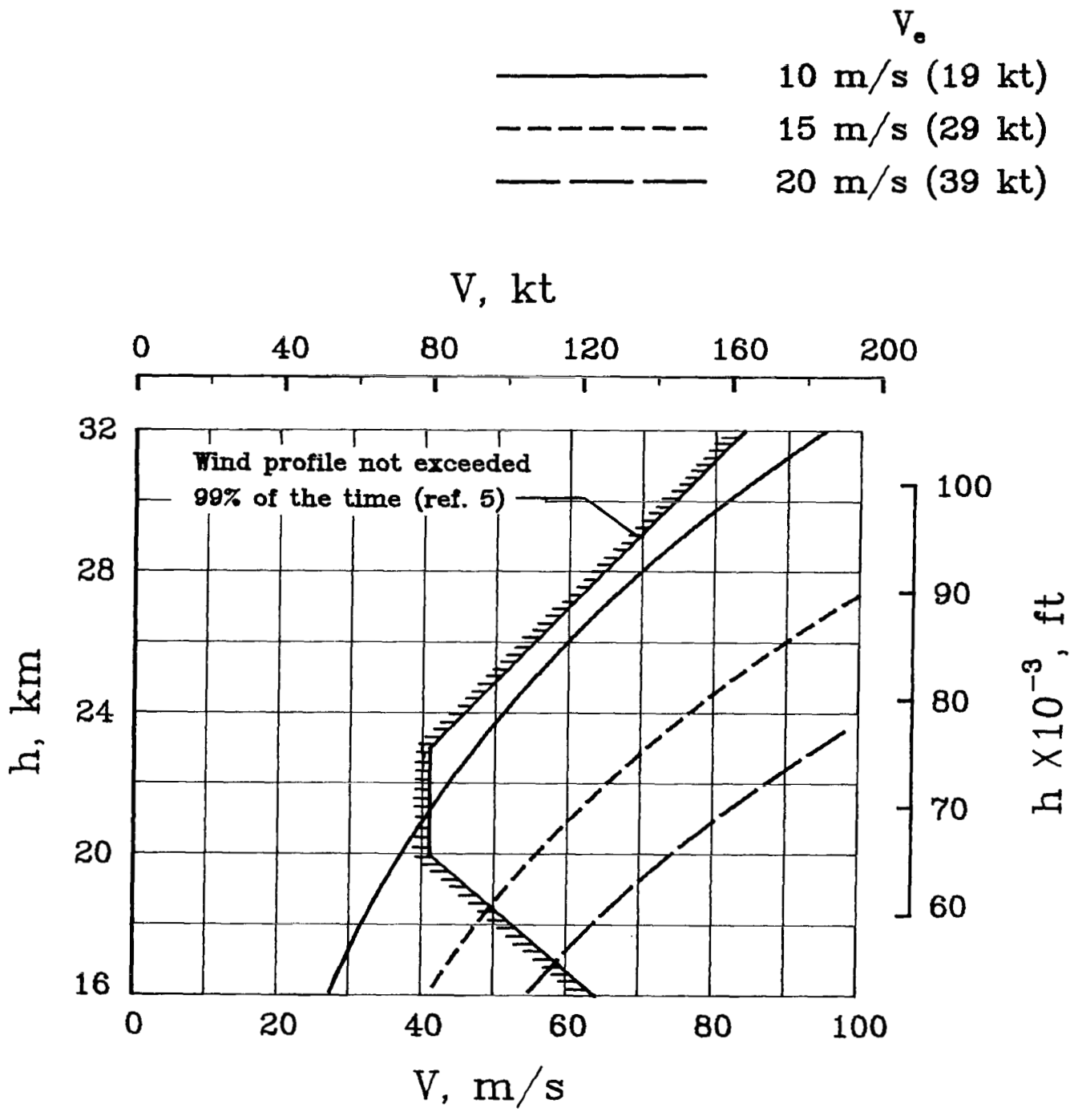

(a) True airspeed profile.

Figure 7.- Comparison of limiting wind profile and vehicle airspeed.

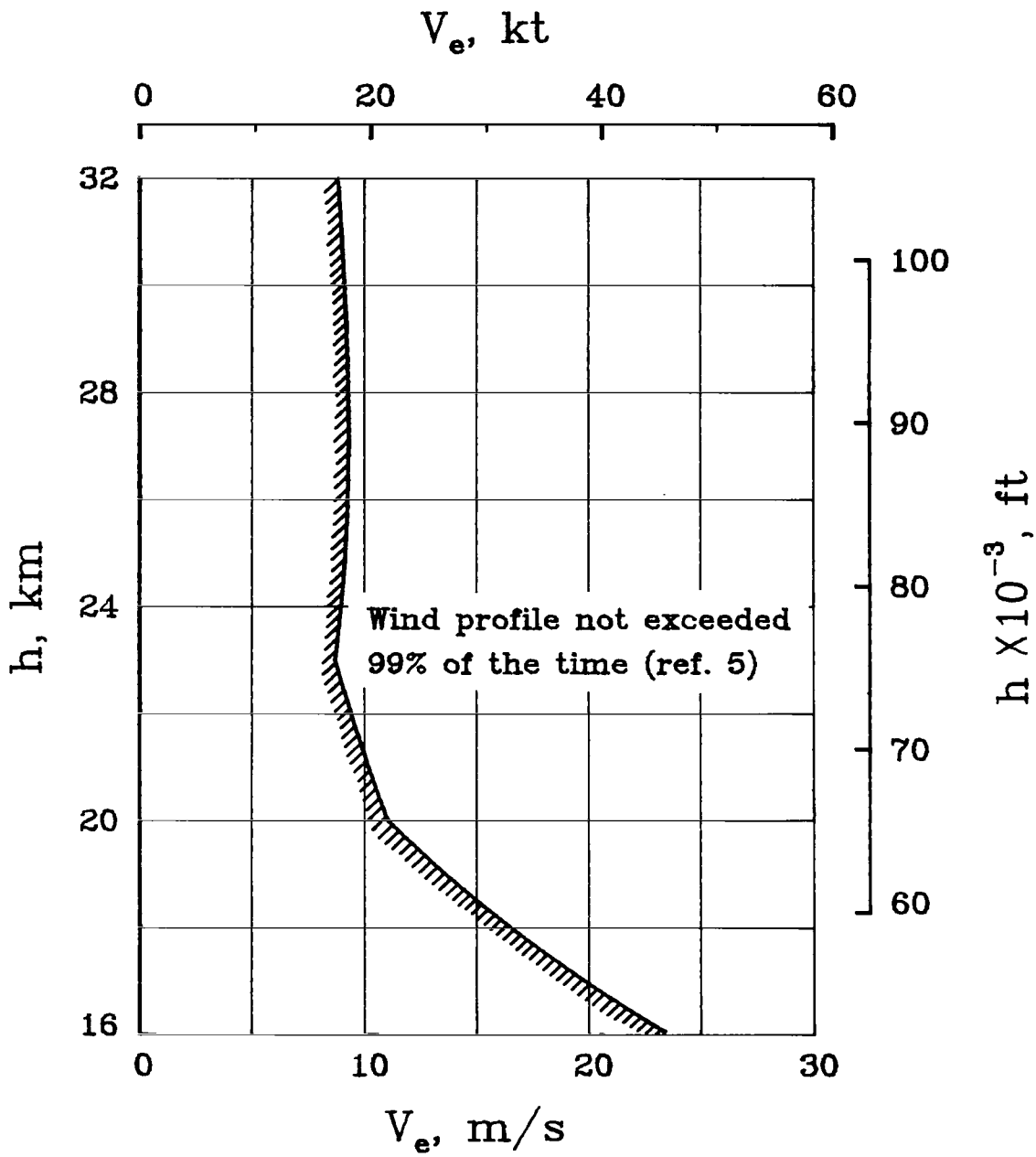

(b) Equivalent airspeed profile.

Figure 7.- Concluded.

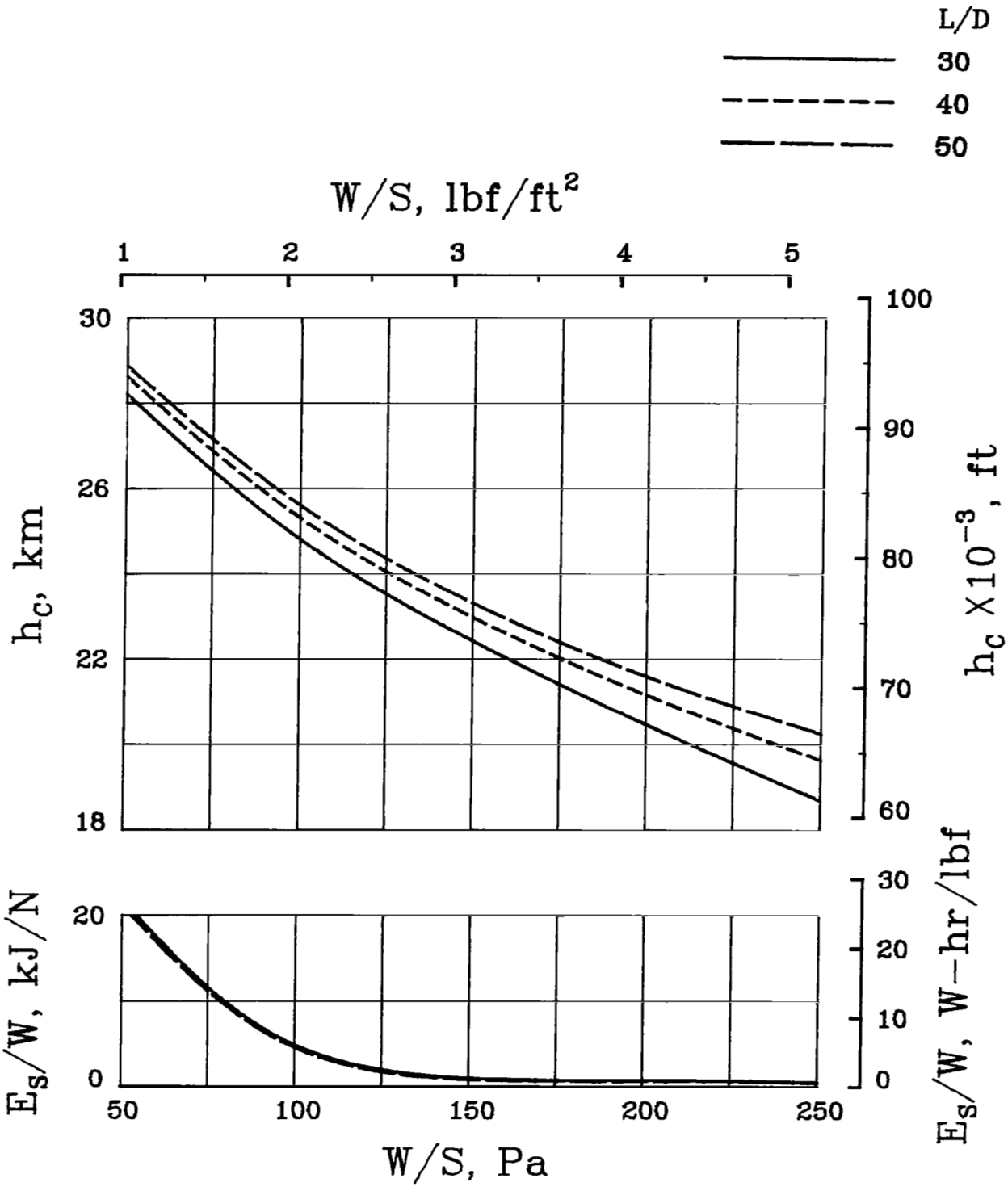

Figure 8.- Effect of wing loading and lift-drag ratio on performance of baseline configuration.

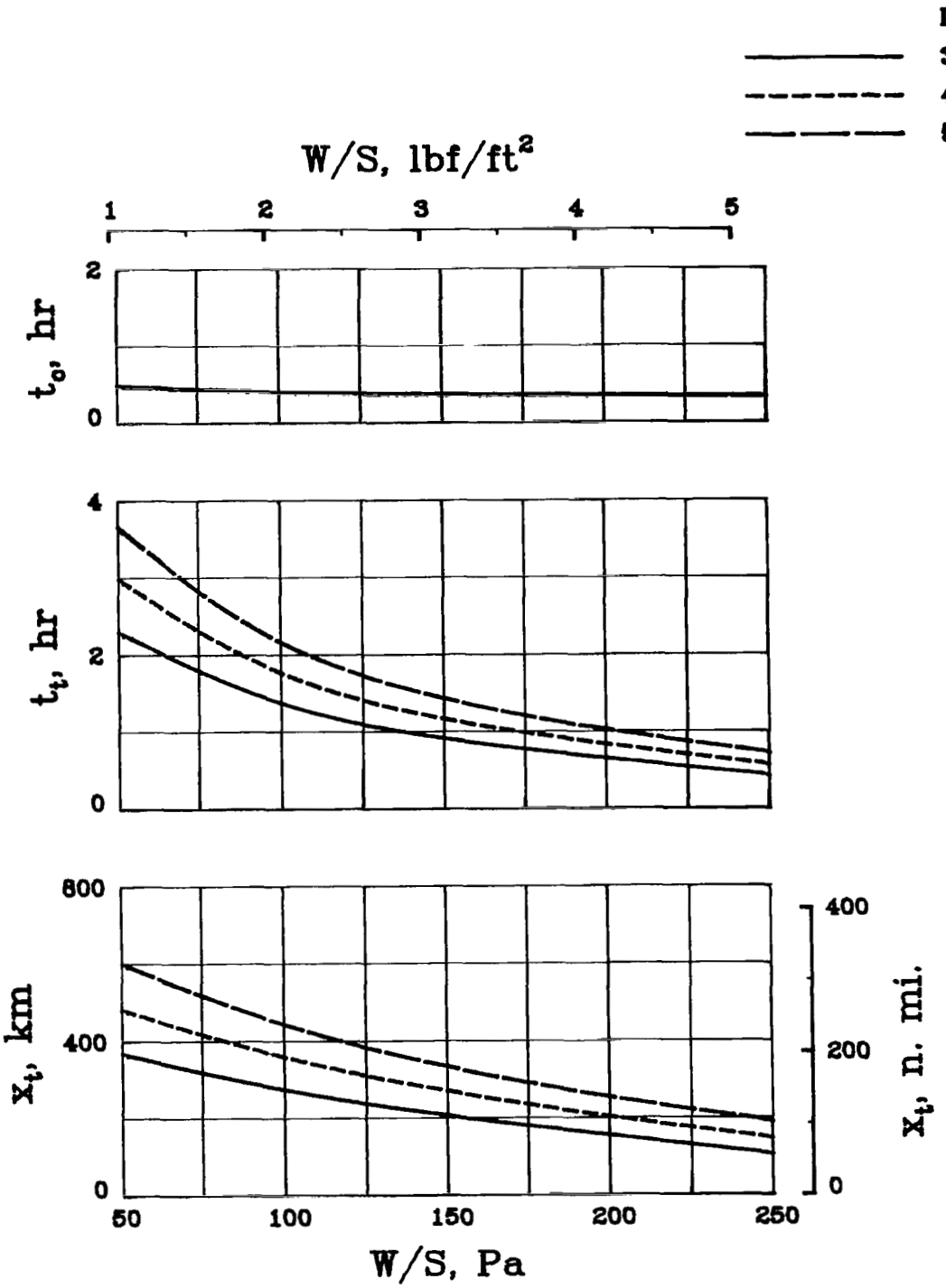

Figure 8.- Concluded.

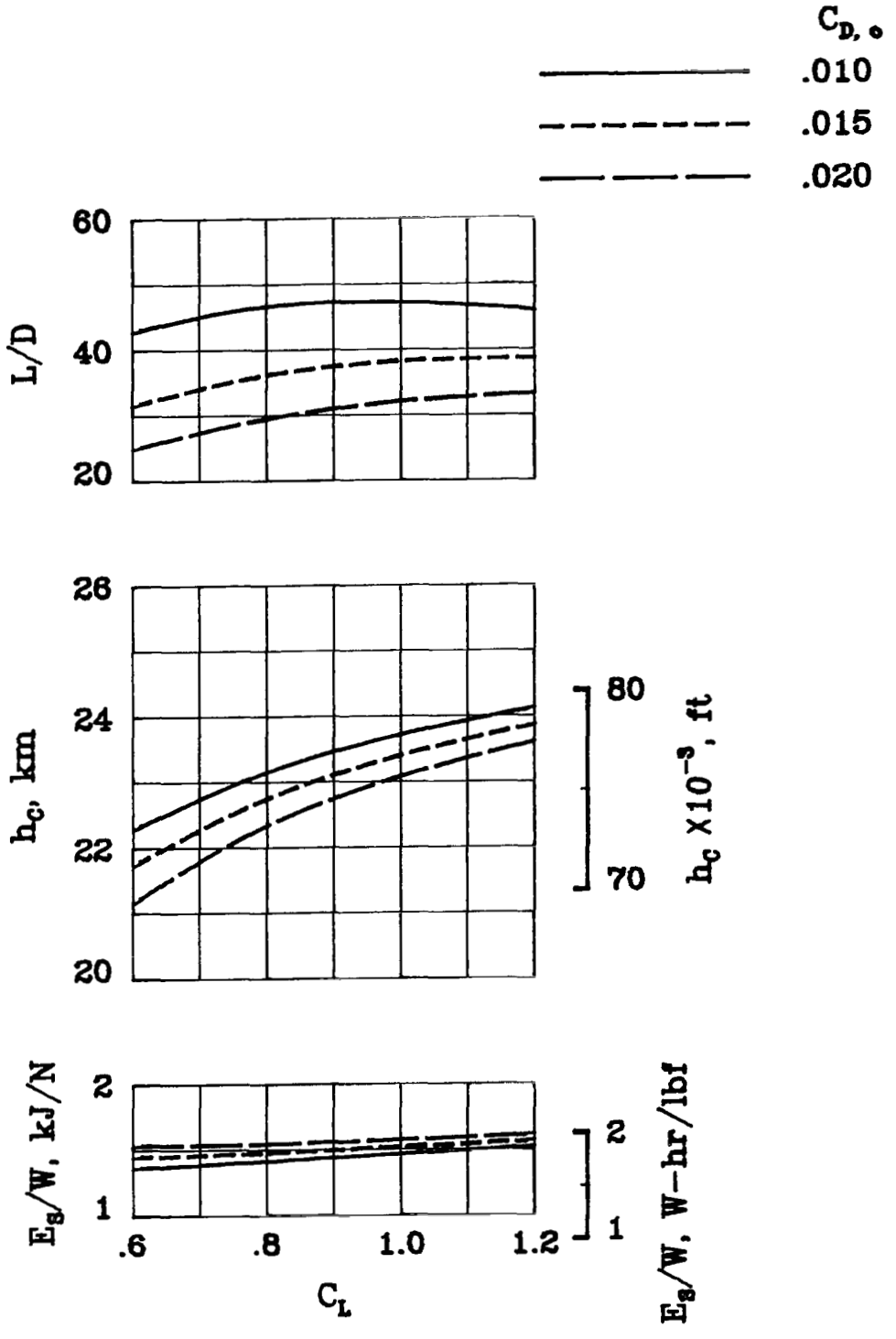

Figure 9.- Effect of airplane lift and drag coefficients on performance.

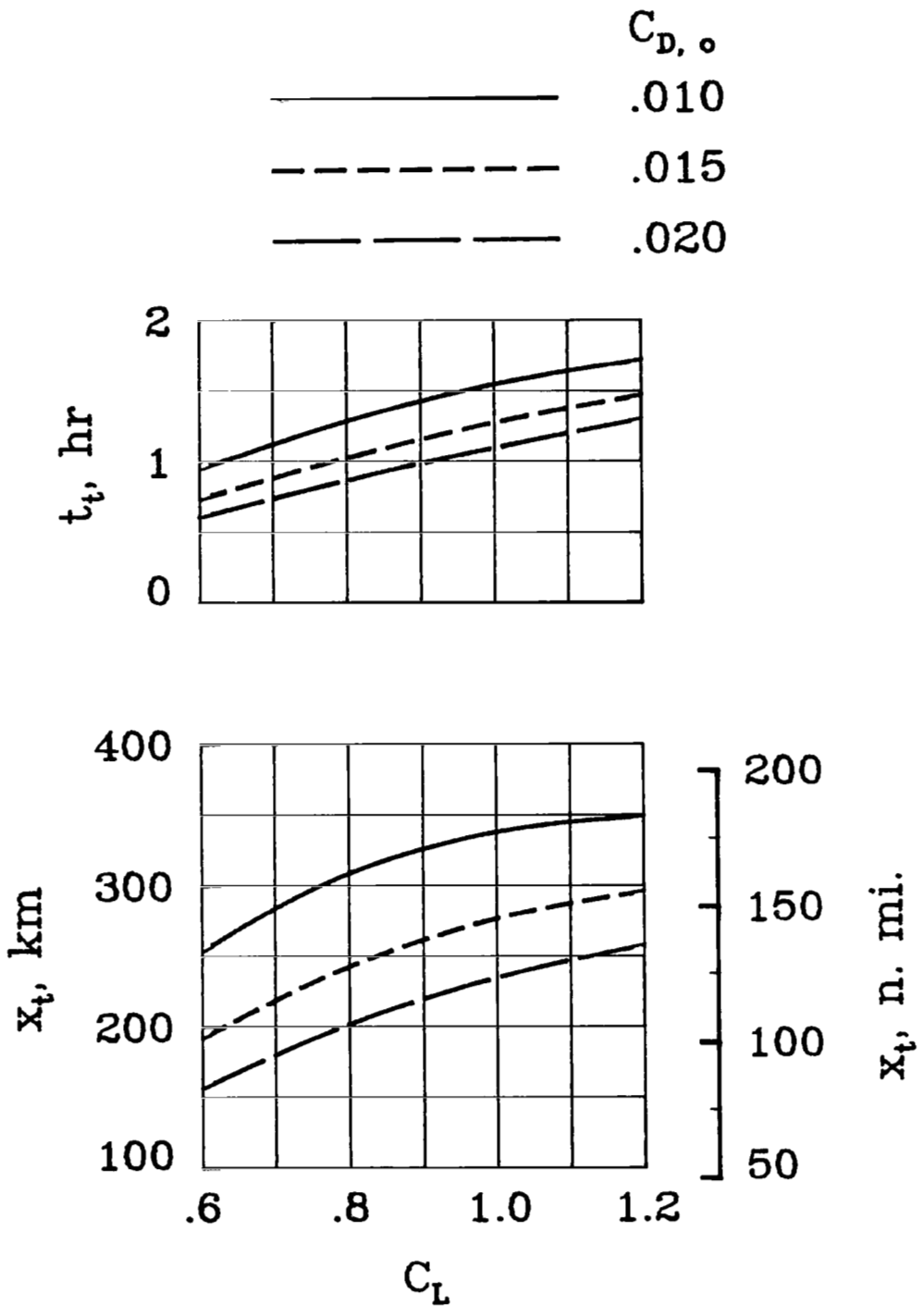

Figure 9.- Concluded.

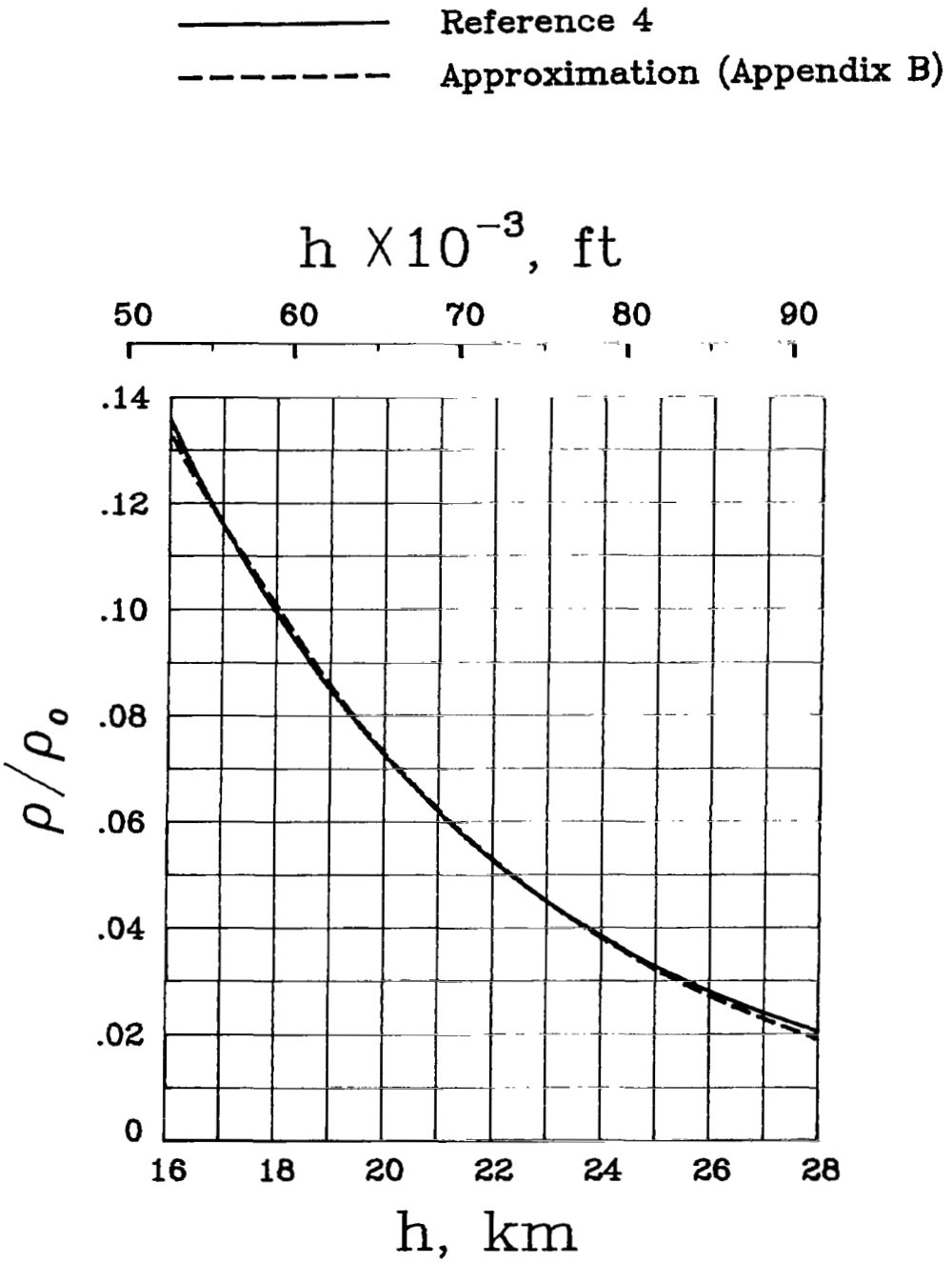

Figure 10.- Comaprison of two models of air density variation with altitude.

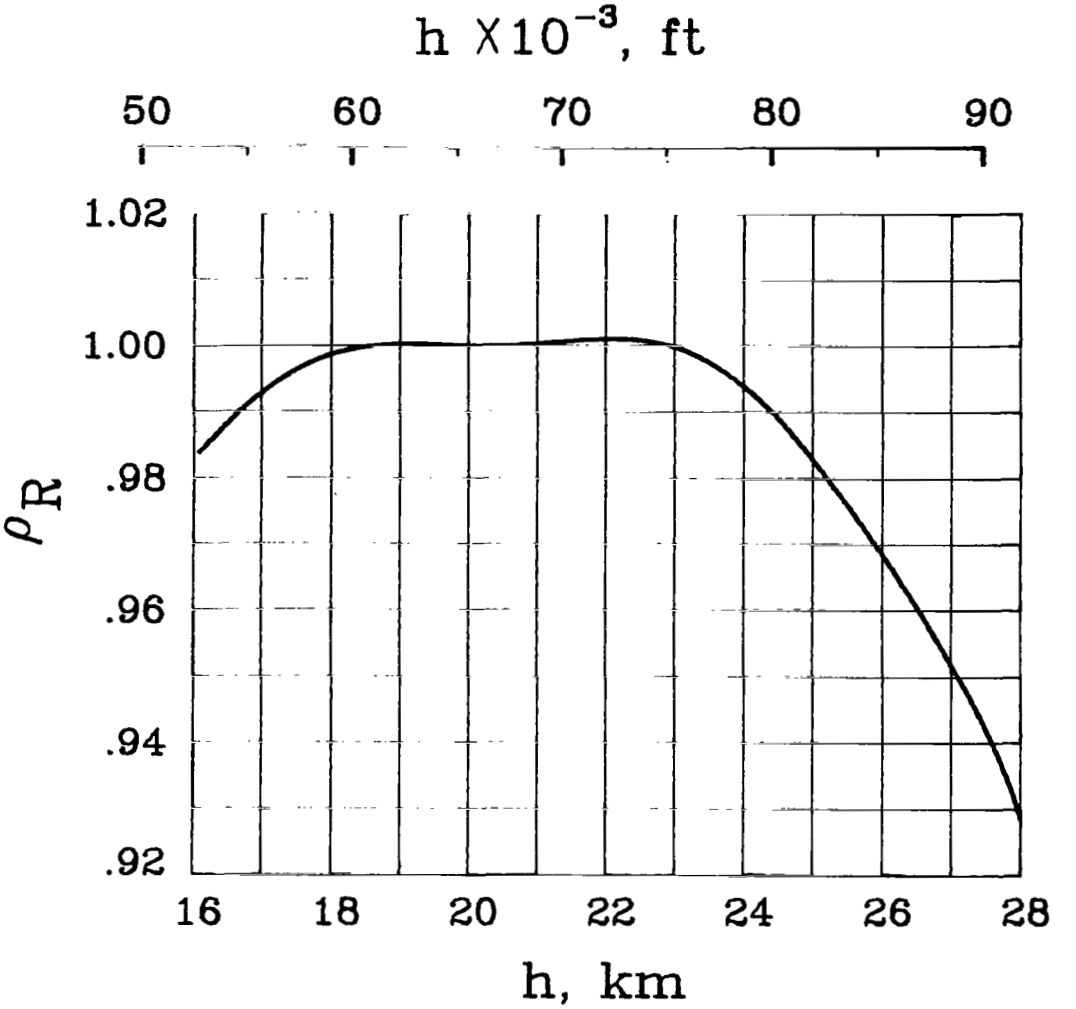

Figure 11.- Ratio of approximate density (appendix B) to density from reference 4.

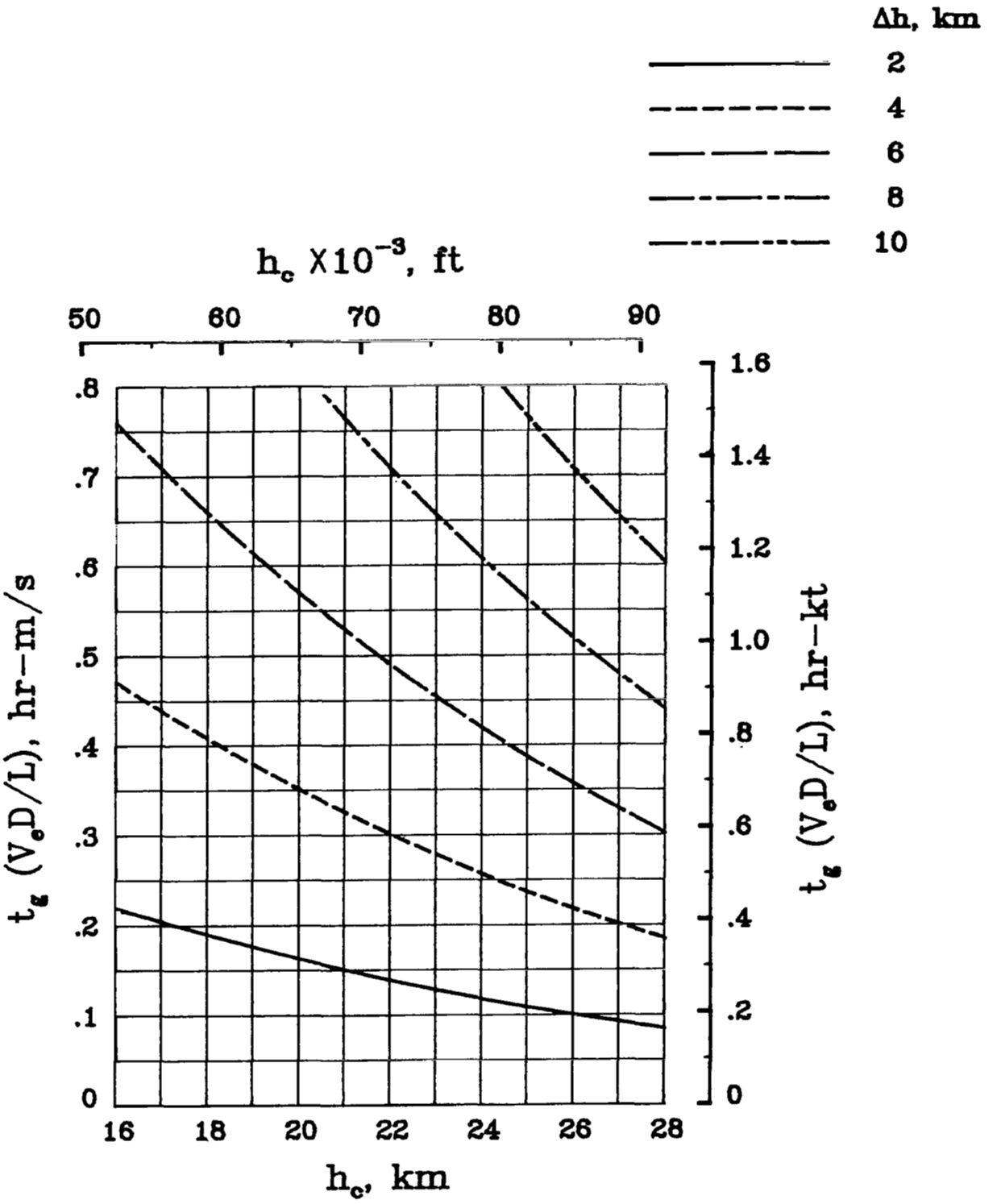

Figure 12.- Variation of glide-time parameter with initial altitude and altitude decrement.

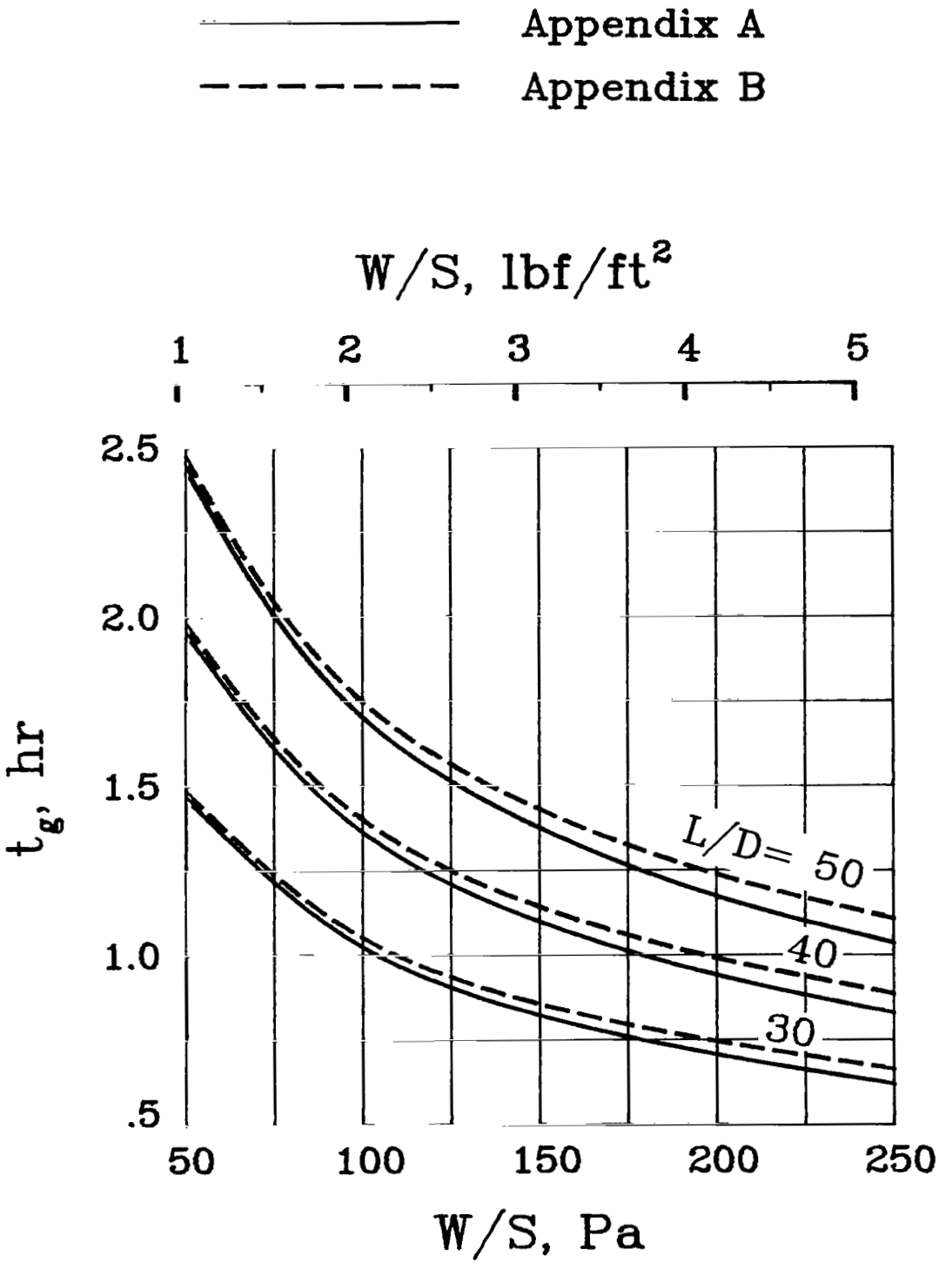

Figure 13.- Variation of time to glide from 25 to 18 km (82 000 to 59 000 ft) with wing loading and lift-drag ratio. C_L = 0.9.

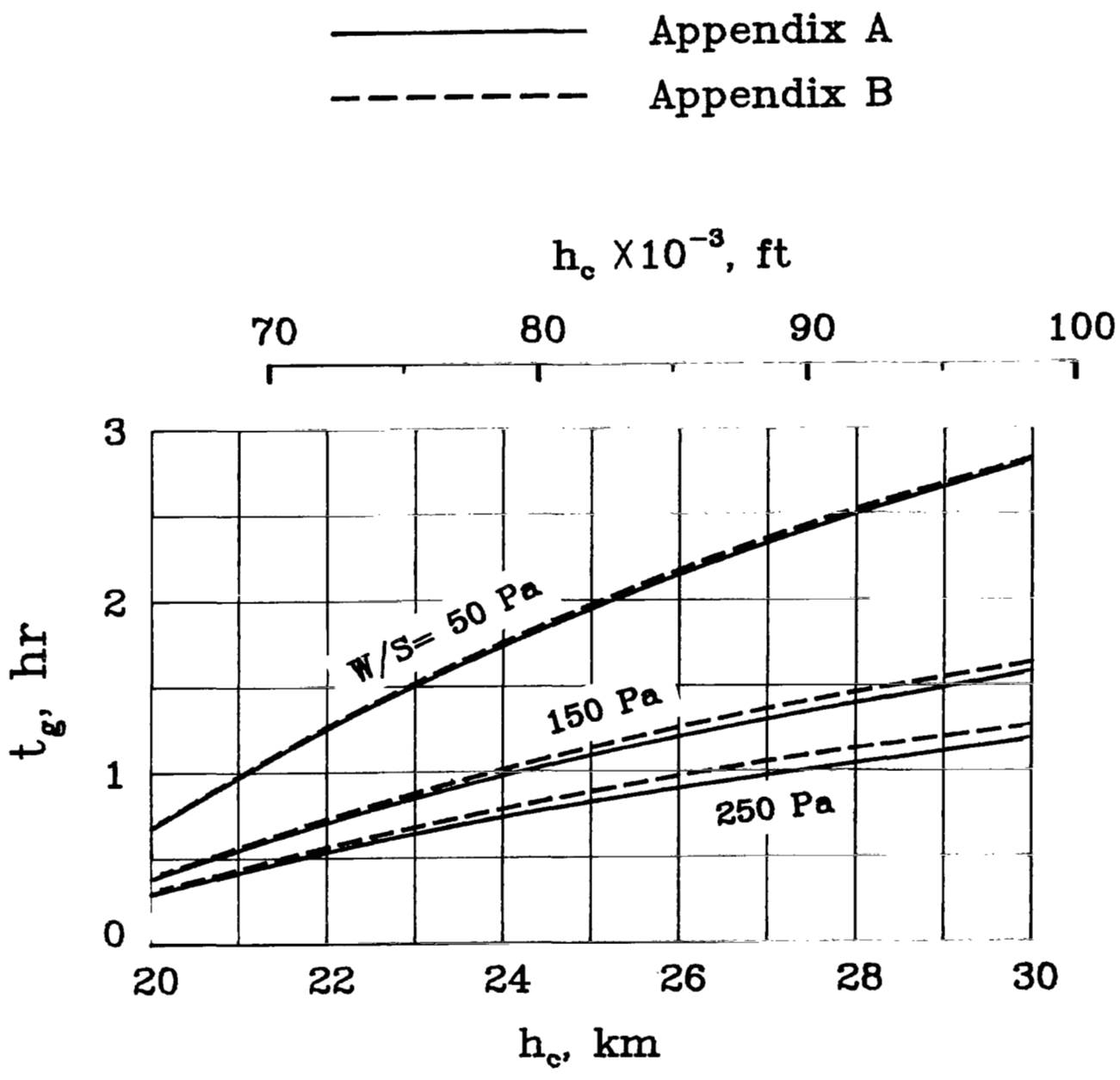

Figure 14.- Variation of glide time with altitude and wing loading. Glide termination at 18 km (59 000 ft); L/D = 40; C_L = 0.9.

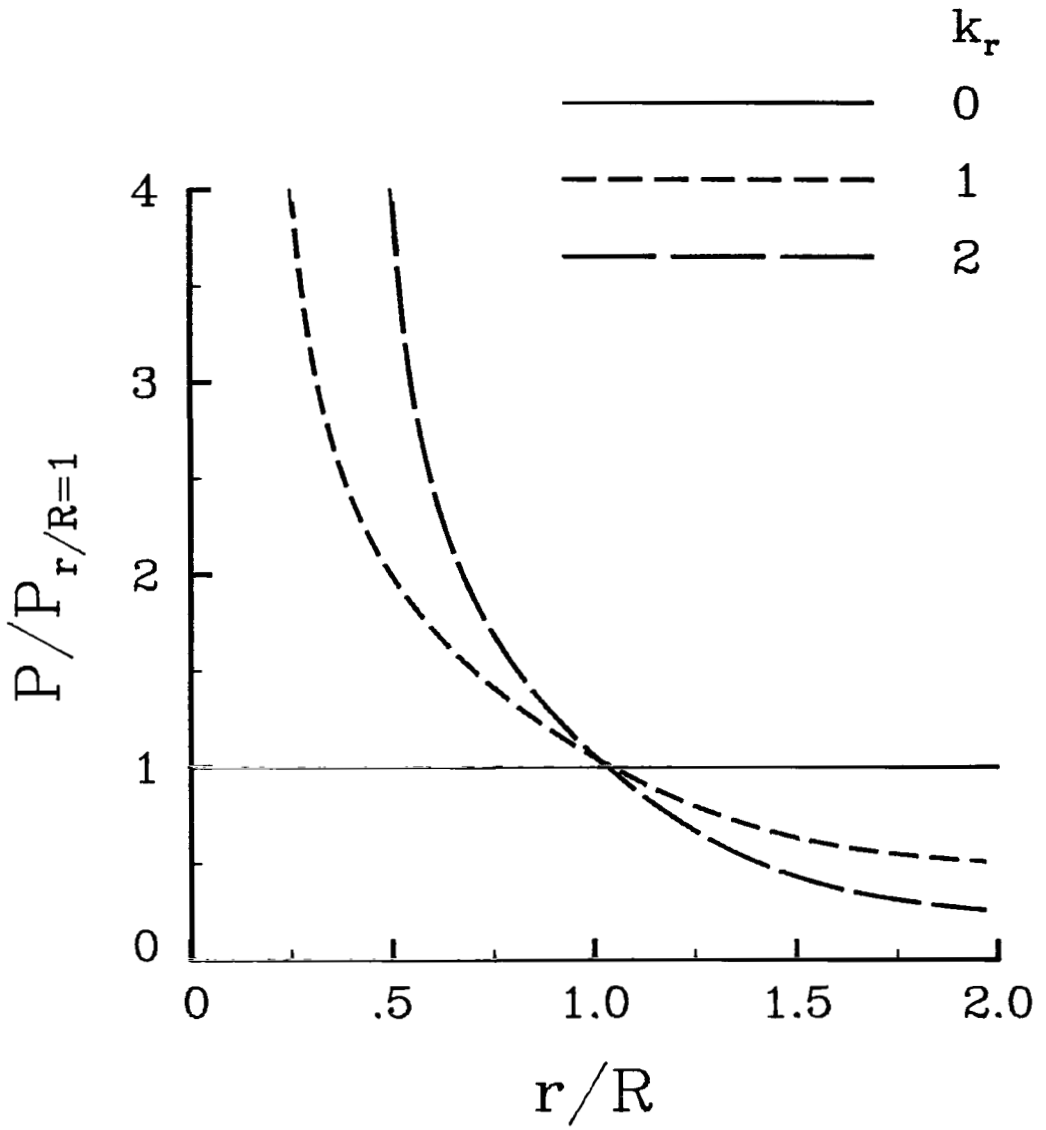

Figure 15.- Relative variation in microwave-beam intensity with range.

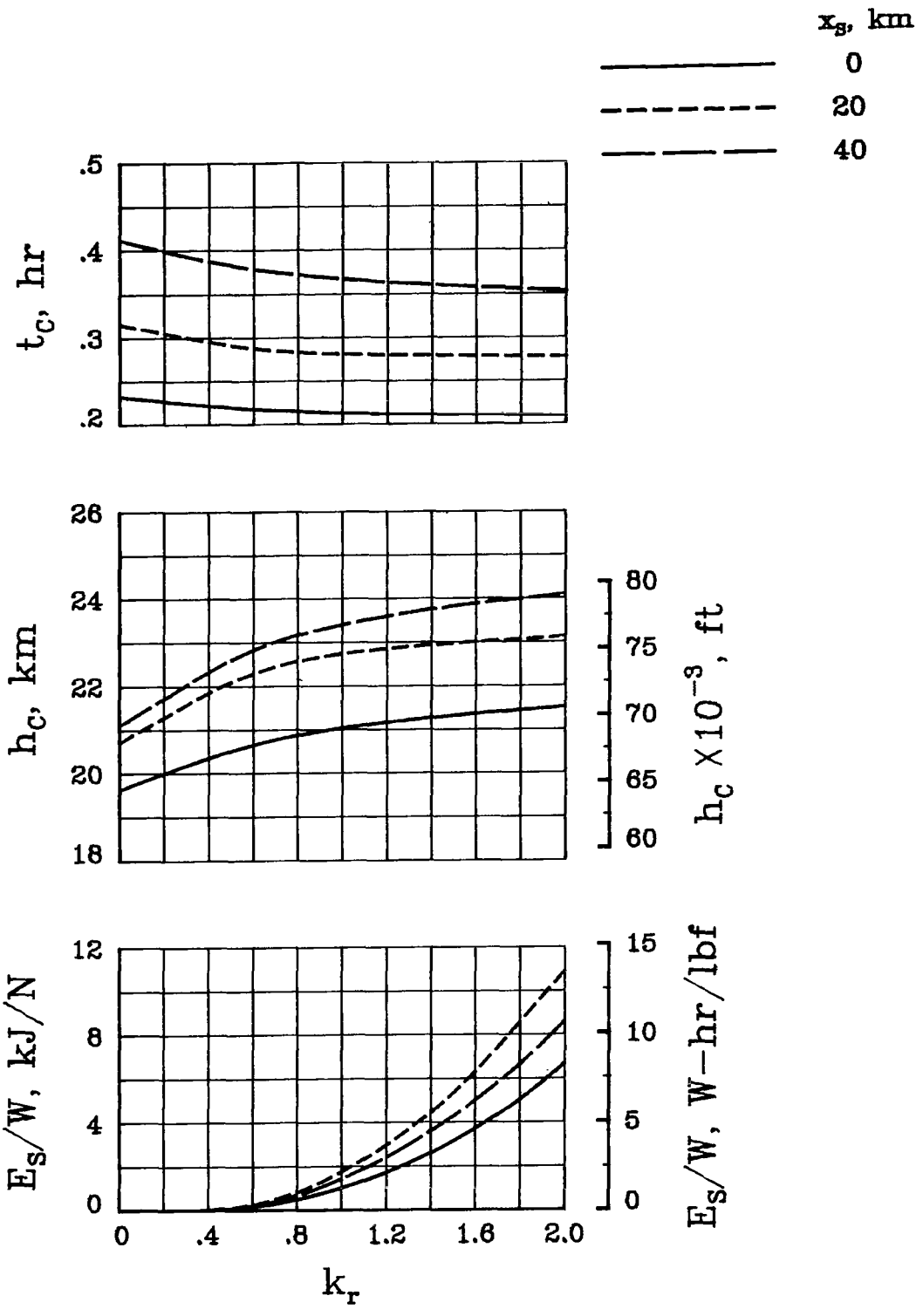

Figure 16.- Variation of baseline configuration climb performance with microwave-beam intensity factor k_r of equation (15).

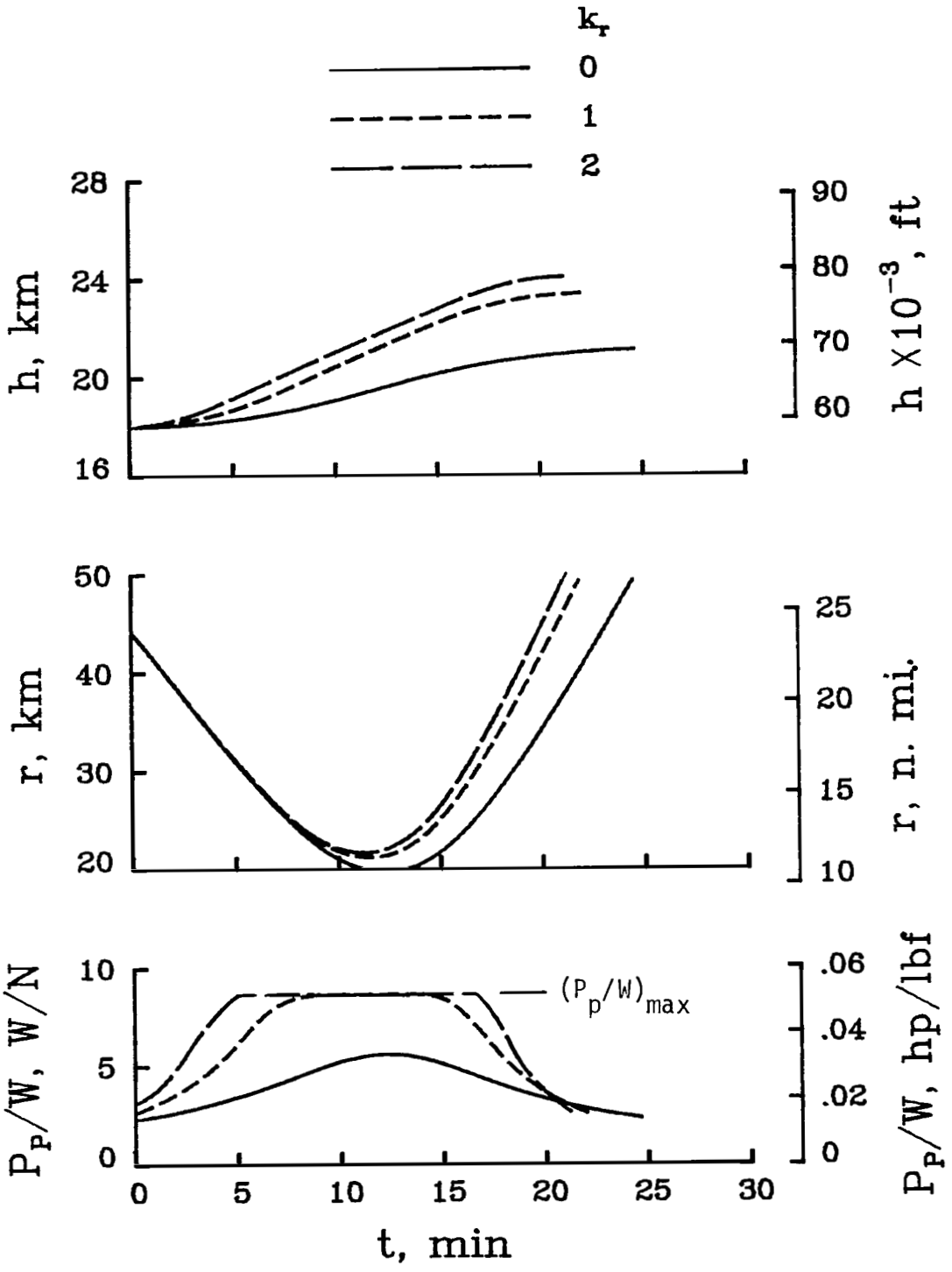

Figure 17.- Climb performance for three values of k_r. Baseline configuration; x_s = 40 km (22 n.mi.).

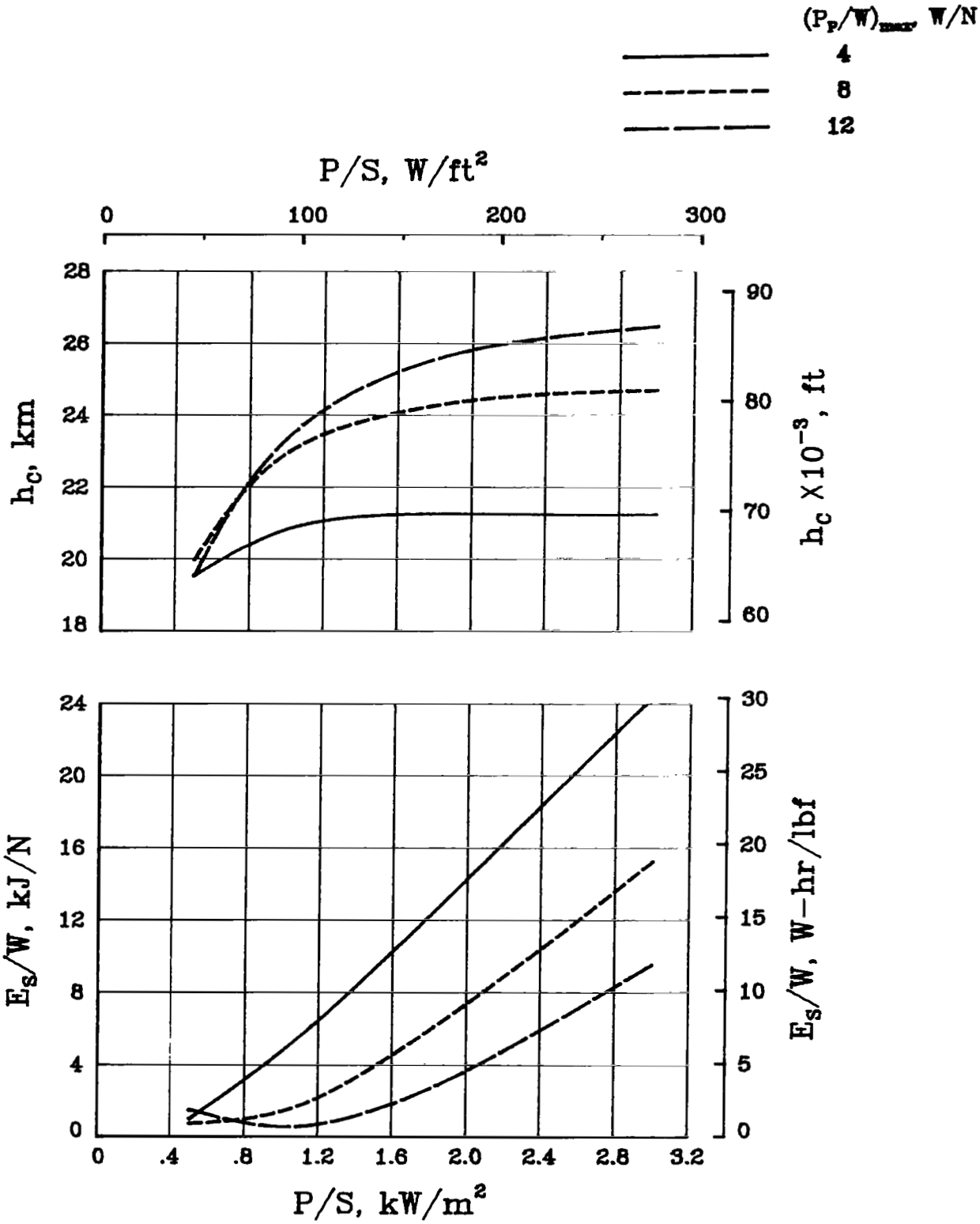

Figure 18.- Effect of beam intensity and motor size on climb performance.

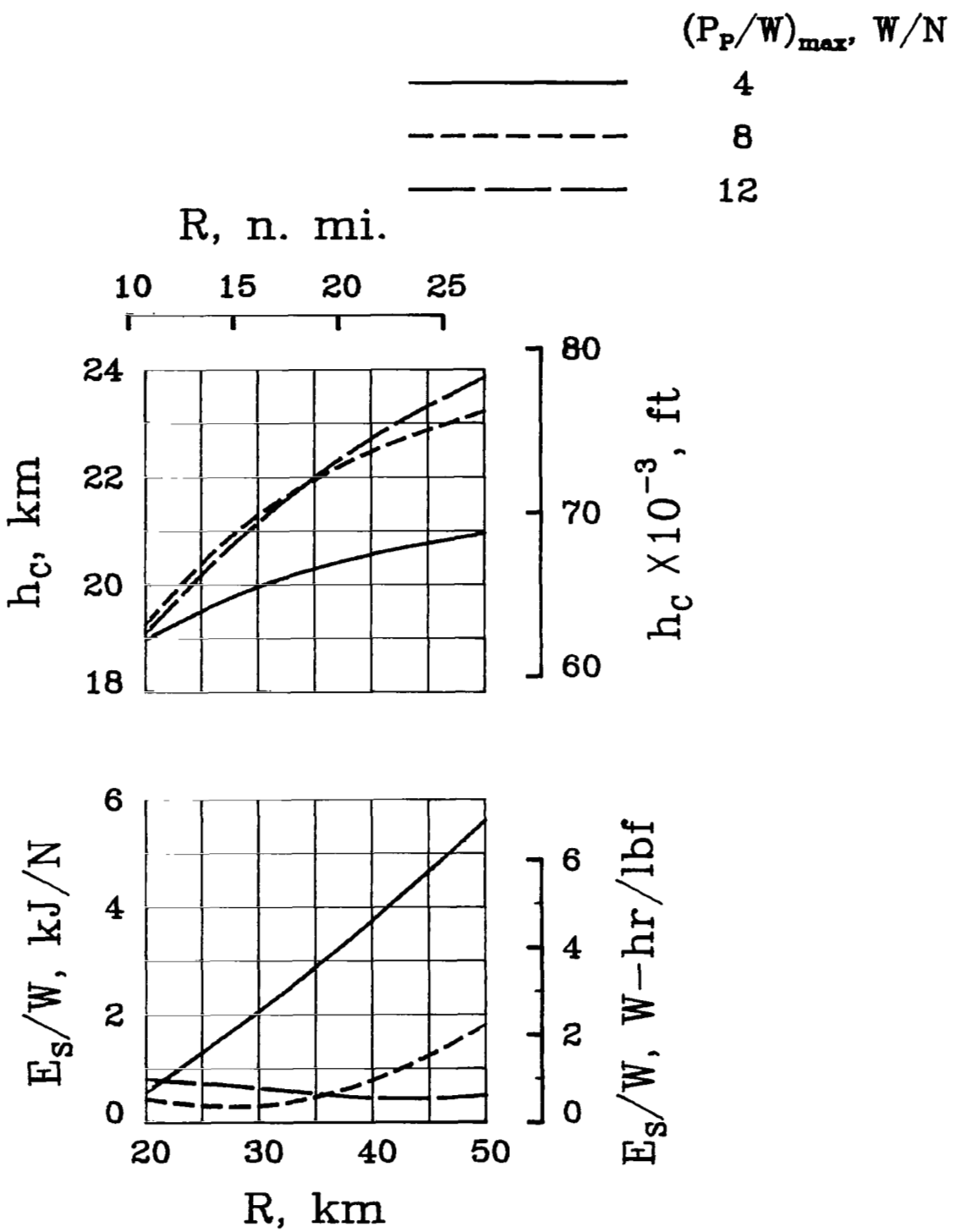

Figure 19.- Effect of variation in reference range and motor size.

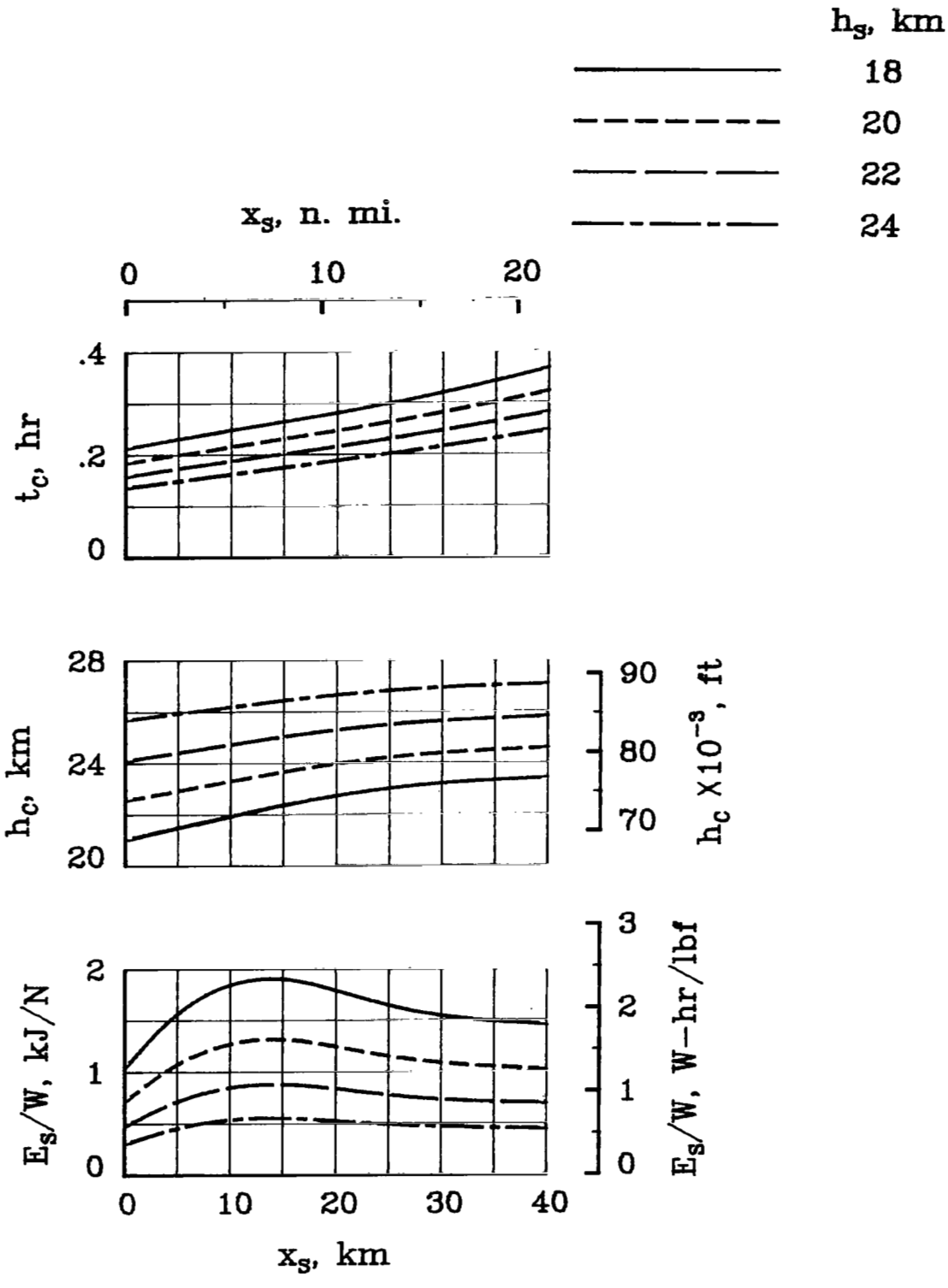

Figure 20.- Effect of initiating climb at different altitudes and horizontal ranges.

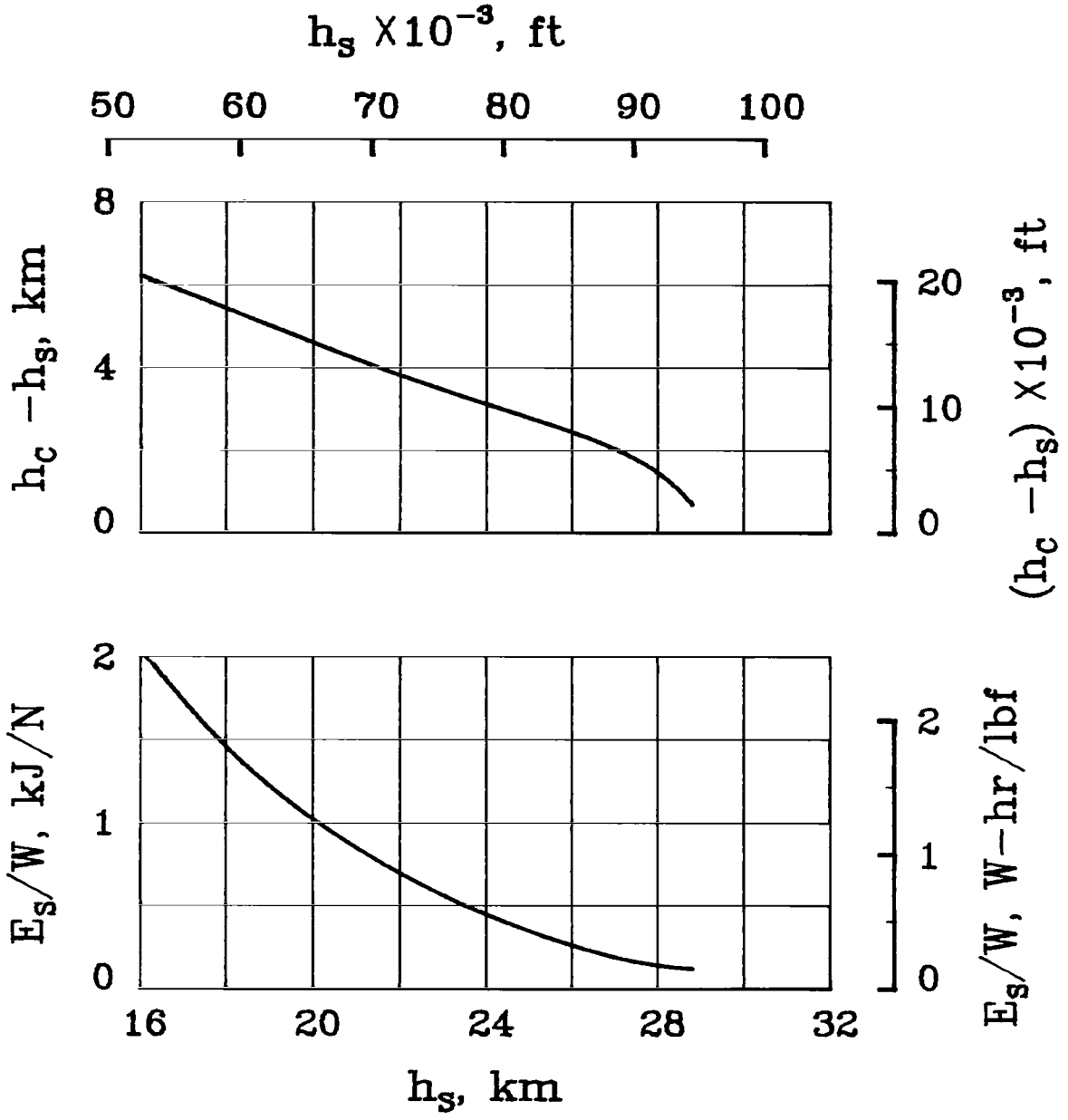

Figure 21.- Effect of variation in initial altitude on climb performance. x_c = 40 km (22 n.mi.).

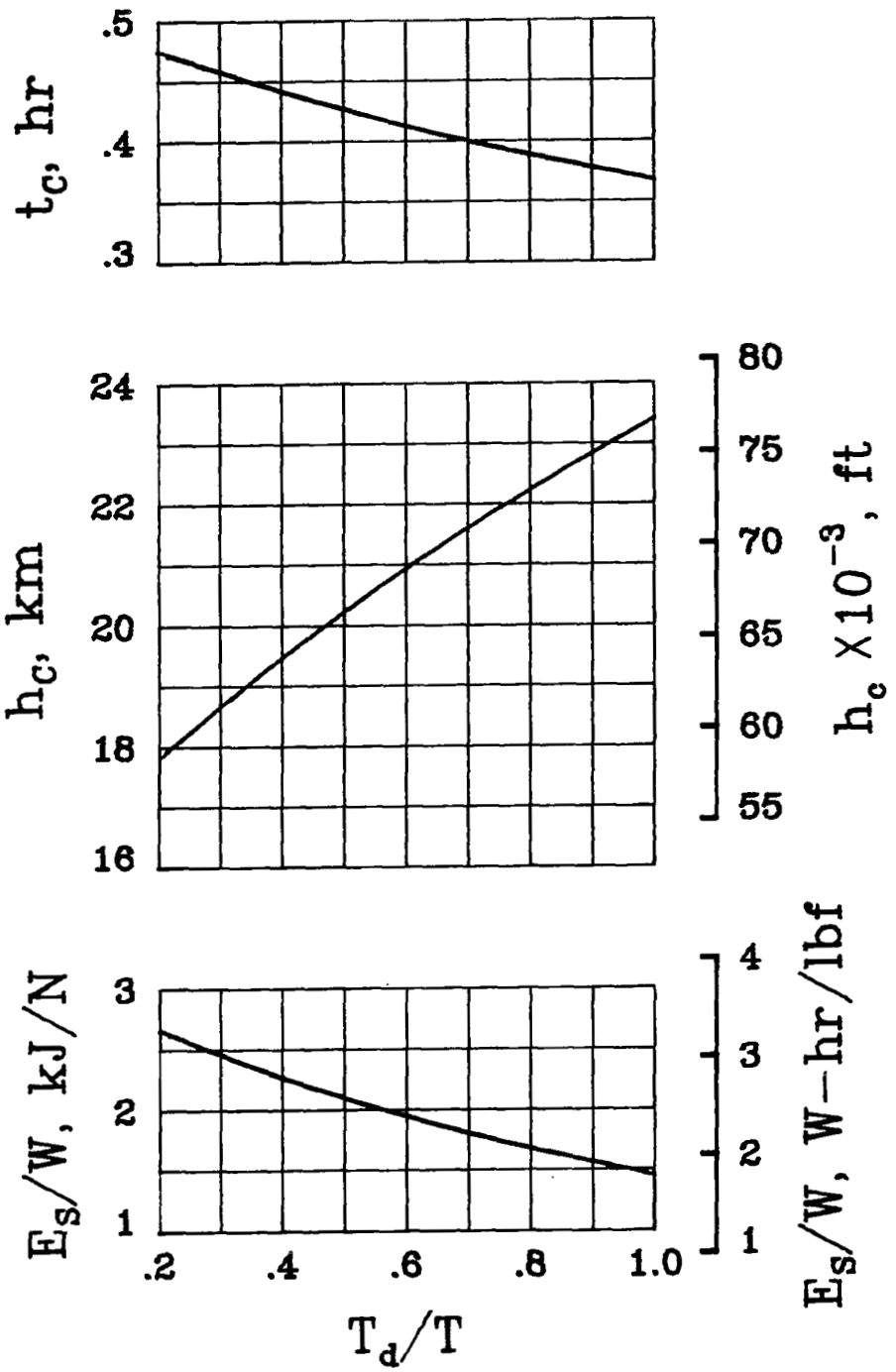

Figure 22.- Effect of degradation of propeller efficiency on climb performance.

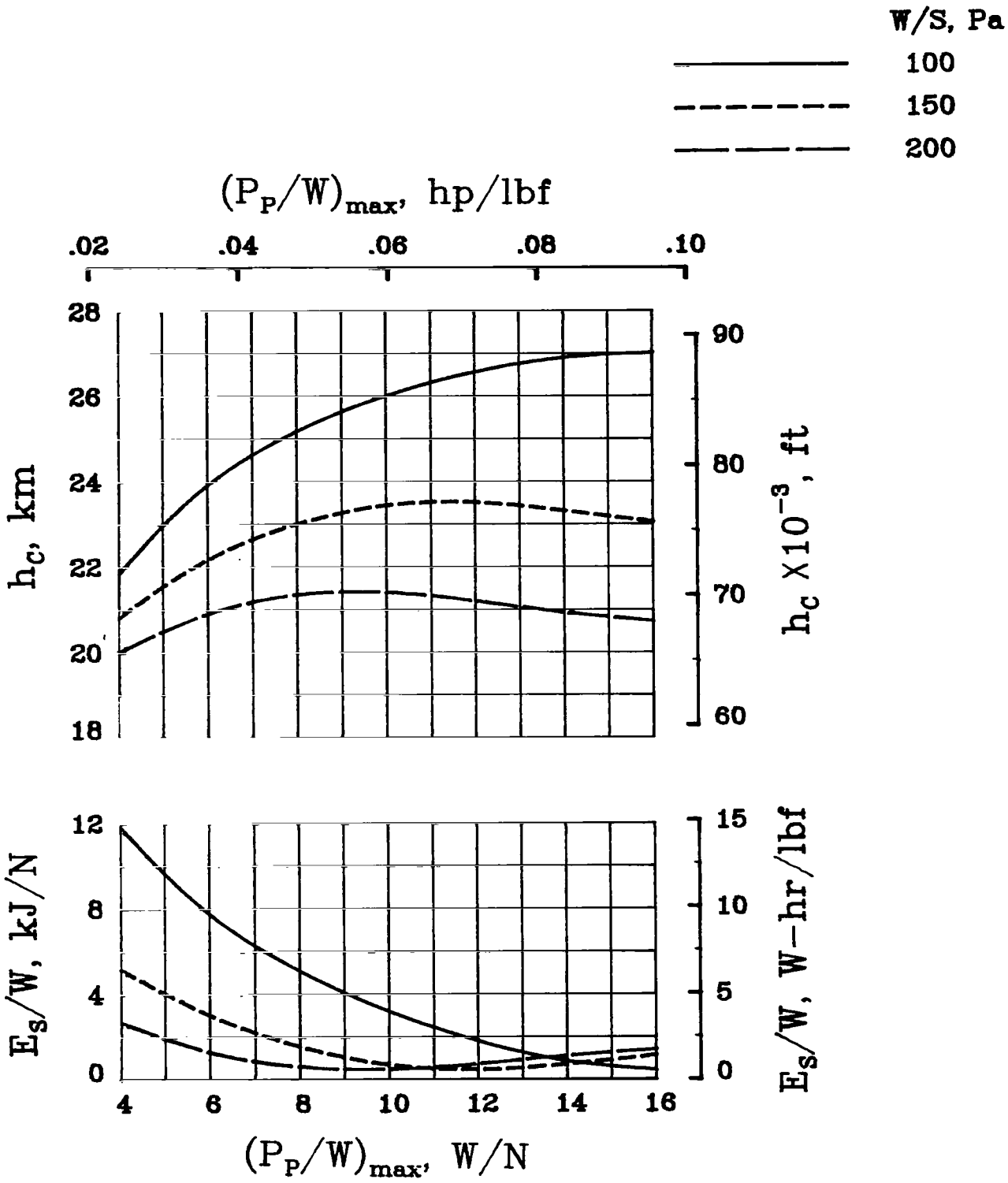

Figure 23.- Effect of motor size and wing loading on climb performance.

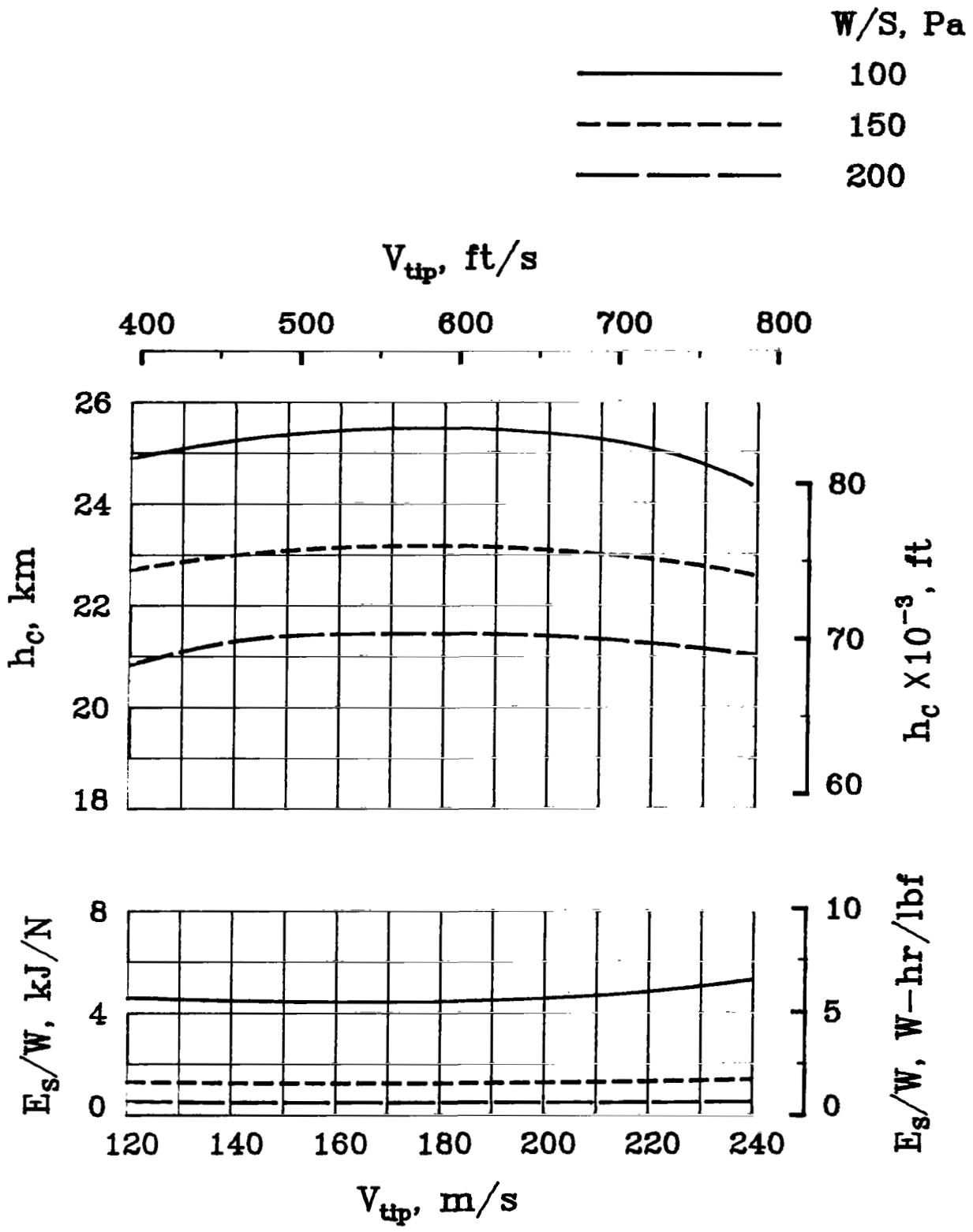

Figure 24.- Effect of propeller tip speed and wing loading on climb performance.

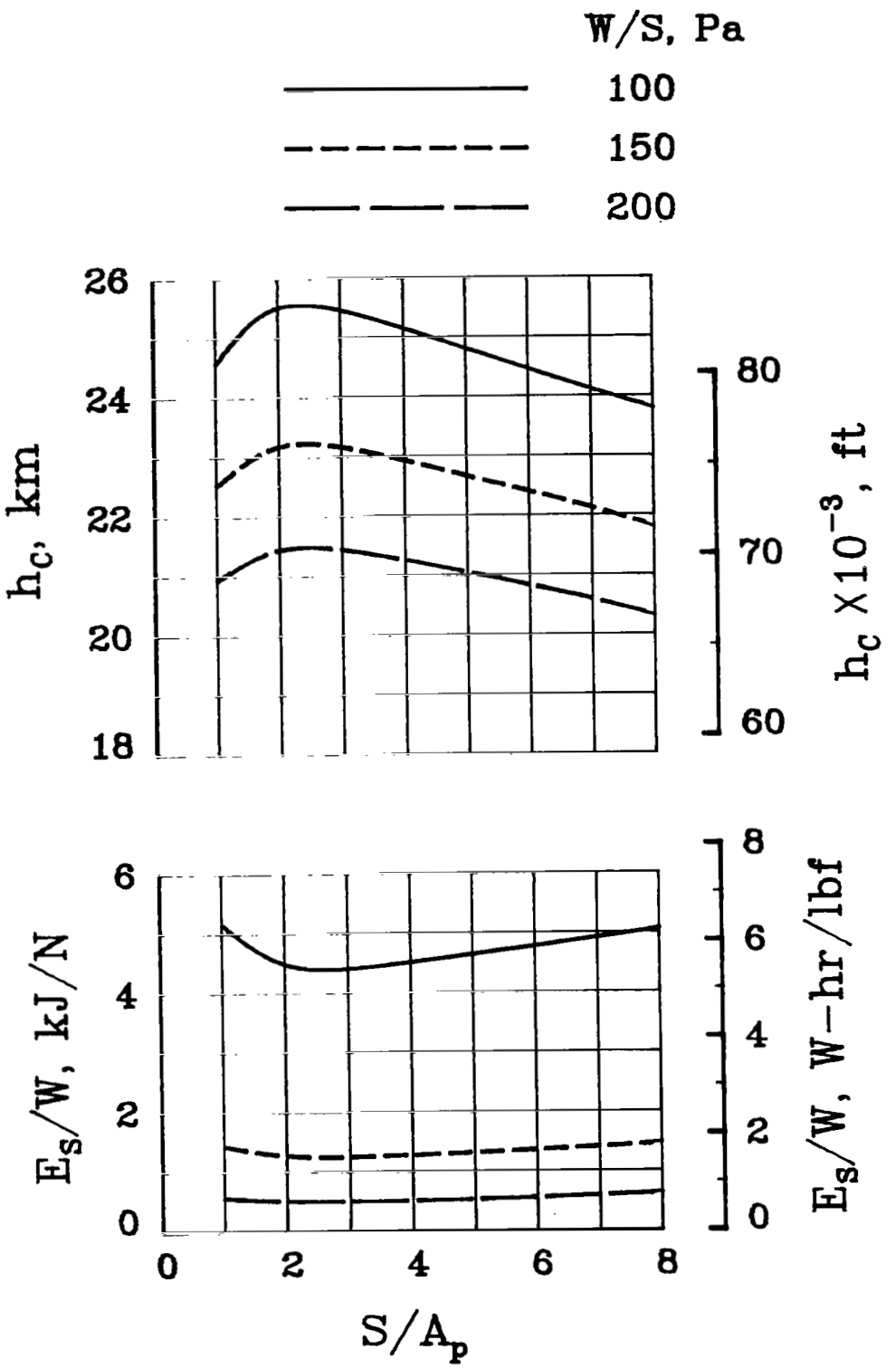

Figure 25.- Effect of propeller size and wing loading on climb performance. V_{tip} = 172 m/s (564 ft/s).

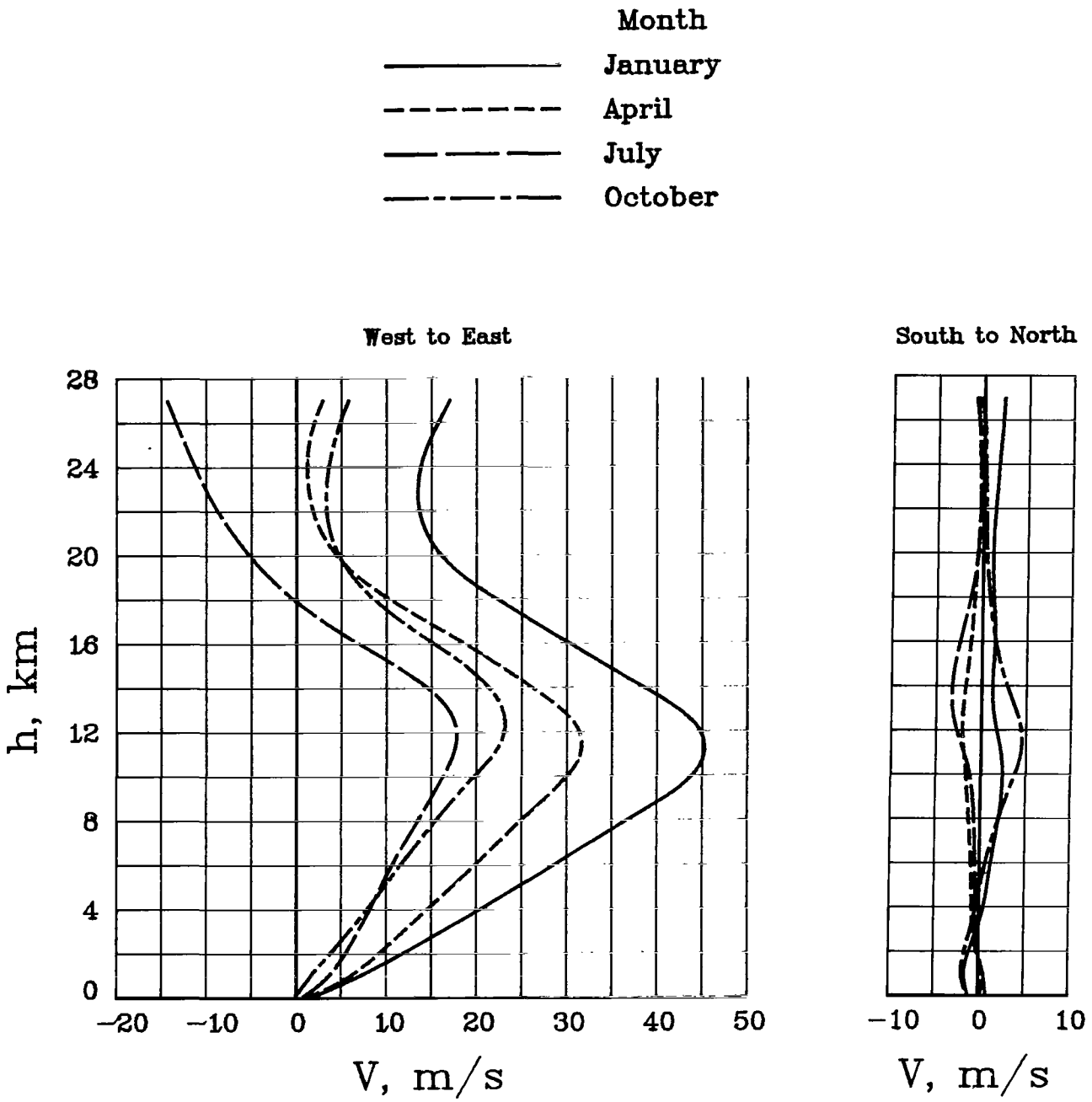

(a) Mean velocities.

Figure 26.- Wind profile data (ref. 19).

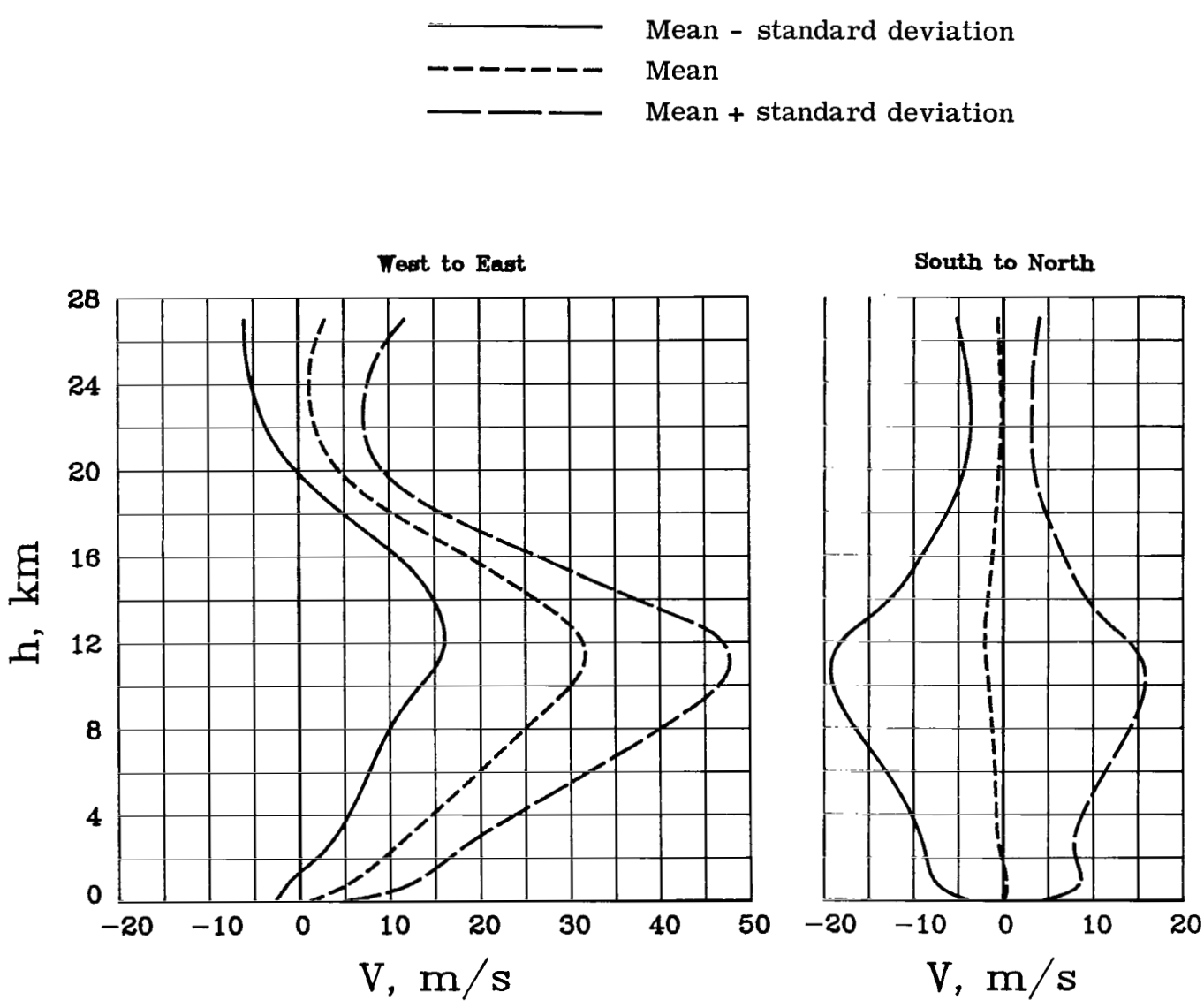

(b) Mean and standard-deviation profiles for April.

Figure 26.- Concluded.

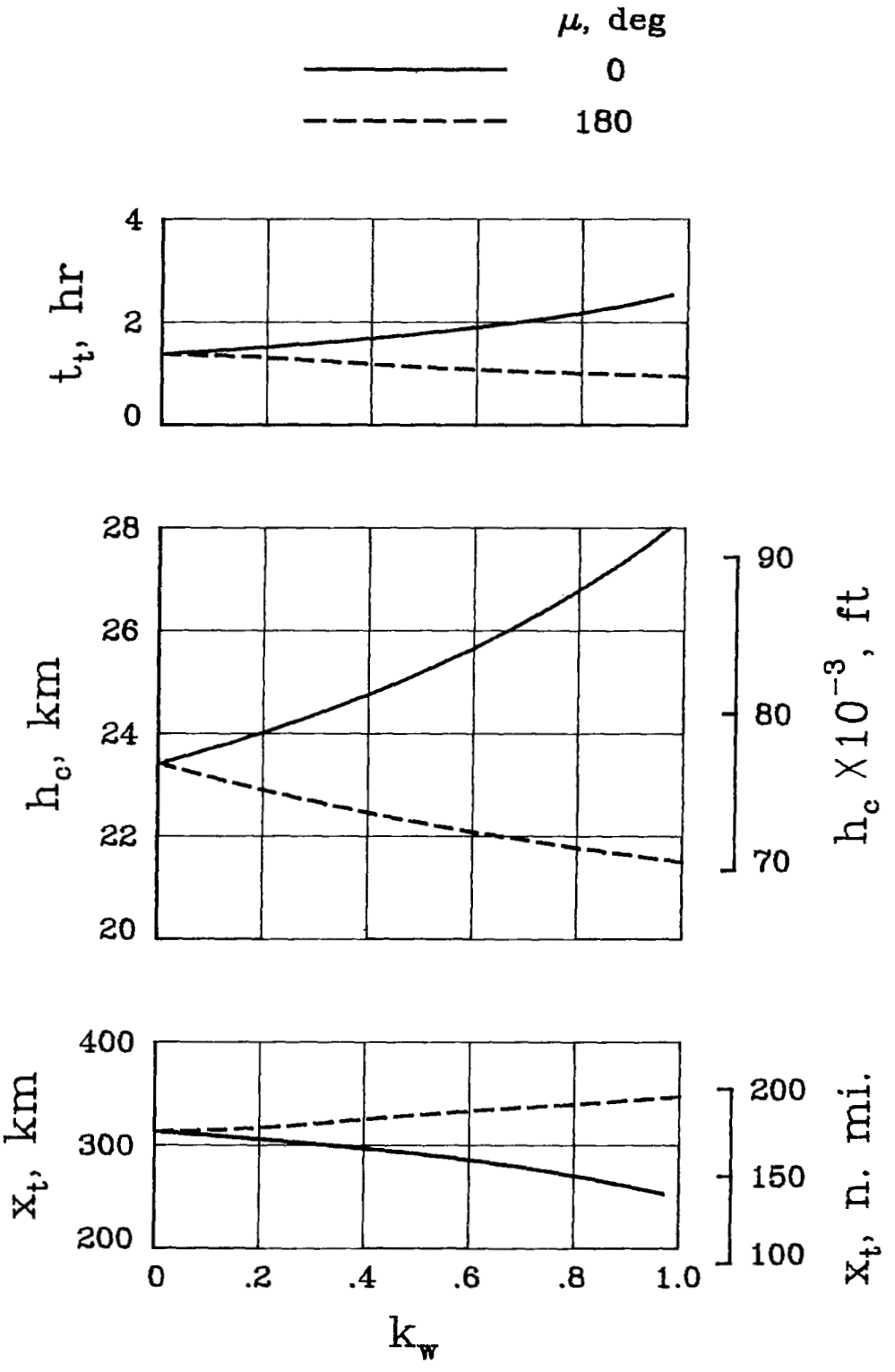

Figure 27.- Effect of head winds and tail winds on performance of baseline configuration.

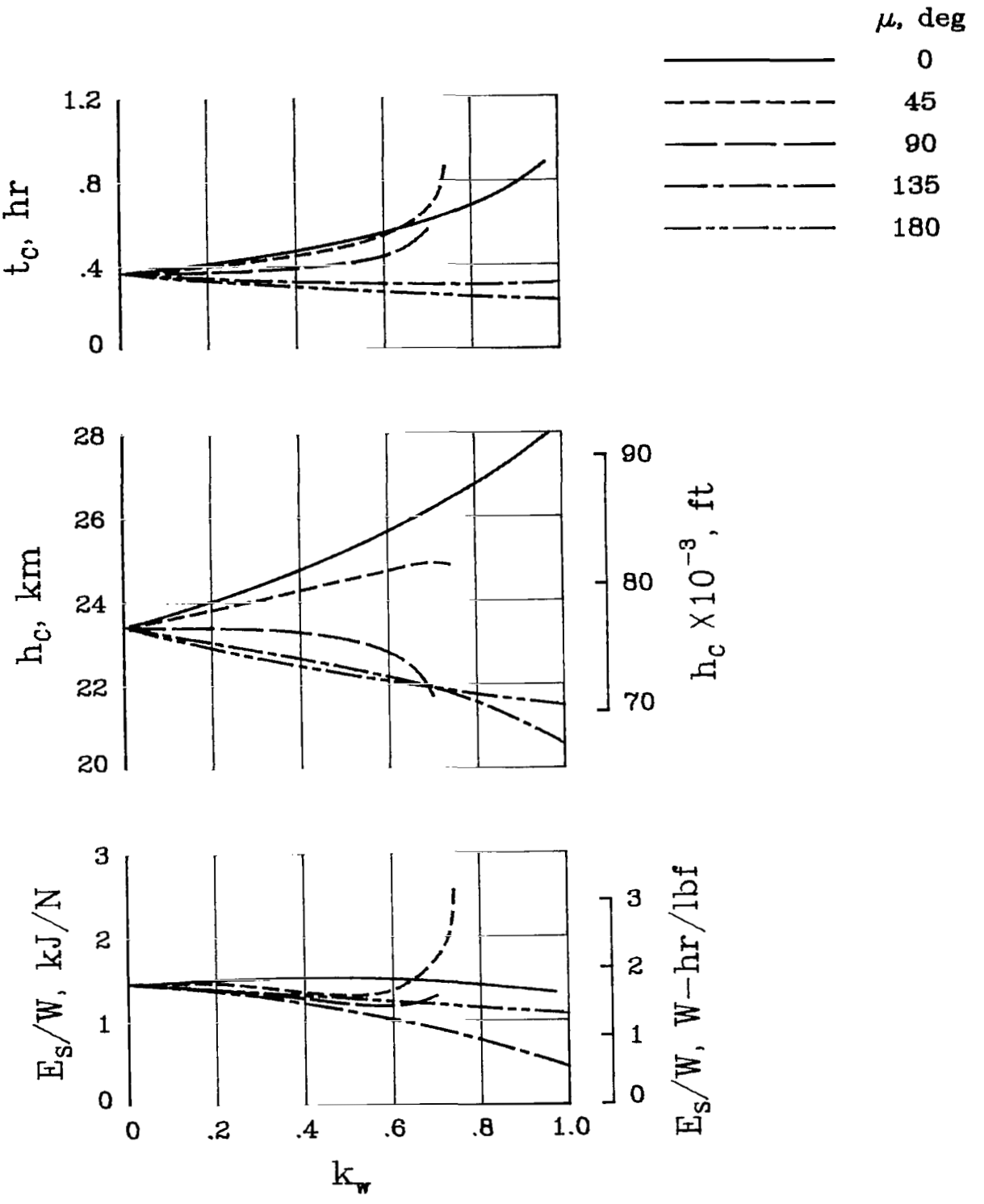

(a) Variation of wind-profile magnitude.

Figure 28.- Effect of wind direction and profile amplitude on performance of baseline configuration.

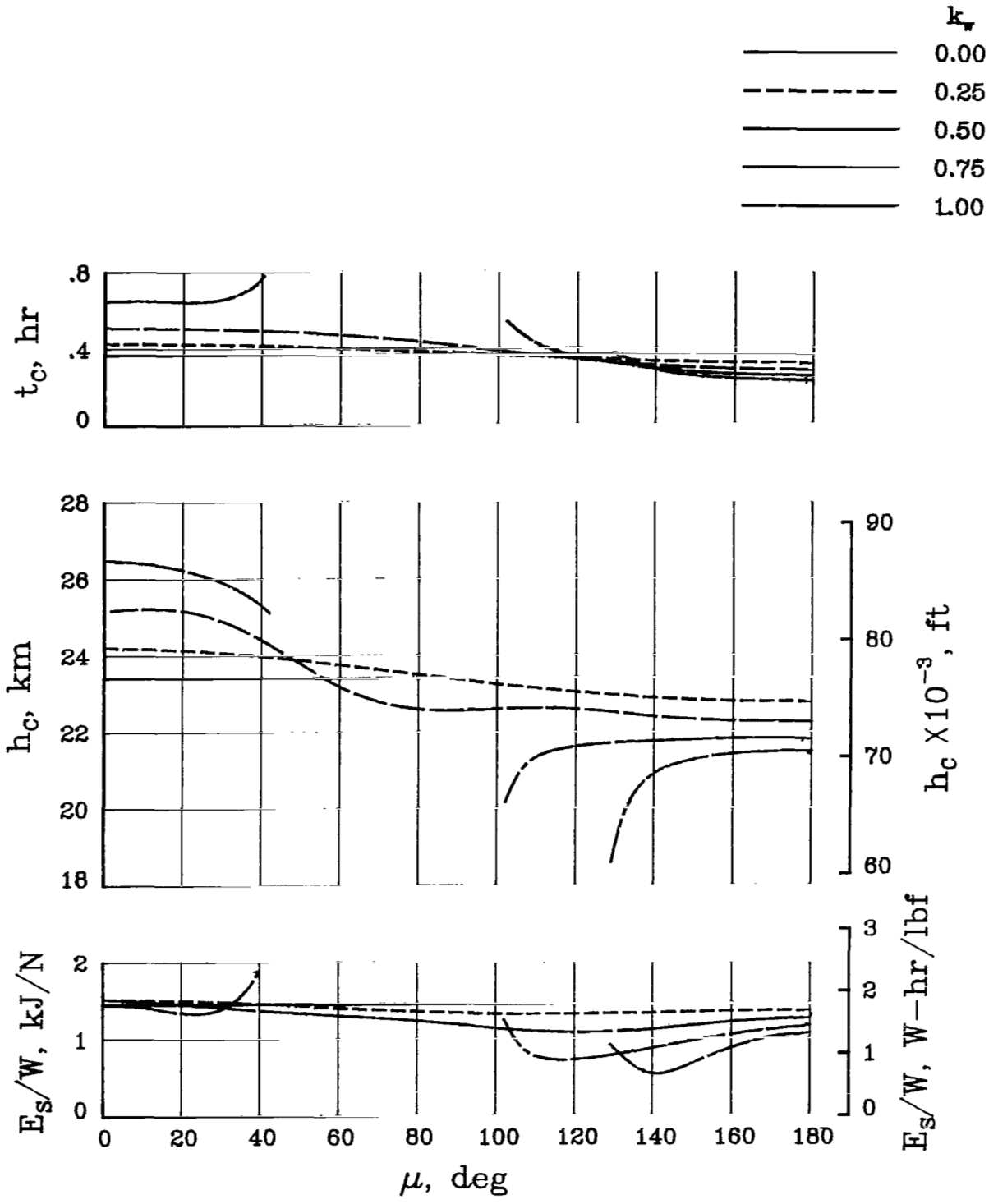

(b) Variation of wind direction.

Figure 28.- Concluded.

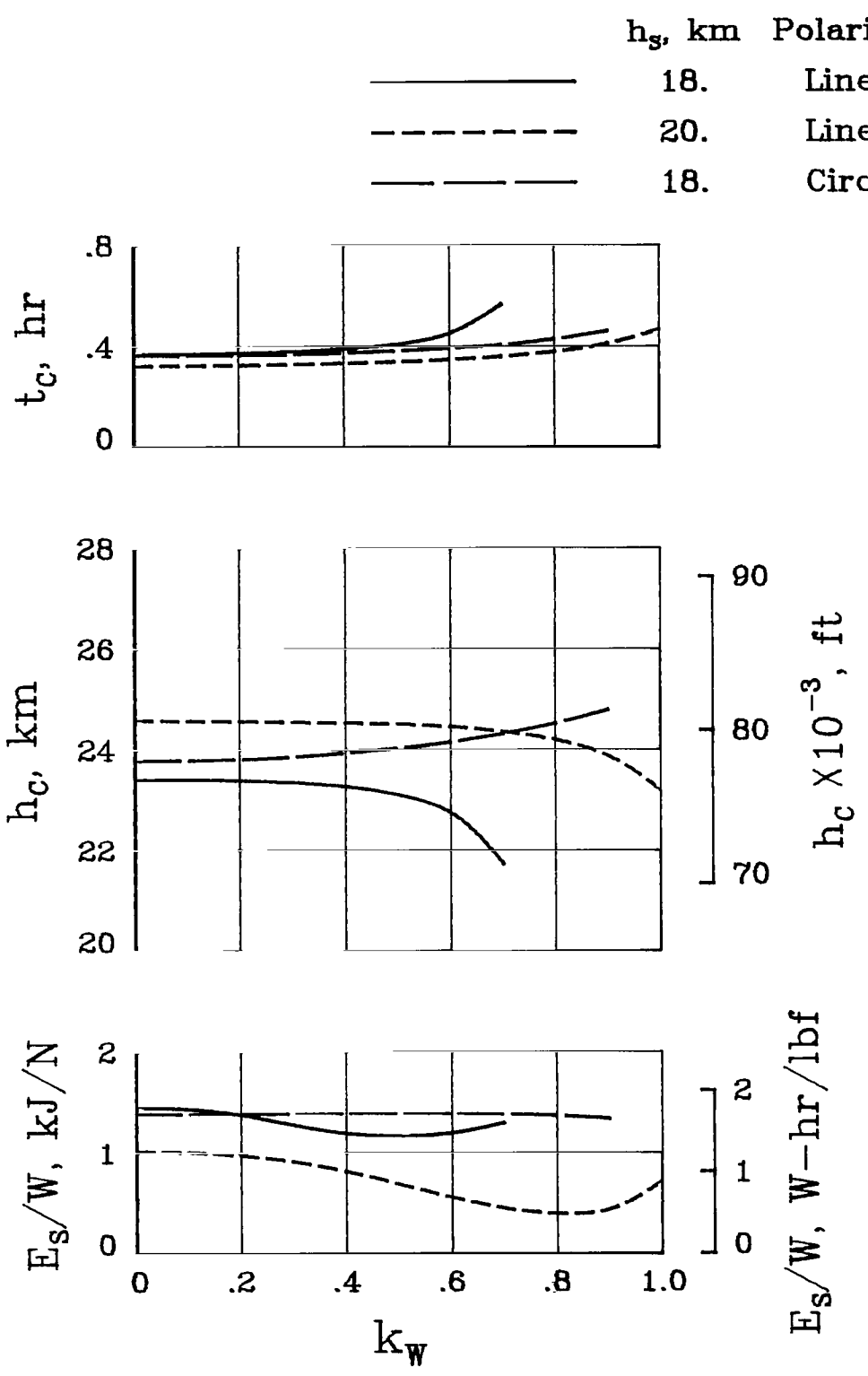

Figure 29.- Climb performance for $\mu = 90°$ and $P/S = 1.1$ kw/m^2 (100 W/ft^2).

1. Report No.	2. Government Accession No.	3. Recipient's Catalog No.
NASA TP-1918		

4. Title and Subtitle
PARAMETRIC STUDY OF MICROWAVE-POWERED HIGH-ALTITUDE AIRPLANE PLATFORMS DESIGNED FOR LINEAR FLIGHT

5. Report Date
November 1981

6. Performing Organization Code
530-01-13-02

7. Author(s)
Charles E. K. Morris, Jr.

8. Performing Organization Report No.
L-14606

10. Work Unit No.

9. Performing Organization Name and Address
NASA Langley Research Center
Hampton, VA 23665

11. Contract or Grant No.

13. Type of Report and Period Covered
Technical Paper

12. Sponsoring Agency Name and Address
National Aeronautics and Space Administration
Washington, DC 20546

14. Sponsoring Agency Code

15. Supplementary Notes

16. Abstract

The performance of a class of remotely piloted, microwave-powered, high-altitude airplane platforms was studied. The first part of each cycle of the flight profile consists of climb while the vehicle is tracked and powered by a microwave beam; this is followed by gliding flight back to a minimum altitude above a microwave station and initiation of another cycle. Parametric variations were used to define the effects of changes in the characteristics of the airplane aerodynamics, the energy-transmission systems, the propulsion system, and winds. Results show that wind effects limit the reduction of wing loading and the increase of lift coefficient, two effective ways to obtain longer range and endurance for each flight cycle. Calculated climb performance showed strong sensitivity to some power and propulsion parameters. A simplified method of computing gliding endurance was developed.

17. Key Words (Suggested by Author(s))	18. Distribution Statement
Microwave power High-altitude observation Sailplanes	Unclassified - Unlimited Subject Category 05

19. Security Classif. (of this report)	20. Security Classif. (of this page)	21. No. of Pages	22. Price
Unclassified	Unclassified	72	A04

For sale by the National Technical Information Service, Springfield, Virginia 22161

NASA-Langley, 1981